Supplementary material for the paper
Scatter broadening measurements of 124 Pulsars at 327 MHz

M.A. Krishnakumar [1,2], D. Mitra [2], A. Naidu [2], B. C. Joshi [2] and P. K. Manoharan [1,2]

kkma@ncra.tifr.res.in

The supplementary material contains three sections. See below for details.

1. Sample and Fit Results

Table 1 gives the observational summary for the sample of 124 pulsars that has been observed with the Ooty Radio Telescope at 327 MHz for scatter broadening (τ_{sc}) measurements. Fig. 1–62 are plots of 124 pulsars for which τ_{sc} measurements are done by fitting Eqn. (1) as explained in Section 2.2 of the main paper. The transfer function used for these fits is $s(t) = exp(-t/\tau_{sc})$. Refer the figure caption of Fig. 1 for the plot details.

[1]Radio Astronomy Centre, NCRA-TIFR, Udagamandalam, India

[2]National Centre for Radio Astrophysics, Tata Institute of Fundamental Research, Pune, India

Table 1. Summary of Observations. For each pulsar the table lists the MJD of observation, period, dispersion measure, rotation measure (taken from catalogue), duration of observation and peak signal to noise ratio.

Sr. No.	Pulsar Name	MJD (days)	Period (secs)	DM (cm^{-3} pc)	RM (Catalog) rad m^2	Duration of Observation (minutes)	SNR (peak)
1	B0447-12	56621.84	0.438011	37.04	13.00	32	33
2	B0450-18	56643.65	0.548955	39.90	13.80	29	43
3	B0458+46	56623.85	0.638556	42.19	-43.00	168	13
4	B0523+11	56621.92	0.354428	79.35	37.00	31	47
5	B0531+21	56623.96	0.033689	56.79	-42.30	10	56
6	B0559-05	56589.98	0.395941	80.54	64.00	30	60
7	B0611+22	56621.96	0.334980	96.91	69.00	17	50
8	B0621-04	56590.06	1.038995	70.83	49.00	30	18
9	B0626+24	56590.09	0.476582	84.19	69.50	9	174
10	B0736-40	56377.71	0.374936	160.80	12.10	19	59
11	B0740-28	56590.86	0.166762	73.78	149.95	16	298
12	J0749-4247	56541.00	1.095428	104.59	125.00	60	7
13	B0808-47	56377.73	0.547216	228.30	105.00	30	15
14	B0818-41	56377.76	0.545464	113.40	57.70	30	56
15	B0833-45	56590.95	0.089378	67.99	31.38	7	503
16	B0835-41	56377.78	0.751649	147.29	135.80	14	365
17	B0840-48	56553.32	0.644358	196.85	-	60	19
18	B0844-35	56590.96	1.116034	94.16	144.00	14	16
19	B0853-33	56590.97	1.267463	86.64	165.00	18	38
20	J0857-4424	56541.11	0.326788	184.43	-75.00	54	8
21	B0903-42	56541.15	0.965168	145.80	284.00	60	19
22	J0905-4536	56545.03	0.988275	179.70	153.00	90	7
23	B0906-49	56545.09	0.106768	180.37	10.00	89	14
24	B0950-38	56545.16	1.373816	167.00	-	90	25
25	B1015-56	56644.86	0.503437	439.10	365.00	61	17
26	J1036-4926	56780.57	0.510386	136.53	-11.00	51	17
27	B1039-55	56643.84	1.170804	306.50	155.00	25	12
28	B1044-57	56756.71	0.369427	240.20	133.00	120	13
29	B1119-54	56747.70	0.535779	204.70	42.00	164	73
30	J1123-4844	56594.31	0.244833	92.92	-7.00	30	15
31	J1210-5559	56770.73	0.279768	174.35	58.00	40	19
32	B1317-53	56594.41	0.279739	97.60	141.00	25	21
33	B1325-49	56547.26	1.478812	118.00	170.00	90	29
34	B1523-55	56770.76	1.048672	362.70	34.00	89	7
35	J1557-4258	56552.52	0.329216	144.50	-41.90	45	14
36	B1600-49	56379.79	0.327393	140.80	-16.00	17	47
37	B1609-47	56552.55	0.382410	161.20	-138.00	45	13
38	J1614-3937	56540.53	0.407330	152.44	133.00	60	15

Table 1—Continued

Sr. No.	Pulsar Name	MJD (days)	Period (secs)	DM (cm^{-3} pc)	RM (Catalog) rad m^2	Duration of Observation (minutes)	SNR (peak)
39	B1620-42	56547.40	0.364624	295.00	-15.00	82	6
40	J1625-4048	56540.64	2.355500	145.00	-7.00	90	22
41	B1635-45	56544.51	0.529168	258.91	-28.00	60	10
42	J1648-3256	56544.55	0.719527	128.28	-60.00	42	22
43	B1647-52	56768.86	0.635018	179.10	-38.00	29	11
44	J1700-3312	56547.46	1.358440	166.97	-15.00	73	6
45	B1658-37	56704.92	2.454391	303.40	-605.90	239	7
46	B1700-32	56379.84	1.211672	110.31	-21.70	21	89
47	J1703-4851	56542.48	1.396528	150.29	-46.00	57	15
48	J1705-3423	56777.79	0.255411	146.36	-44.00	163	13
49	J1708-3426	56542.52	0.692182	190.70	-176.00	60	5
50	B1718-32	56399.85	0.477119	126.06	90.00	25	47
51	B1727-47	56399.89	0.829842	123.33	-429.10	14	239
52	B1729-41	56768.91	0.627947	195.30	-	21	7
53	B1737-30	56779.89	0.606924	152.15	-168.00	419	24
54	B1738-08	56751.82	2.042895	74.90	124.00	44	24
55	B1737-39	56544.59	0.512260	158.50	204.00	40	28
56	B1740-13	56544.61	0.405376	116.30	-	33	32
57	B1740-31	56544.64	2.414876	193.05	-215.00	90	8
58	B1742-30	56768.97	0.367405	88.37	101.00	29	28
59	J1750-3503	56547.52	0.684079	189.35	173.00	90	7
60	B1756-22	56769.02	0.460942	177.16	6.00	29	20
61	B1758-03	56547.58	0.921577	120.37	32.00	27	39
62	B1804-12	56543.50	0.522668	122.41	-	49	34
63	B1804-08	56386.84	0.163712	112.38	166.00	22	62
64	B1804-27	56652.43	0.827780	312.98	-47.00	45	19
65	J1808-0813	56653.37	0.876040	151.27	77.00	19	12
66	B1813-26	56543.68	0.592942	128.12	90.00	47	20
67	J1817-3837	56543.71	0.384523	102.85	102.90	54	10
68	B1818-04	56653.45	0.598082	84.43	69.20	29	165
69	B1819-22	56386.88	1.874079	121.20	124.00	31	53
70	J1823-0154	56543.75	0.759845	135.87	153.00	34	16
71	B1821-19	56392.86	0.189320	224.65	-303.00	31	17
72	B1823-11	56548.47	2.093333	320.58	229.00	120	8
73	B1826-17	56392.90	0.307106	217.11	306.00	24	19
74	B1829-08	56545.48	0.647389	300.87	39.00	90	8
75	B1831-03	56392.94	0.686665	234.54	-41.00	30	70
76	J1835-1106	56392.96	0.165904	132.68	42.00	24	12

Table 1—Continued

Sr. No.	Pulsar Name	MJD (days)	Period (secs)	DM (cm^{-3} pc)	RM (Catalog) rad m^2	Duration of Observation (minutes)	SNR (peak)
77	B1834-10	56545.56	0.562769	316.98	-1000.00	85	6
78	B1839-04	56747.93	1.839770	195.98	326.00	190	11
79	B1841-04	56545.62	0.991115	123.16	7.00	82	12
80	B1844-04	56408.90	0.597752	141.98	117.00	31	30
81	B1845-01	56408.92	0.659379	159.53	580.00	31	10
82	J1848-1414	56545.68	0.297796	134.47	-	73	6
83	B1846-06	56545.73	1.451478	148.17	-35.00	38	24
84	B1852+10	56545.76	0.573240	207.20	502.00	38	7
85	B1851-14	56545.79	1.146701	130.40	103.00	32	30
86	B1859+01	56545.81	0.288244	105.39	-122.00	27	51
87	B1859+03	56922.67	0.655511	402.08	-237.40	119	25
88	B1859+07	56777.92	0.643948	252.81	282.00	179	6
89	B1900+05	56769.04	0.746522	177.49	-113.00	22	8
90	B1900+06	56748.09	0.673447	502.90	-	239	11
91	B1900+01	56408.97	0.729244	245.17	72.30	31	26
92	B1900-06	56546.56	0.431925	195.61	203.00	60	56
93	J1904+0004	56546.61	0.139536	233.61	289.00	90	9
94	J1904-1224	56546.75	0.750875	118.23	-	33	24
95	B1902-01	56771.03	0.643126	229.13	-	25	12
96	J1908+0500	56547.67	0.291045	201.42	-	90	5
97	B1907+02	56539.74	0.989907	171.73	-	16	68
98	B1907+10	56539.75	0.283661	149.98	540.00	10	41
99	B1907-03	56539.77	0.504645	205.53	152.00	30	38
100	J1910+0714	56547.76	2.712634	124.06	-	44	16
101	B1907+12	56539.80	1.441841	258.64	978.00	50	7
102	B1911-04	56752.00	0.825861	89.39	4.40	18	519
103	B1911+13	56548.62	0.521509	145.05	435.00	120	22
104	B1914+13	56540.75	0.281863	237.01	280.00	30	9
105	B1915+13	56752.03	0.194620	94.54	233.00	37	233
106	B1918+19	56540.78	0.821082	153.85	160.00	30	19
107	B1920+21	56541.71	1.077988	217.09	282.00	19	70
108	B1922+20	56549.60	0.237807	213.00	-	90	5
109	B1923+04	56541.79	1.074155	102.24	0.00	23	42
110	B1924+14	56549.68	1.325011	211.41	-	120	8
111	B1924+16	56542.73	0.579868	176.88	320.00	57	12
112	B1929+20	56544.78	0.268235	211.15	10.00	28	14
113	B1930+22	56544.80	0.144503	219.20	173.00	32	29
114	B1933+16	56409.04	0.358716	158.52	-10.20	31	279

Table 1—Continued

Sr. No.	Pulsar Name	MJD (days)	Period (secs)	DM (cm^{-3} pc)	RM (Catalog) rad m^2	Duration of Observation (minutes)	SNR (peak)
115	B1944+22	56553.62	1.334527	140.00	2.00	116	12
116	B1946+35	56410.85	0.717274	129.07	116.00	31	89
117	B2000+32	56551.55	0.696853	142.21	-	120	13
118	B2002+31	56544.84	2.111386	234.82	30.00	38	48
119	B2011+38	56551.63	0.230206	238.22	78.00	65	8
120	B2027+37	56542.86	1.216841	190.66	-	60	26
121	B2053+36	56752.19	0.221499	97.31	-68.00	13	19
122	B2106+44	56410.94	0.414852	139.83	-146.00	31	13
123	B2111+46	56410.96	1.014643	141.26	-224.00	31	109
124	B2319+60	56752.32	2.256526	94.59	-230.00	50	11

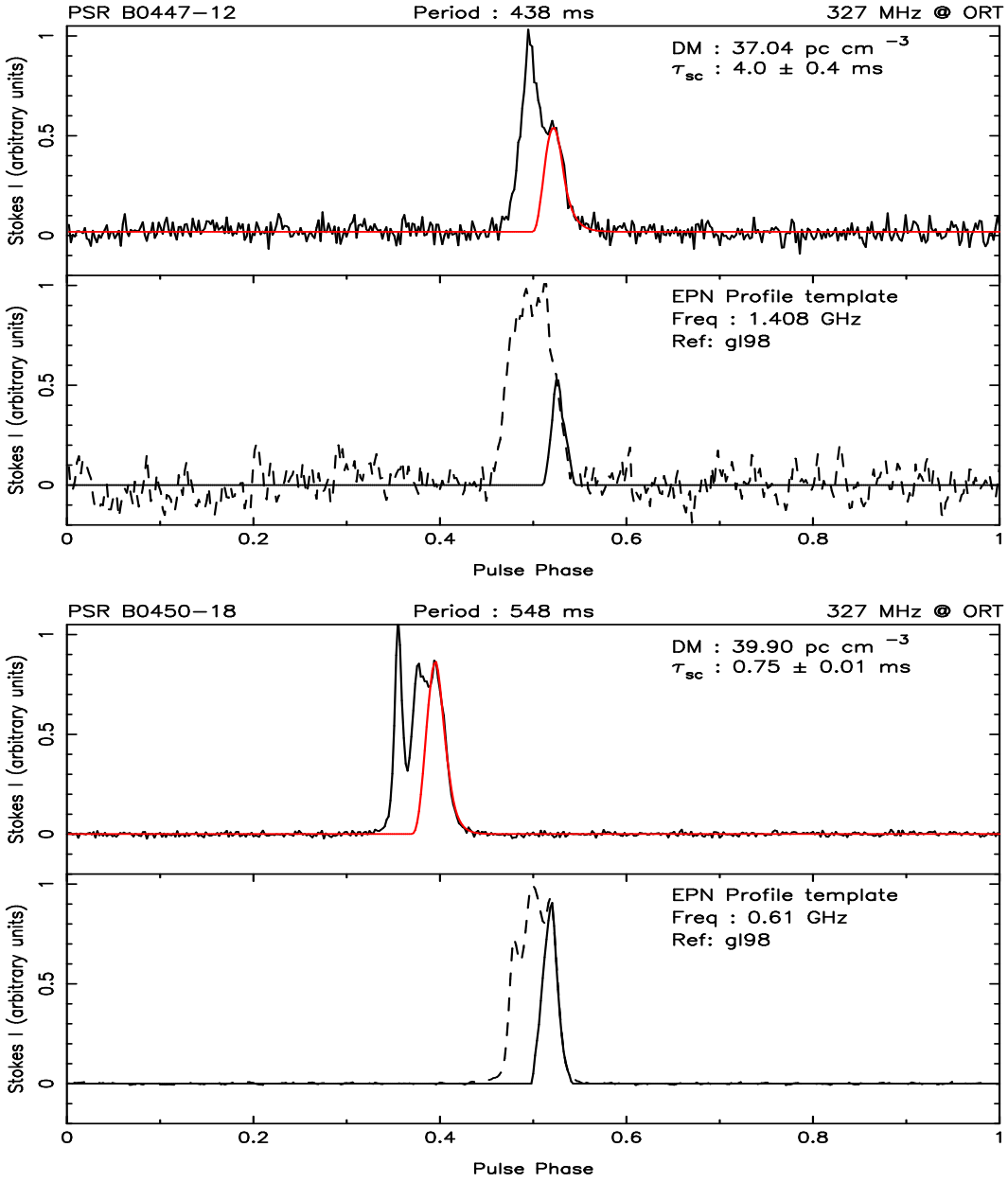

Fig. 1.— Each plot consists of two panels, and the plot title gives the pulsar name, pulsar period, observing frequency and observatory name (ORT). **Top panel** shows the observed profile as *solid black line* and the best fit model as *solid red line*. The legend in the top right gives the DM of the pulsar and the estimated τ_{sc} with error bars. **Bottom panel** shows the high frequency template profile (*solid black line*) that has been used to fit the scattered profile as explained in section 2.2 of the paper. Wherever possible, we have used the high frequency profile from the EPN database (http://www.jb.man.ac.uk/research/pulsar/Resources/epn/browser.html) as templates for the fitting purpose. For pulsars, whose high frequency profiles were not available at EPN database, we created the template profile using the width estimates available in the literature. For some multi-component pulsars, only part of the profile is fitted to get a reliable estimate of the τ_{sc}. In such cases, the black dashed line shows the actual EPN profile and black solid line shows the template profile used for fitting (see main paper for details). The details of the reference IDs given in each plot are provided in the bibliography at the end of this supplementary material.

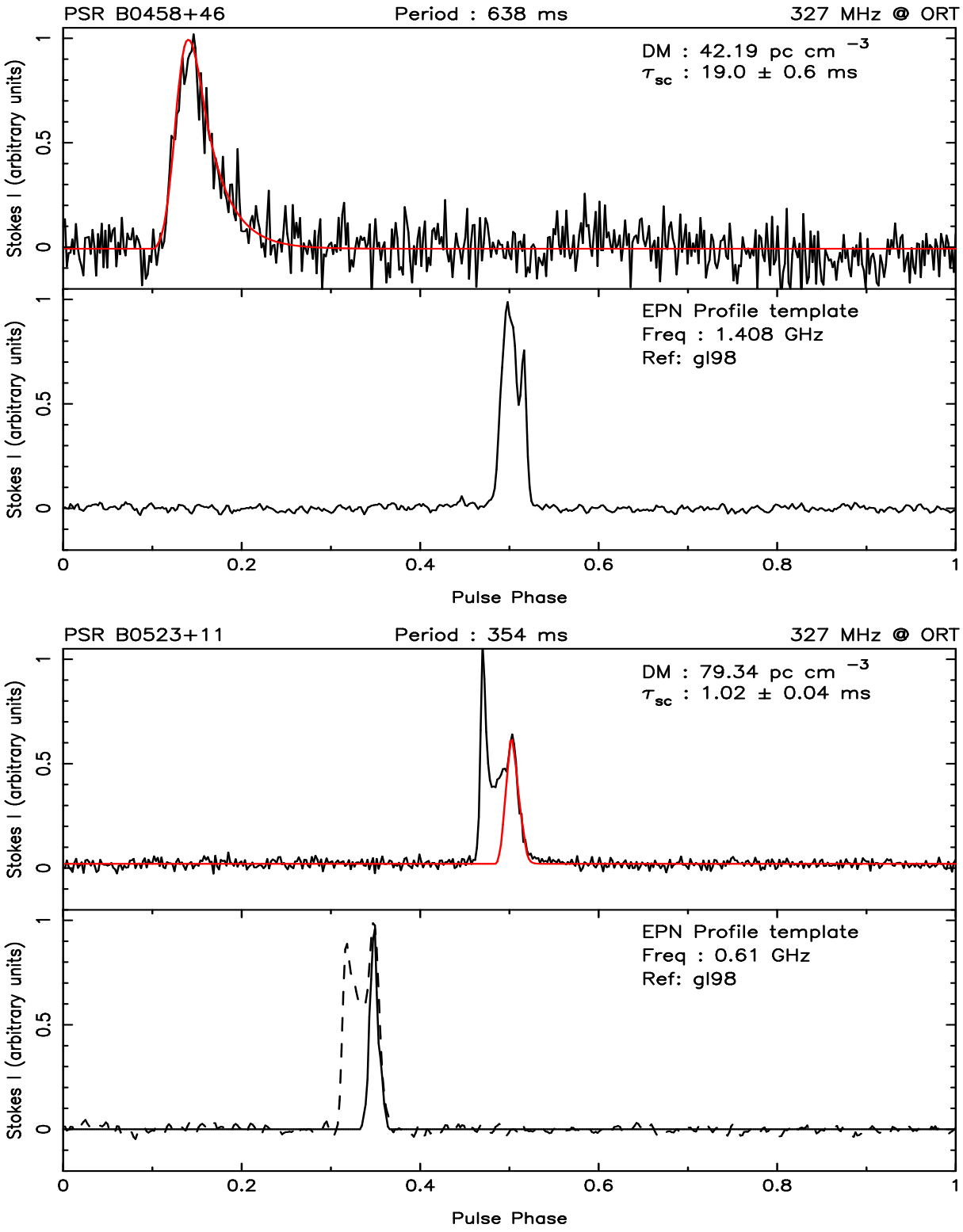

Fig. 2.— Same as in Fig. 1

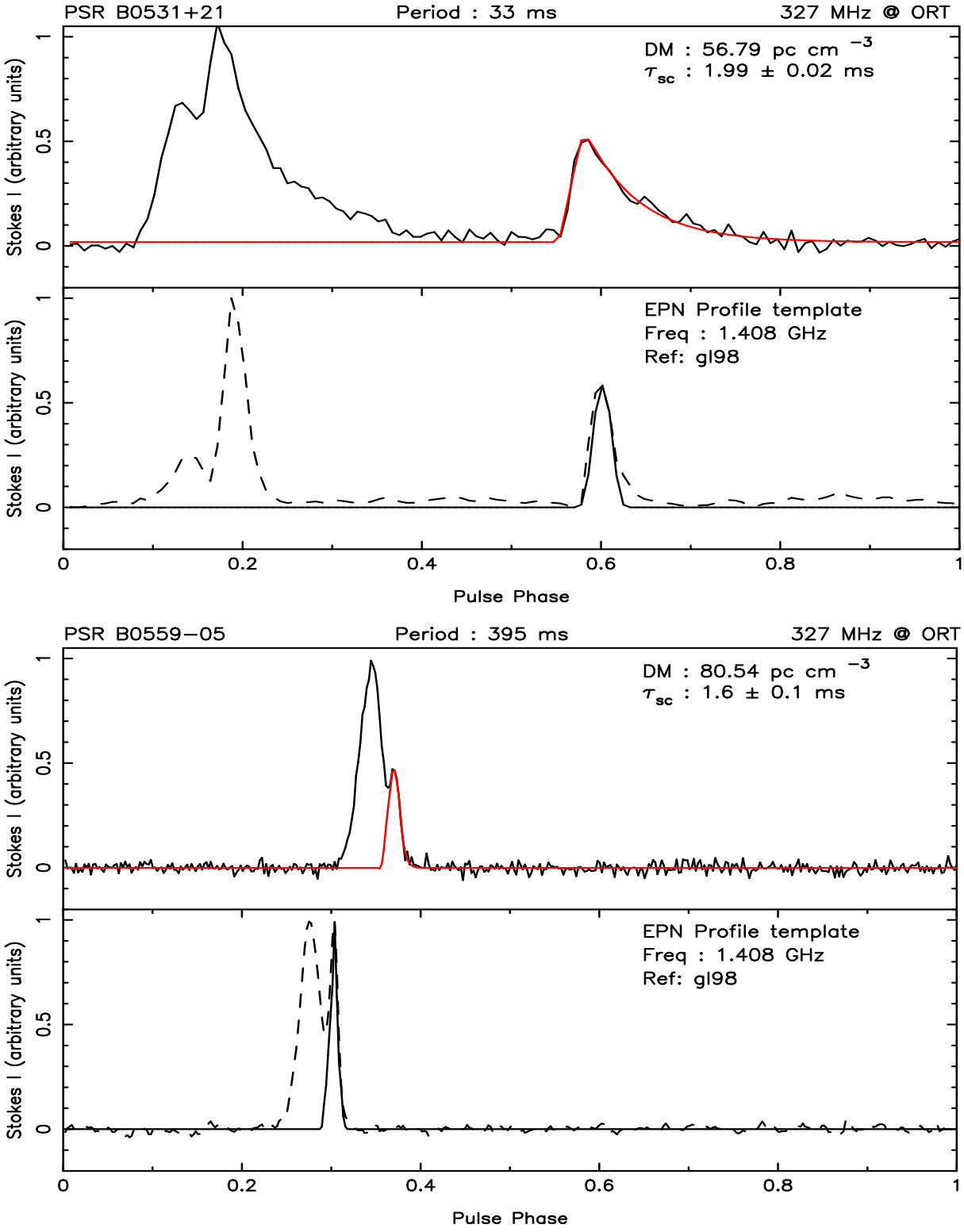

Fig. 3.— Same as in Fig. 1

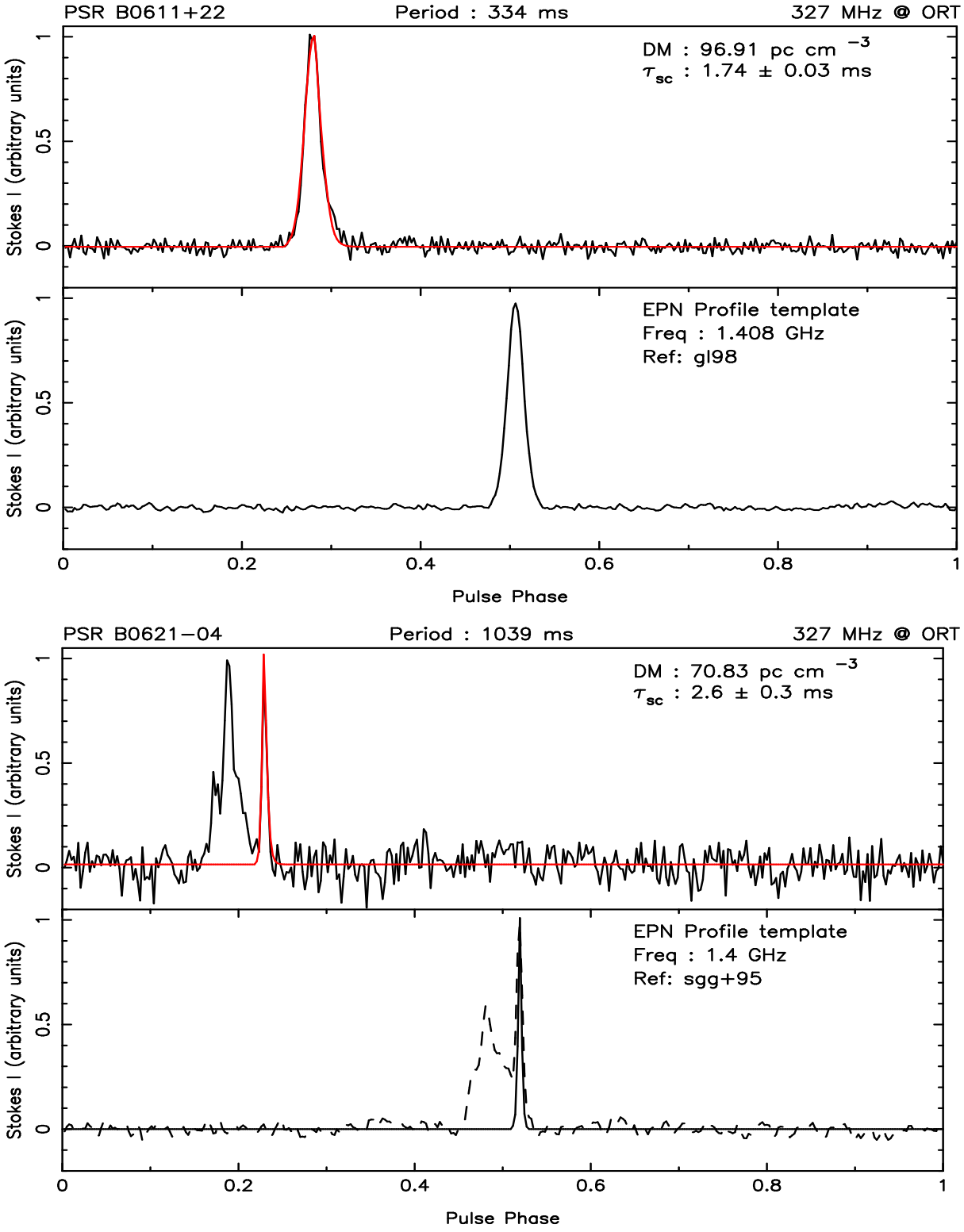

Fig. 4.— Same as in Fig. 1

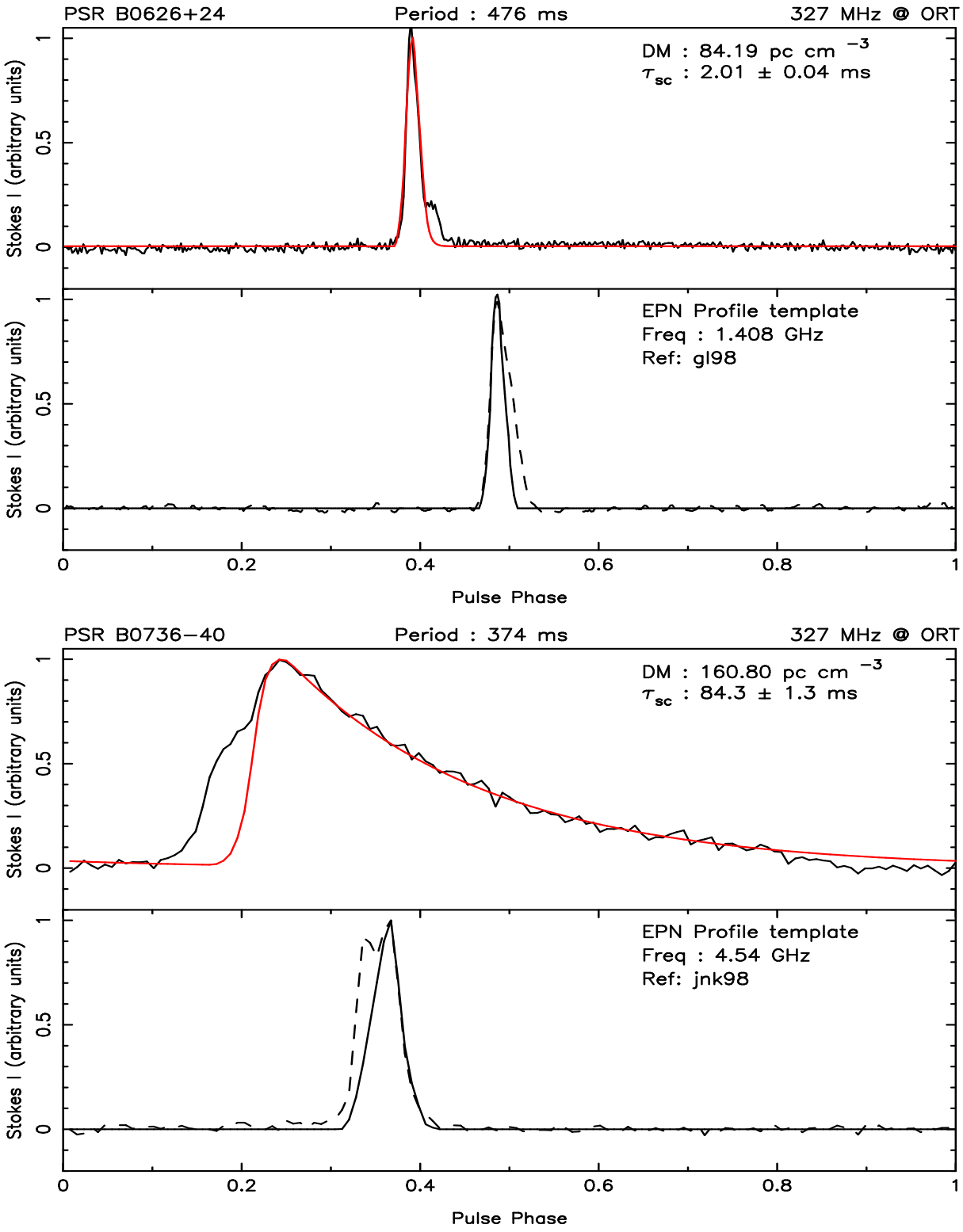

Fig. 5.— Same as in Fig. 1

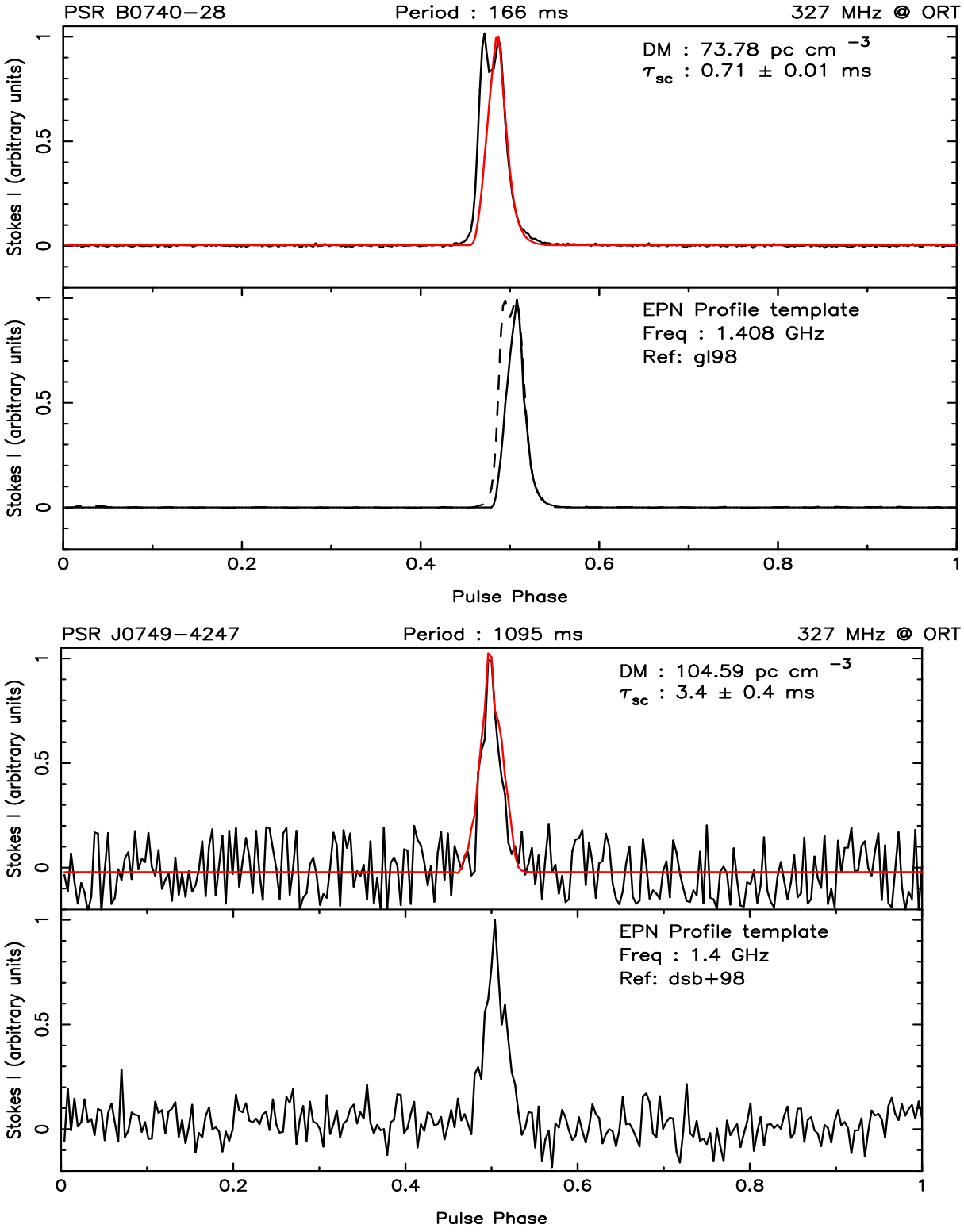

Fig. 6.— Same as in Fig. 1

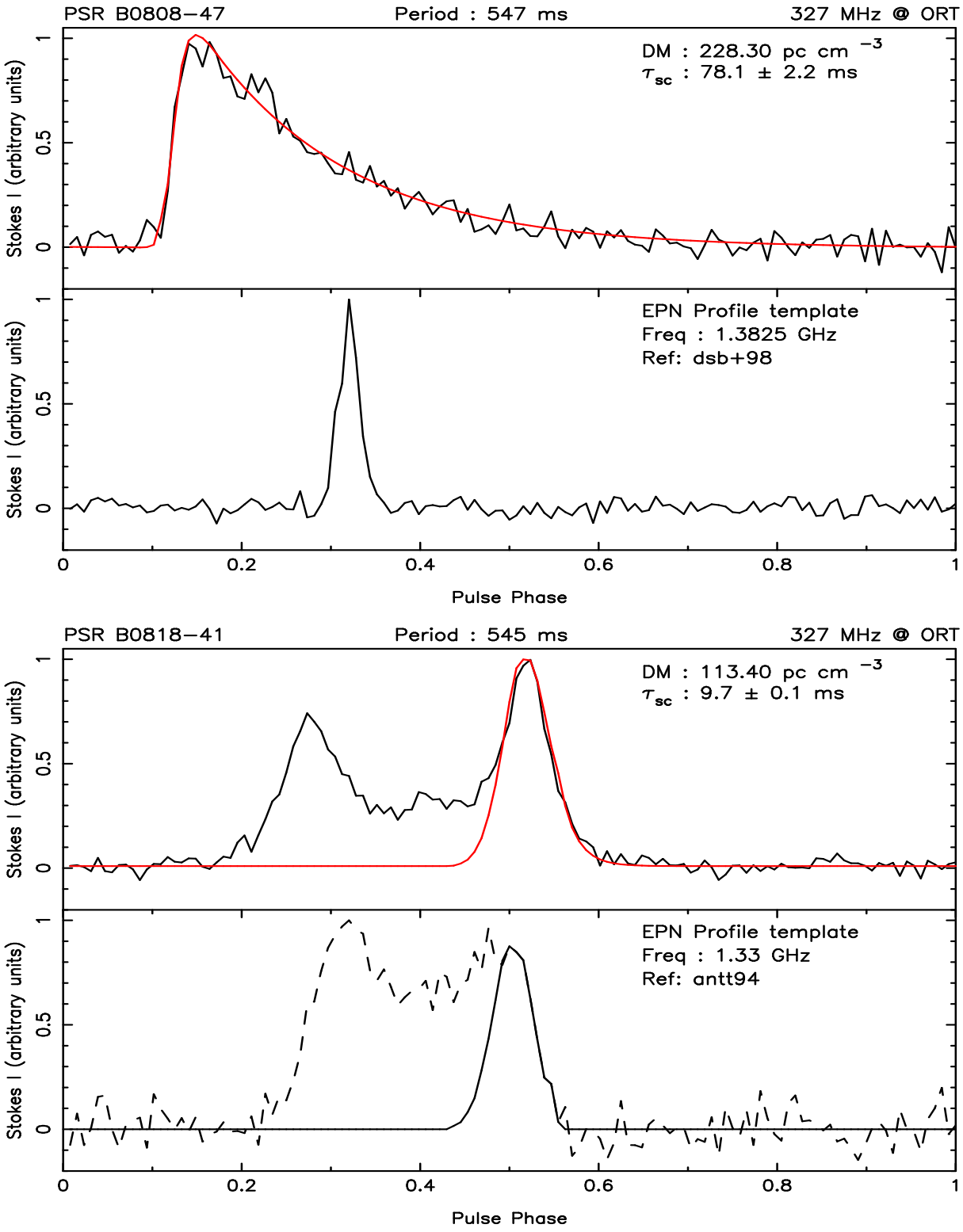

Fig. 7.— Same as in Fig. 1

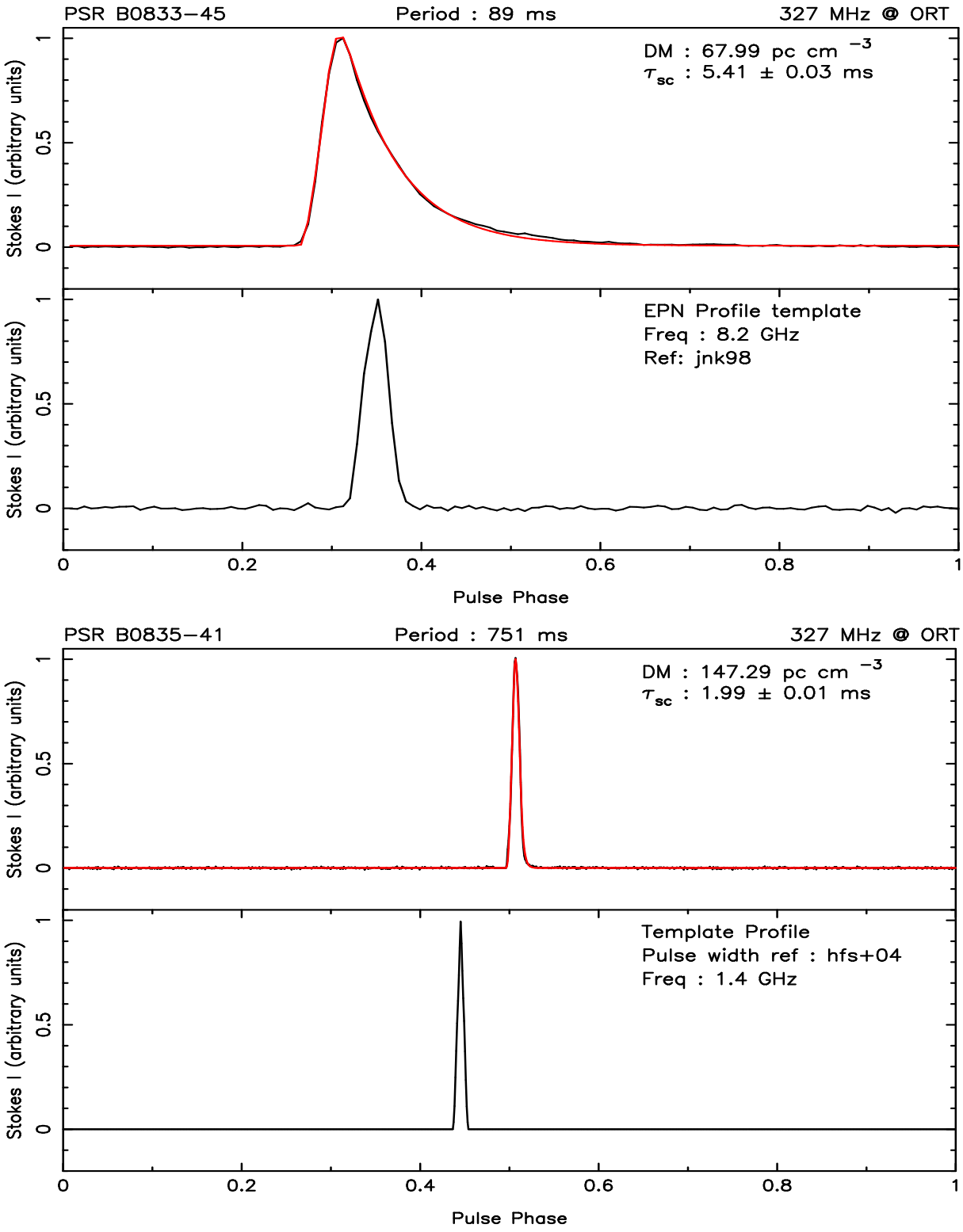

Fig. 8.— Same as in Fig. 1

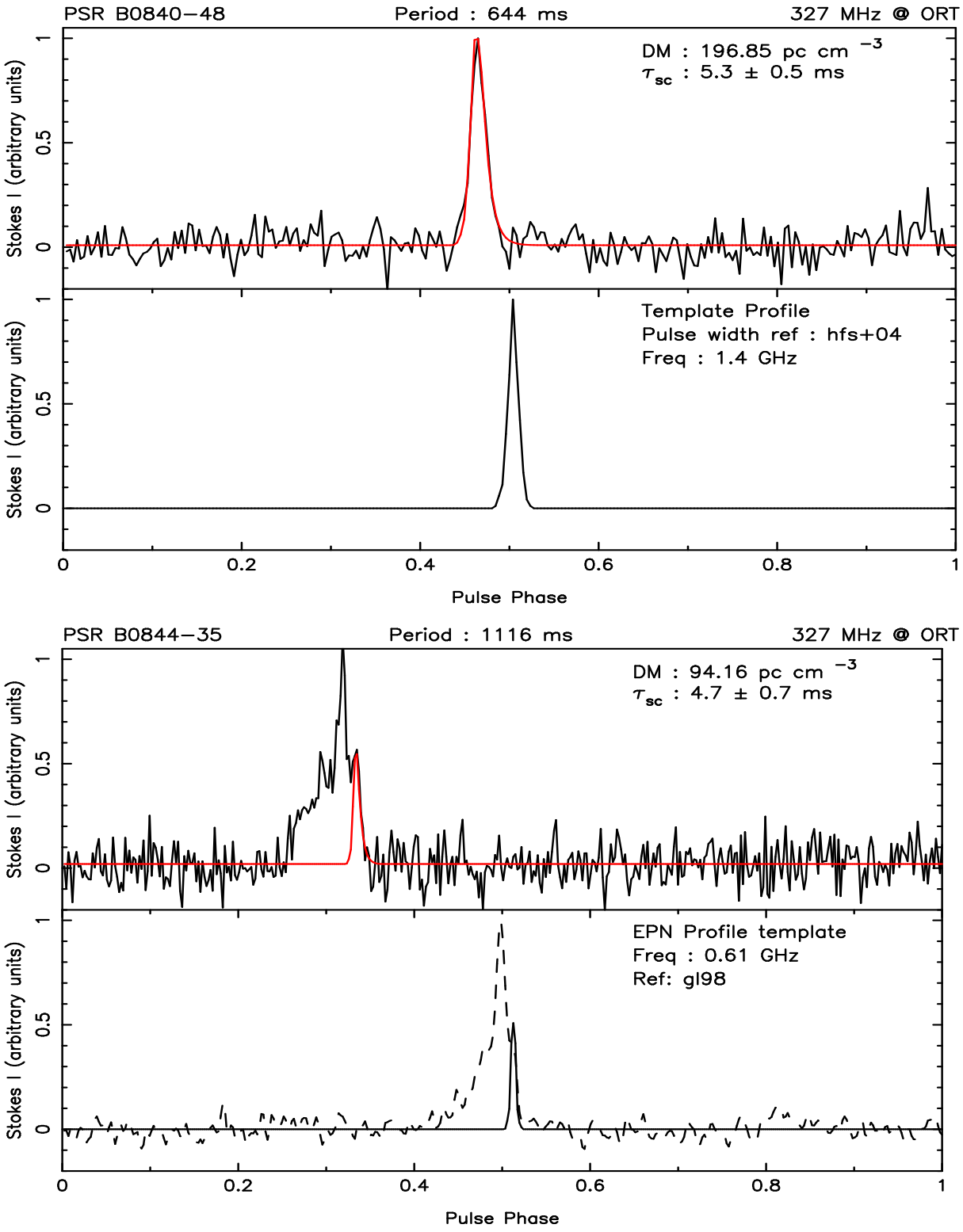

Fig. 9.— Same as in Fig. 1

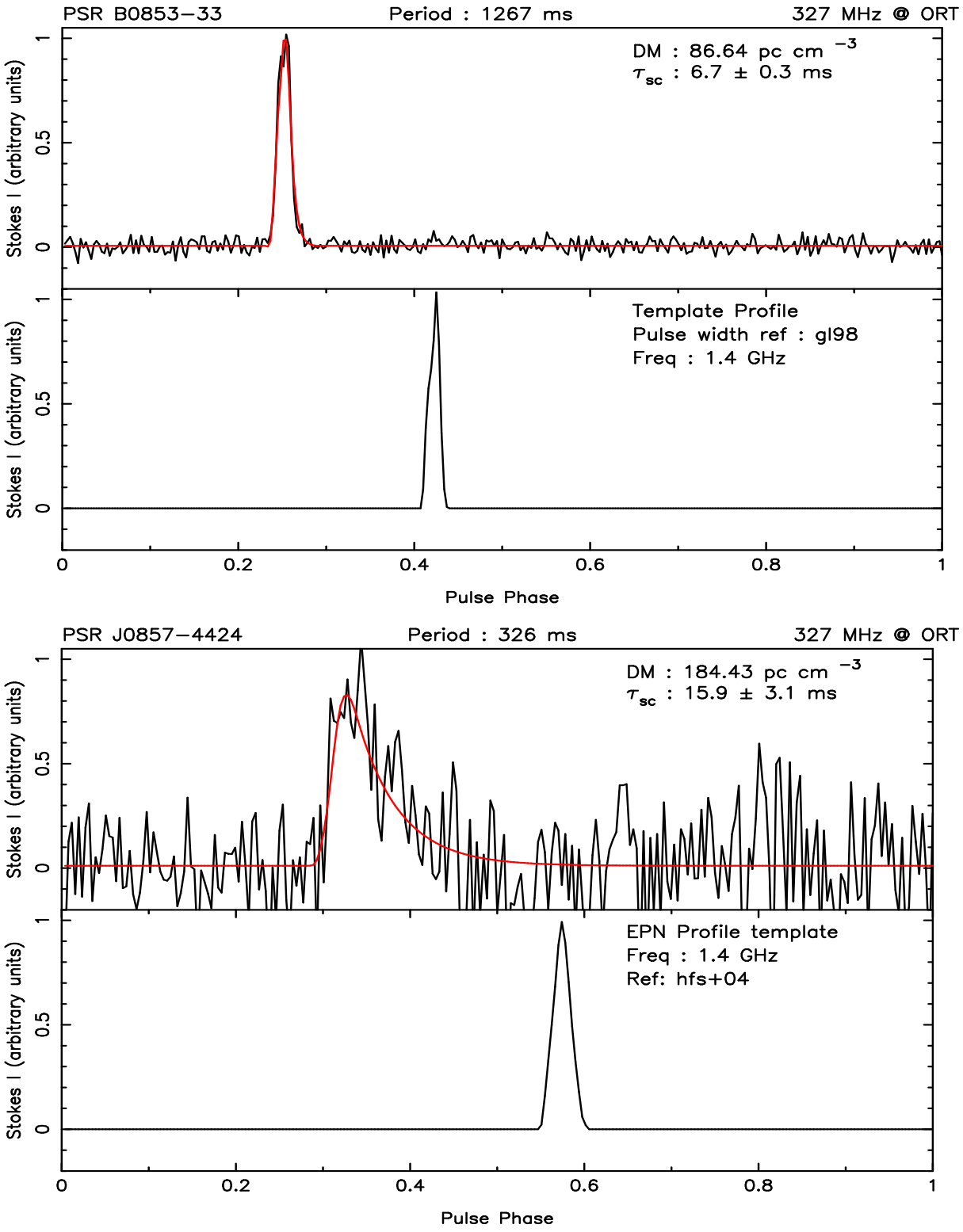

Fig. 10.— Same as in Fig. 1

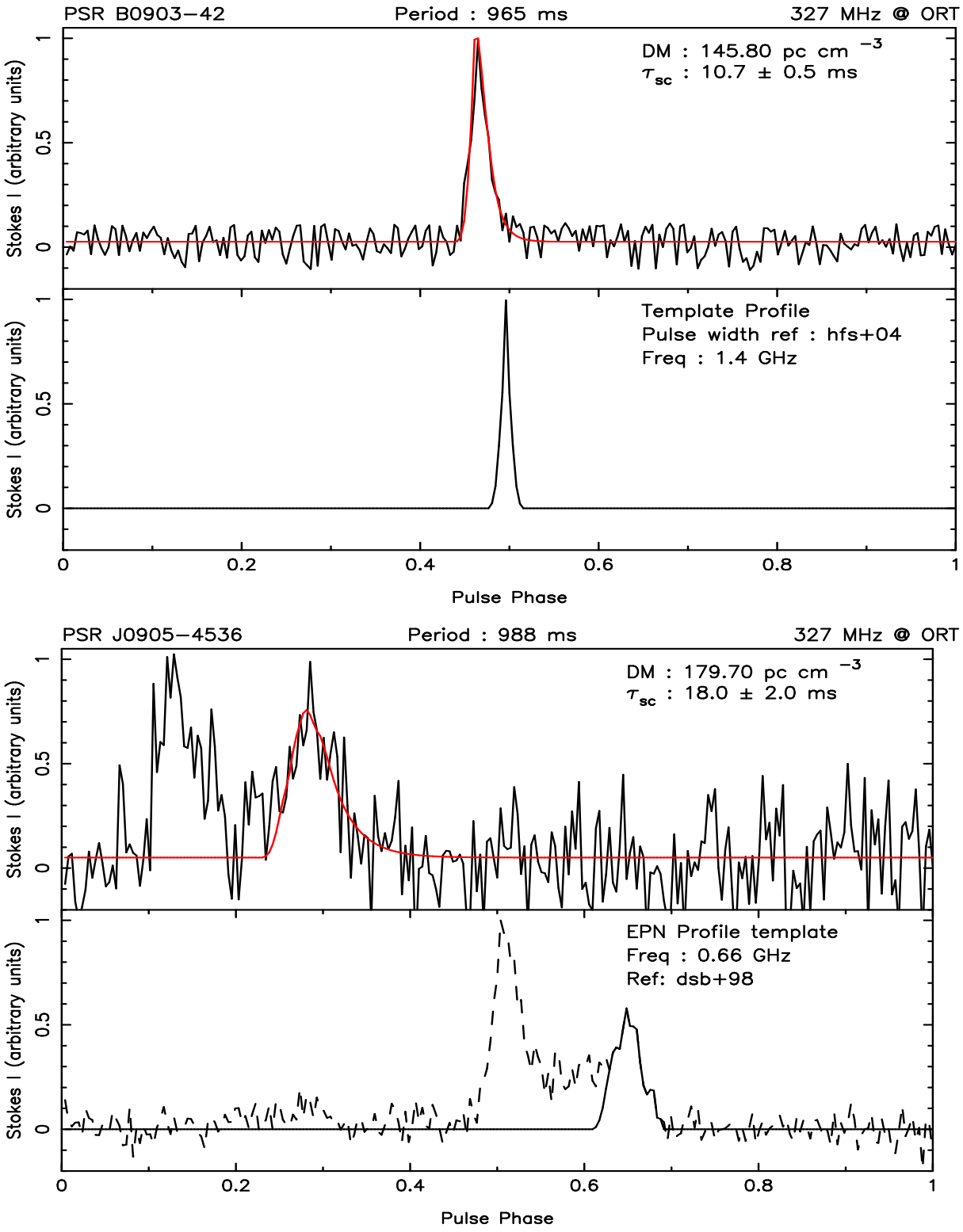

Fig. 11.— Same as in Fig. 1

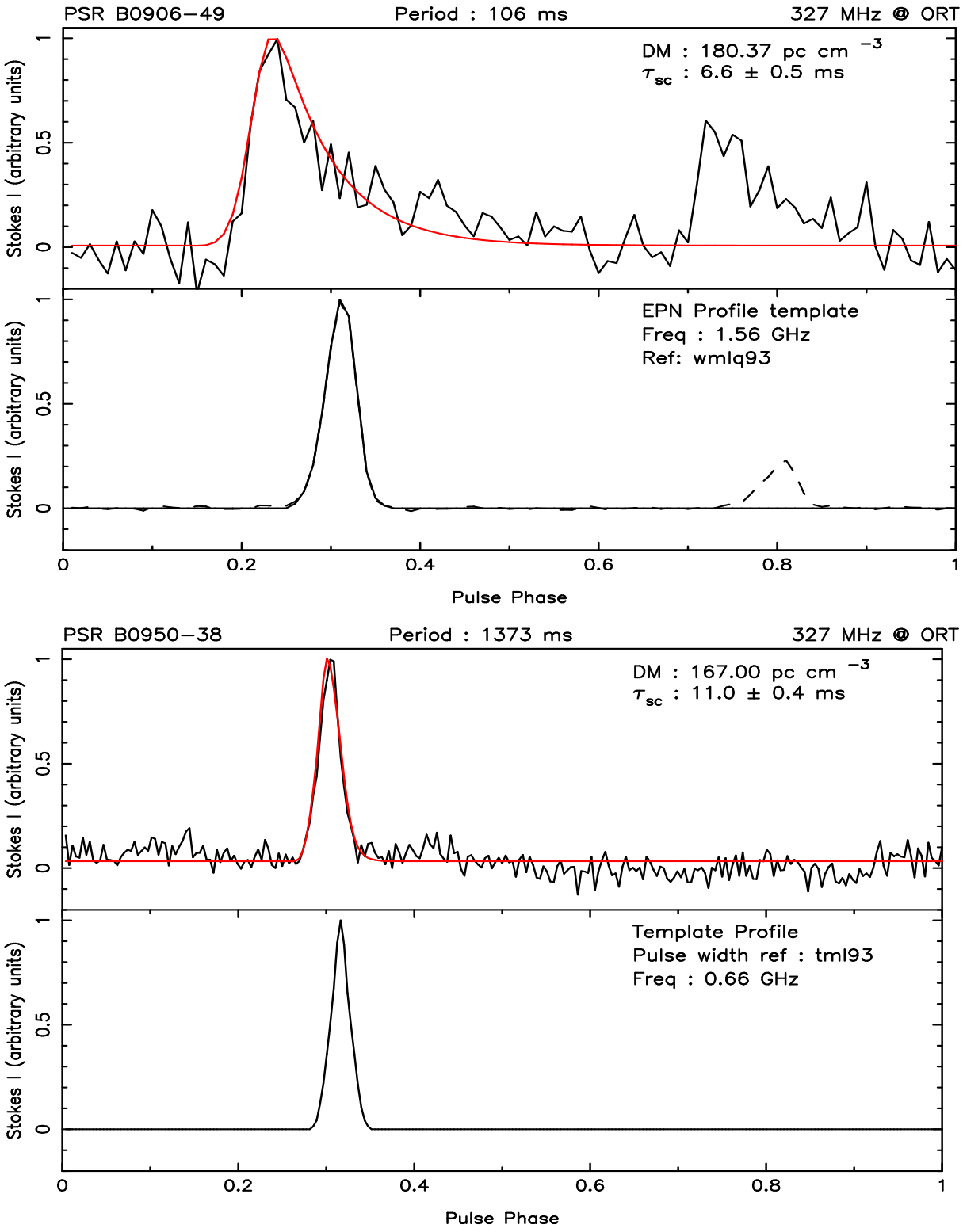

Fig. 12.— Same as in Fig. 1

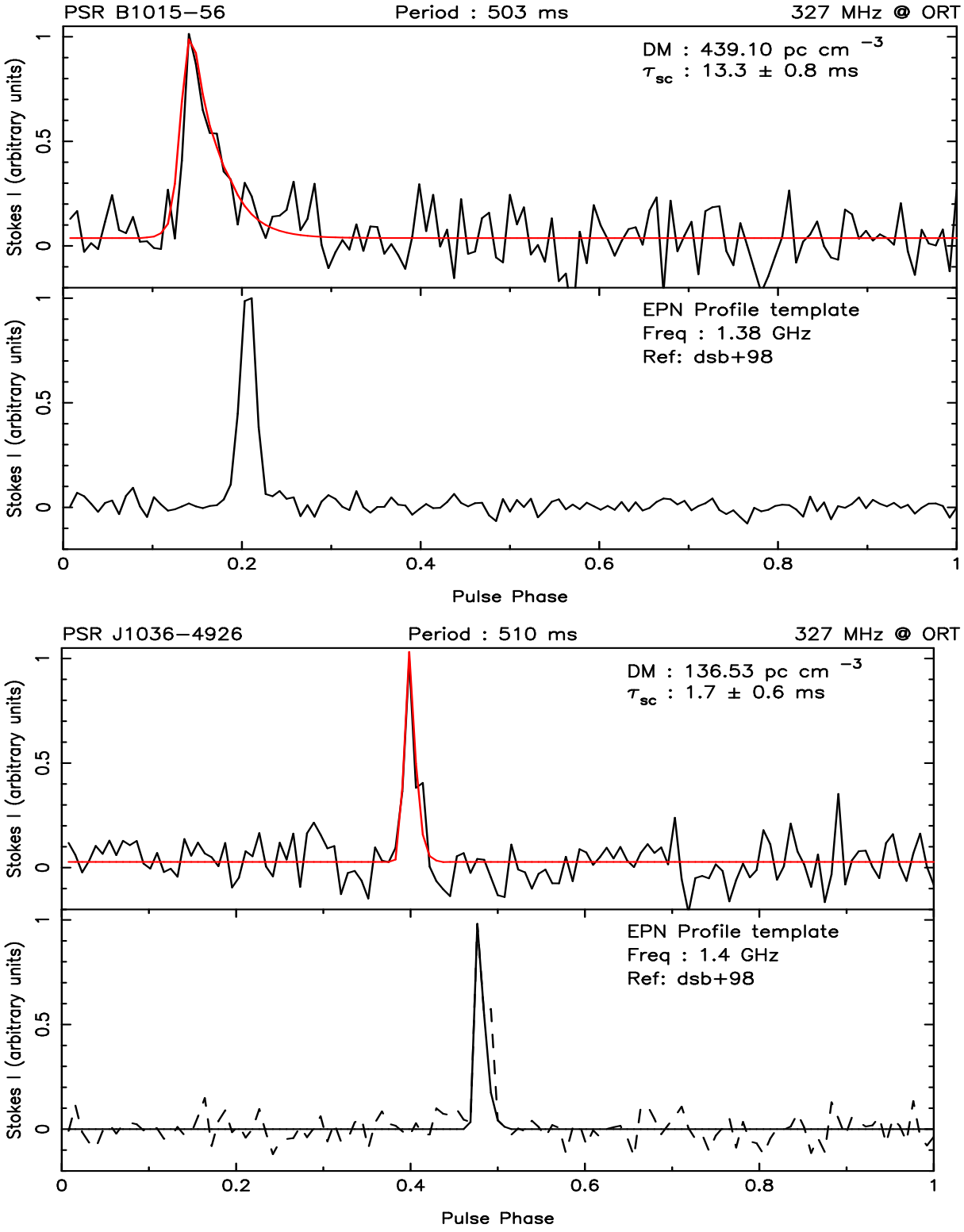

Fig. 13.— Same as in Fig. 1

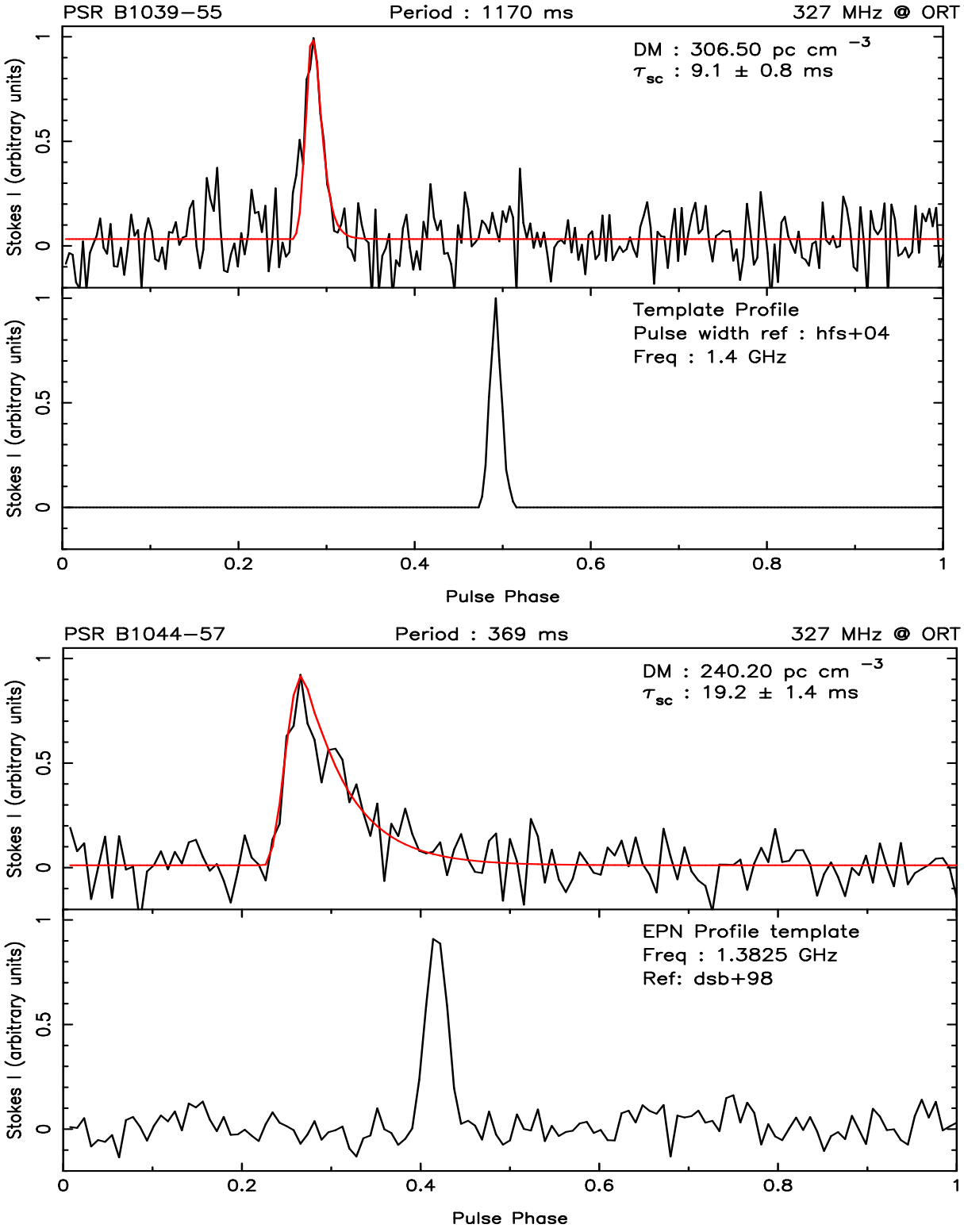

Fig. 14.— Same as in Fig. 1

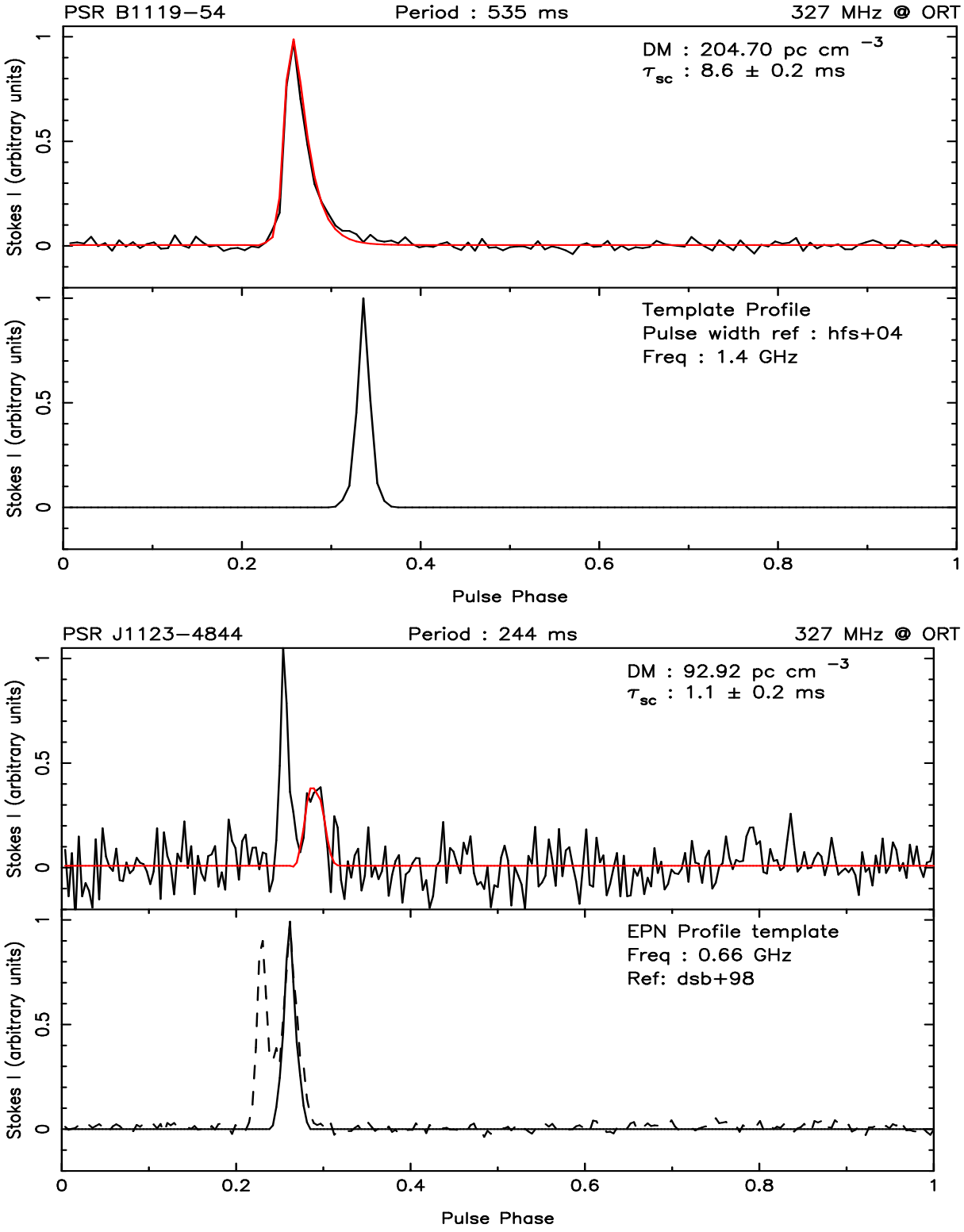

Fig. 15.— Same as in Fig. 1

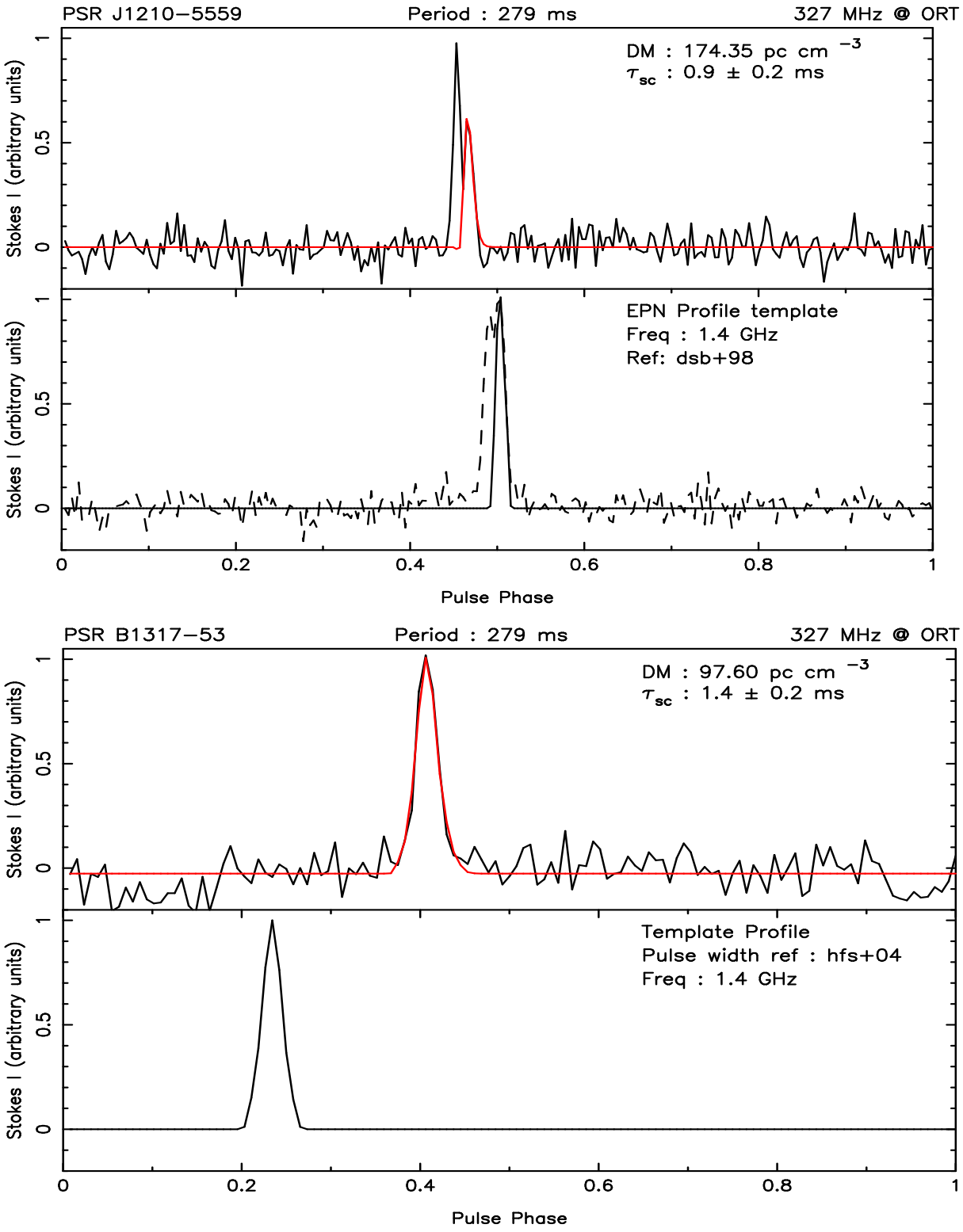

Fig. 16.— Same as in Fig. 1

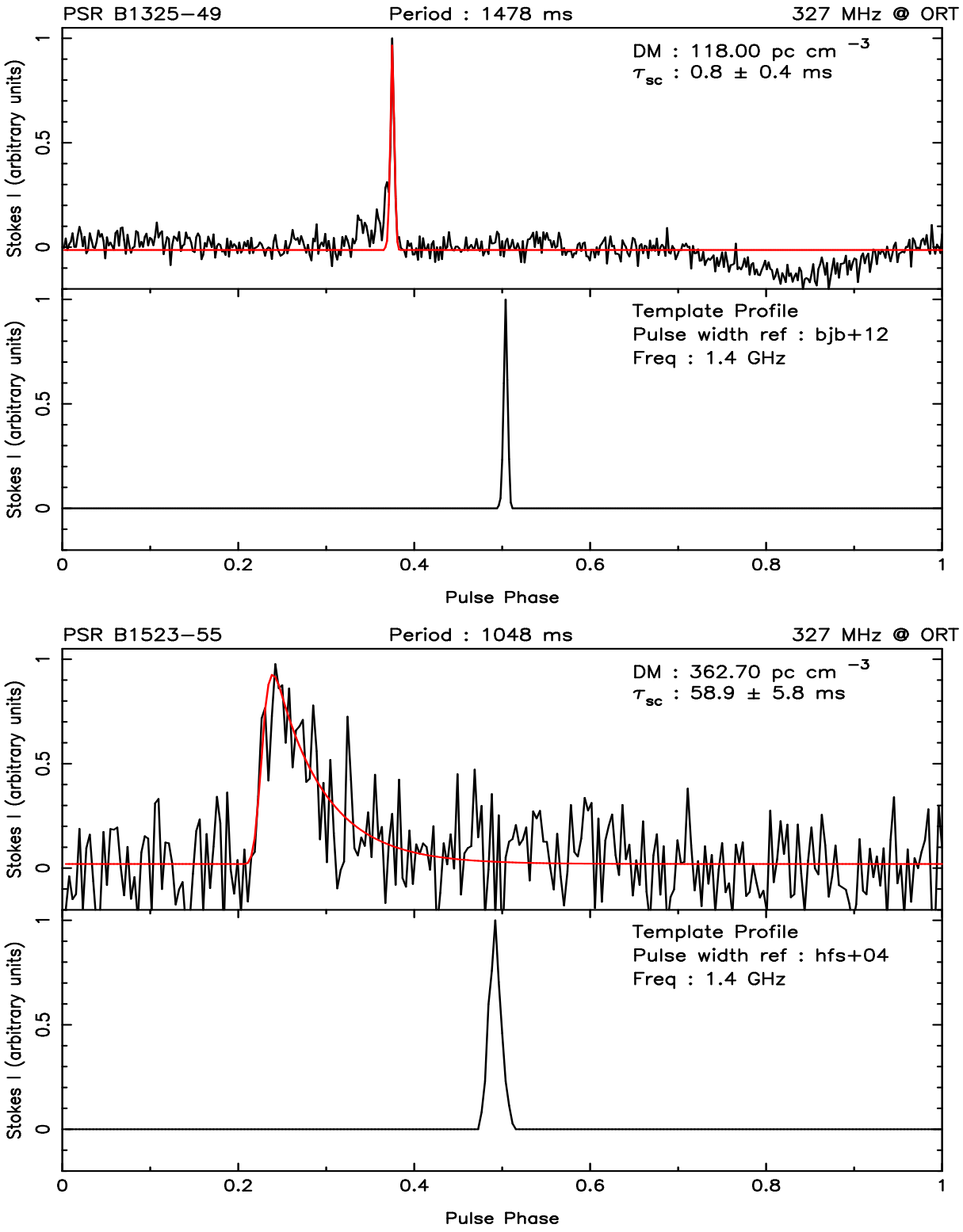

Fig. 17.— Same as in Fig. 1

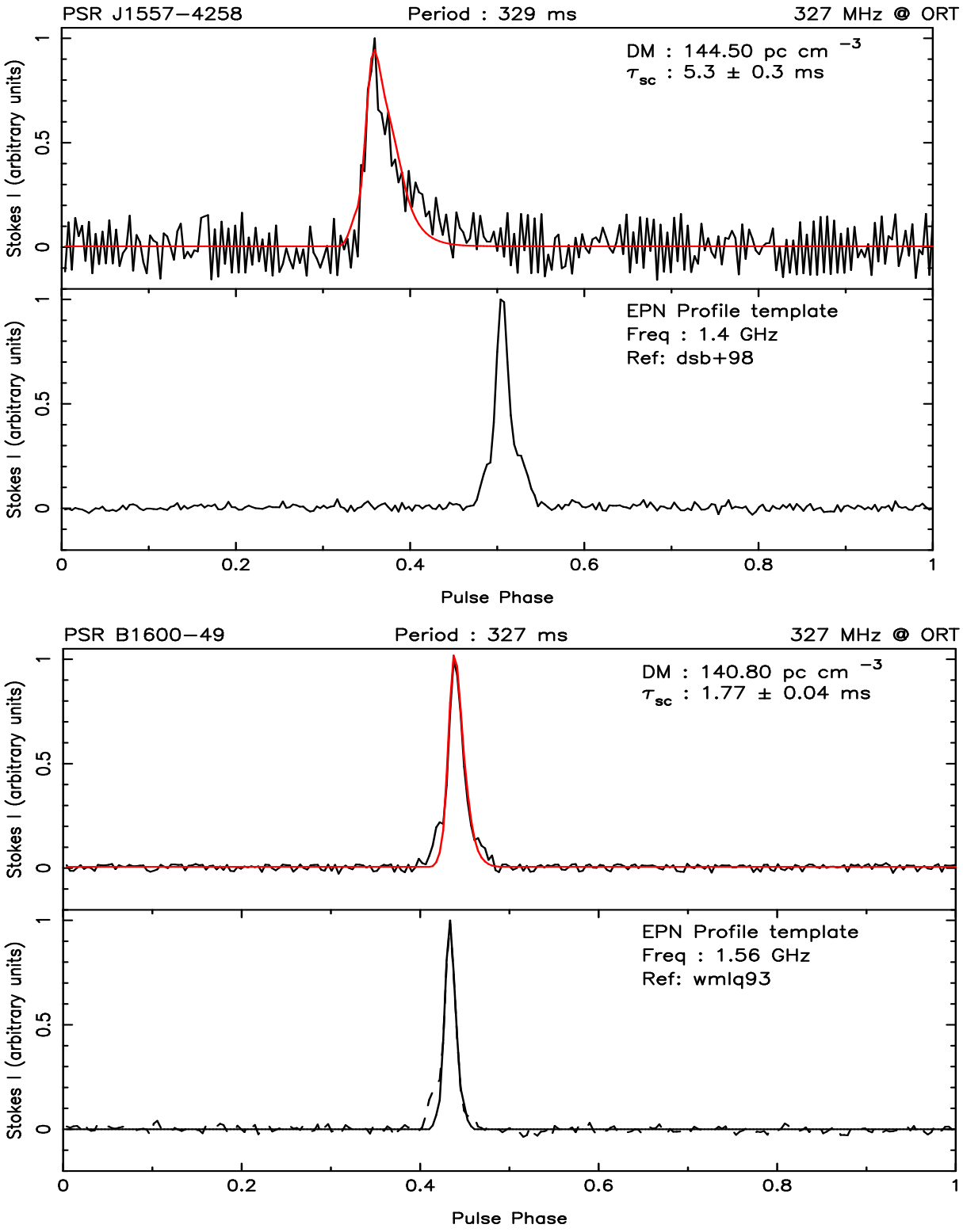

Fig. 18.— Same as in Fig. 1

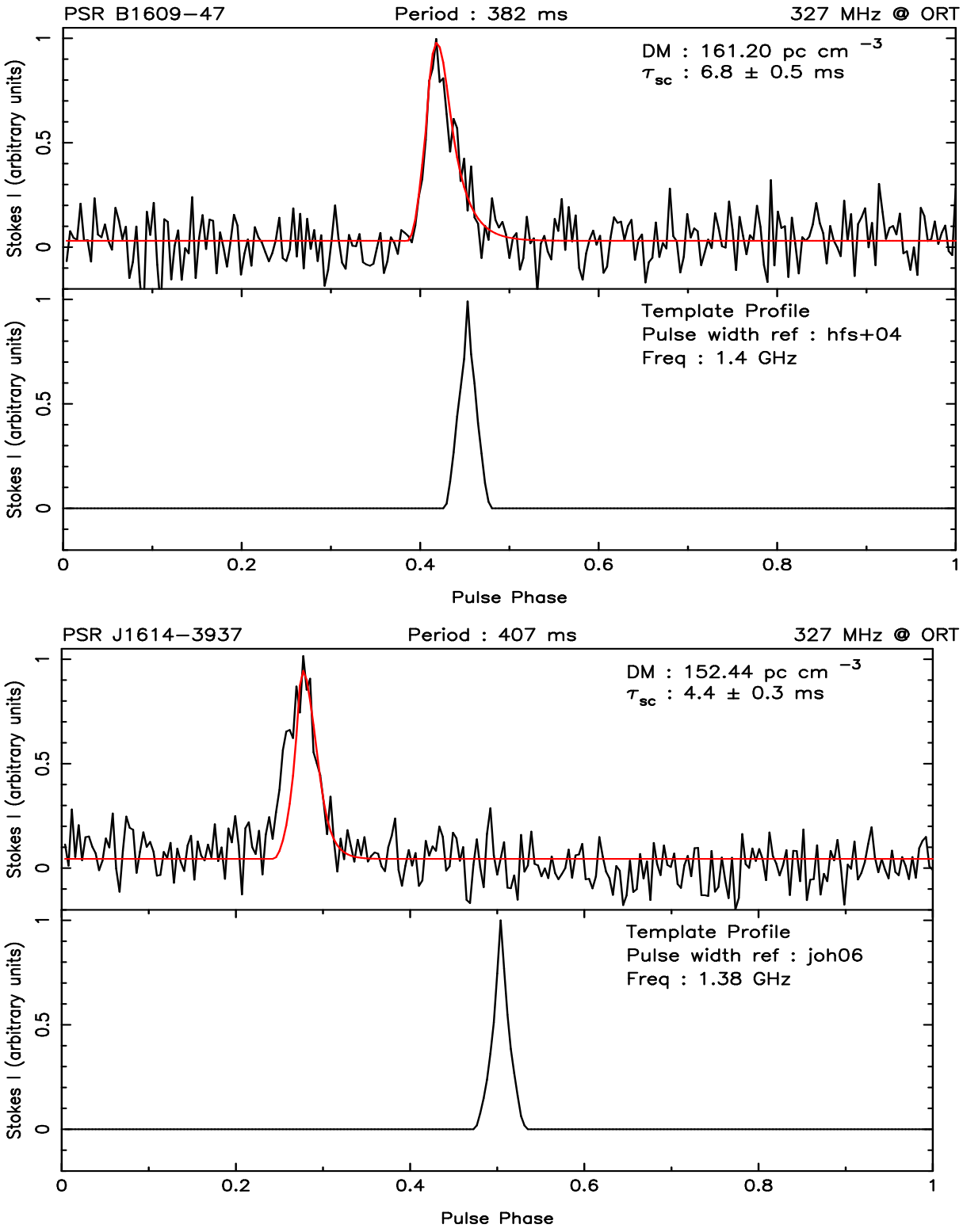

Fig. 19.— Same as in Fig. 1

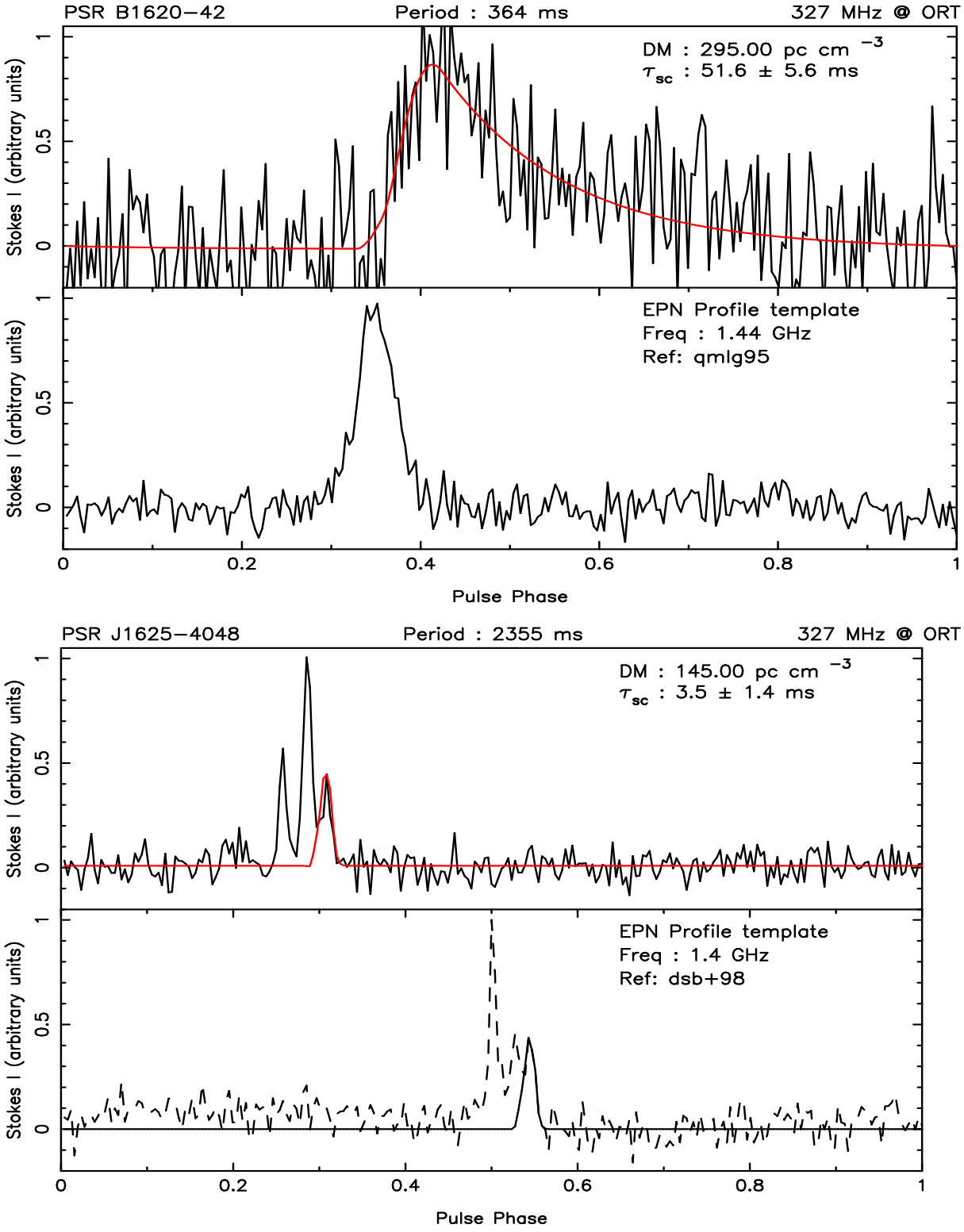

Fig. 20.— Same as in Fig. 1

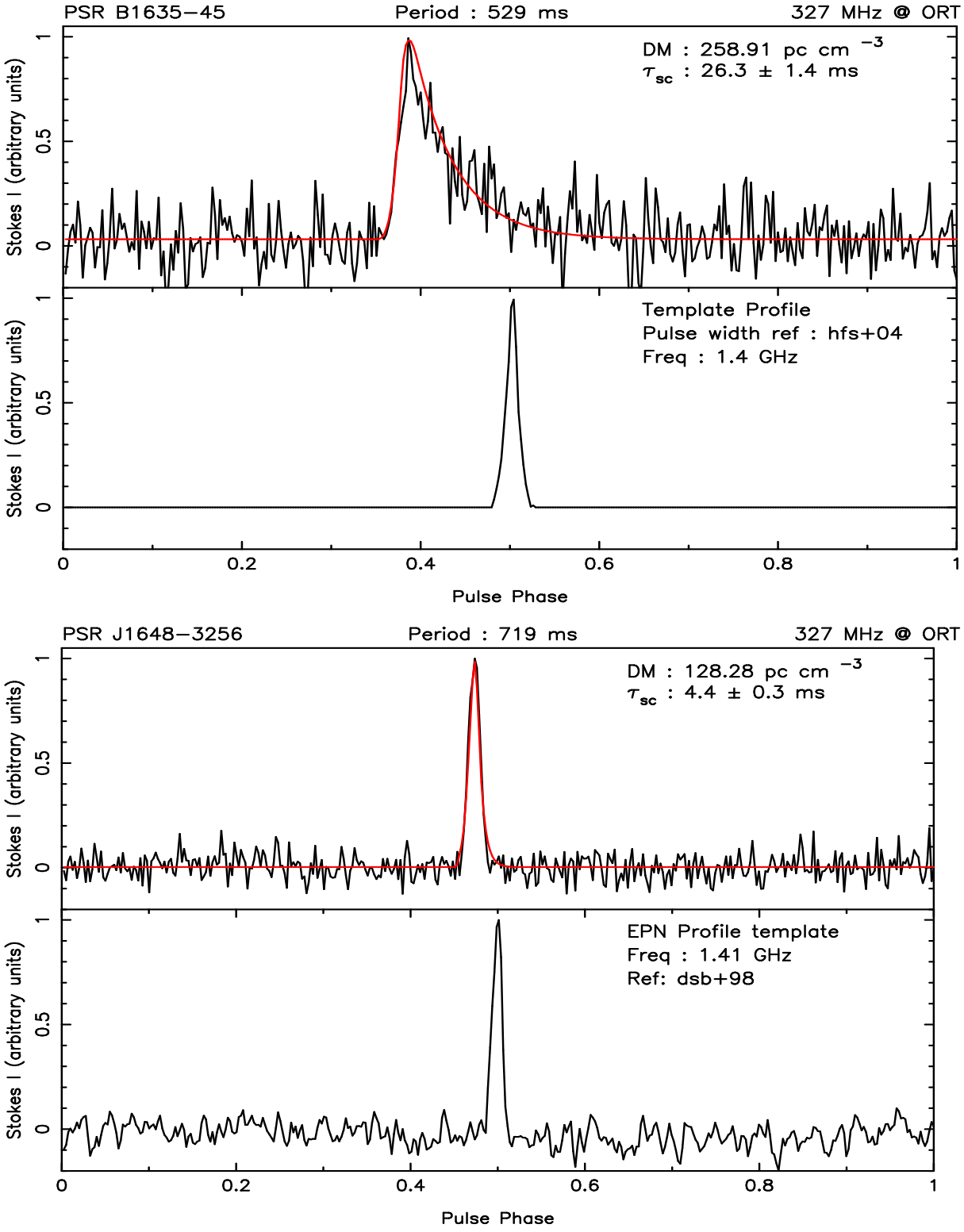

Fig. 21.— Same as in Fig. 1

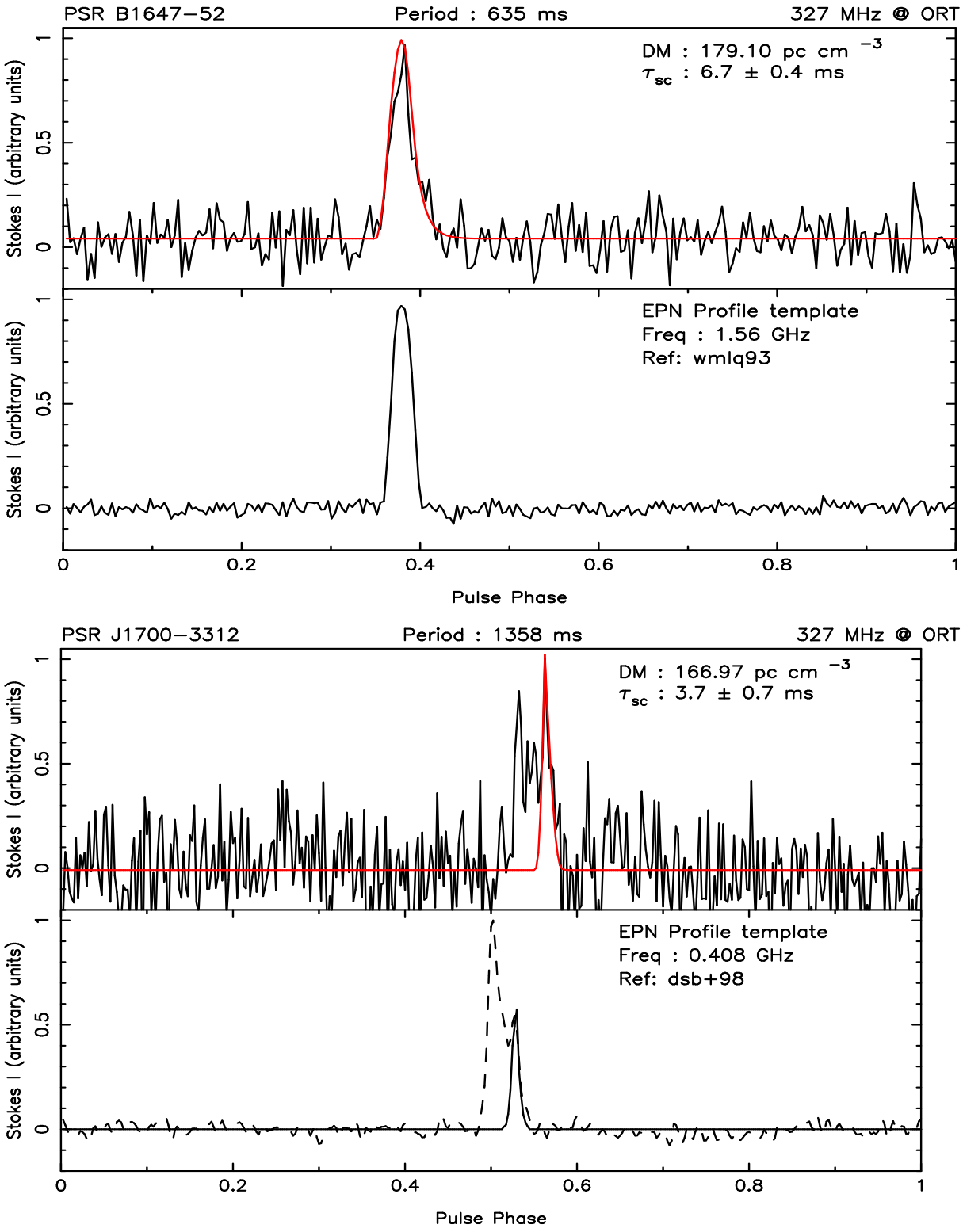

Fig. 22.— Same as in Fig. 1

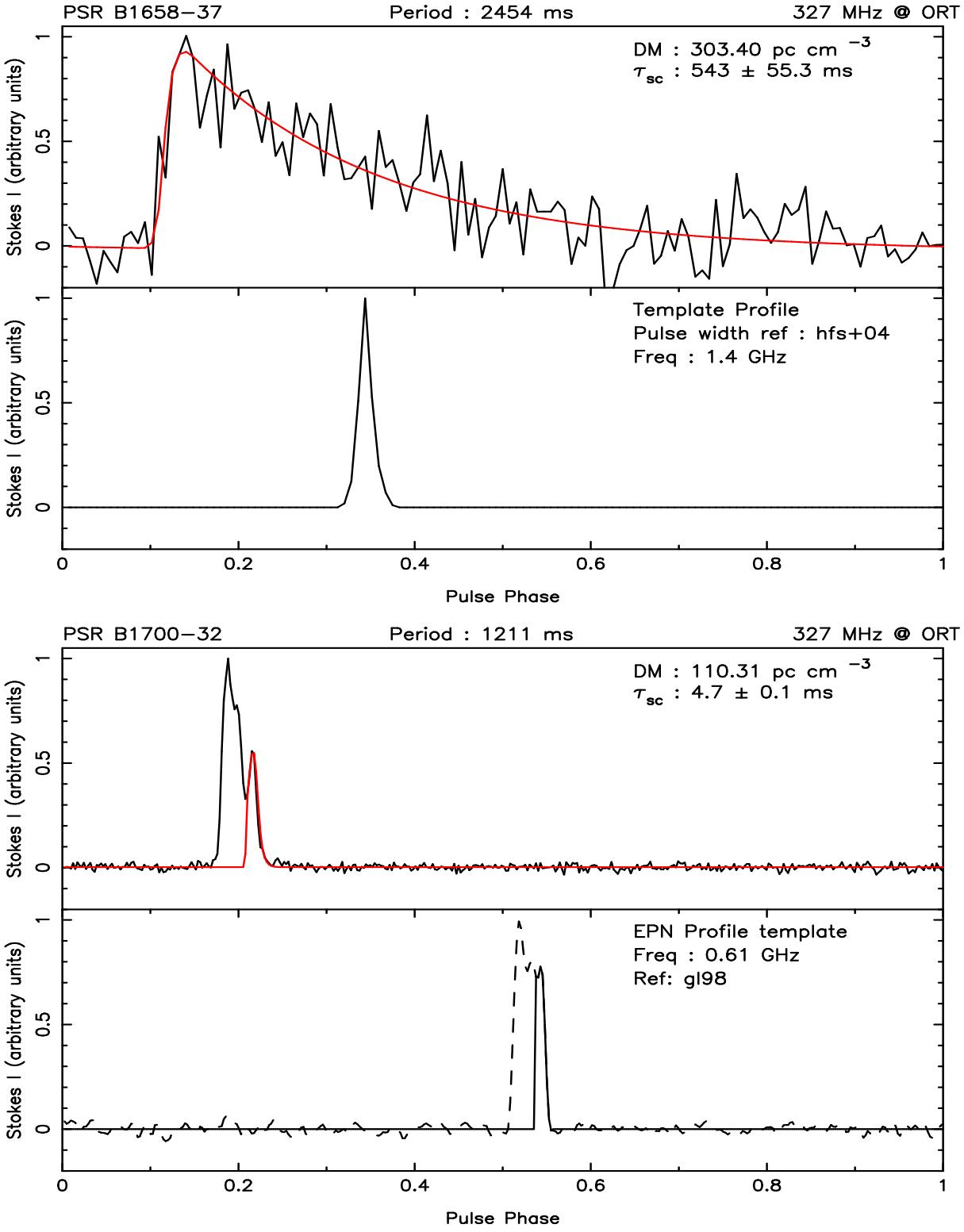

Fig. 23.— Same as in Fig. 1

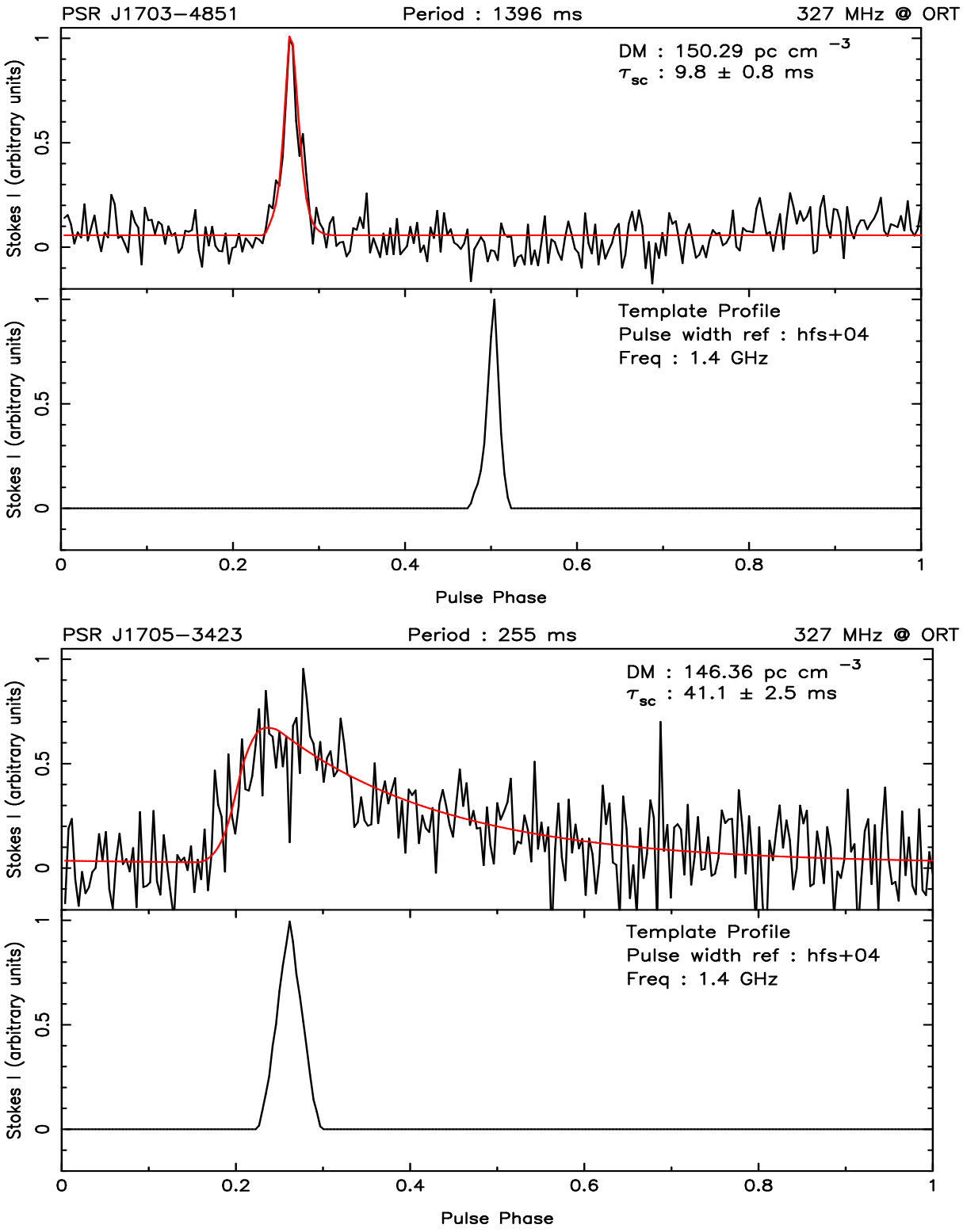

Fig. 24.— Same as in Fig. 1

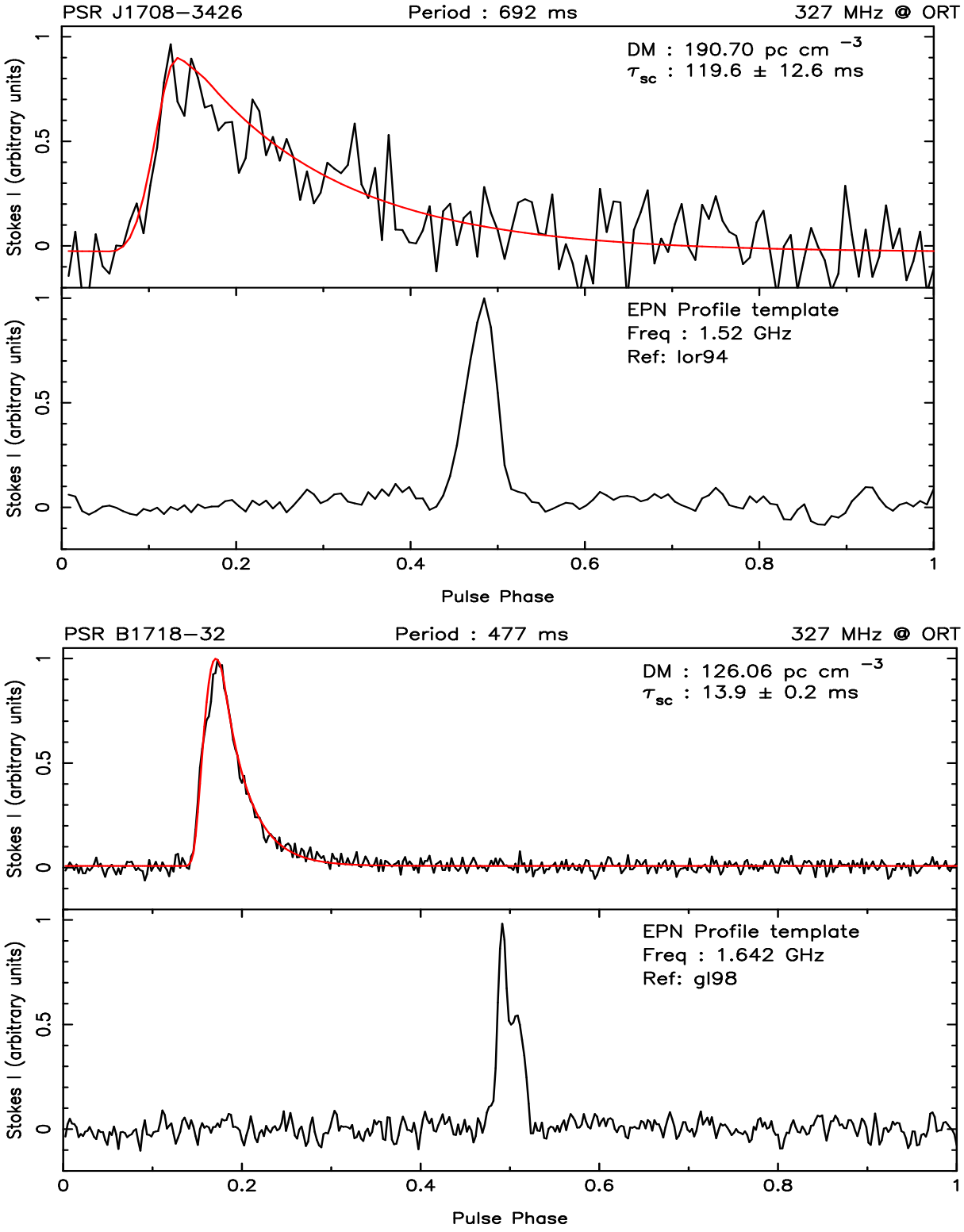

Fig. 25.— Same as in Fig. 1

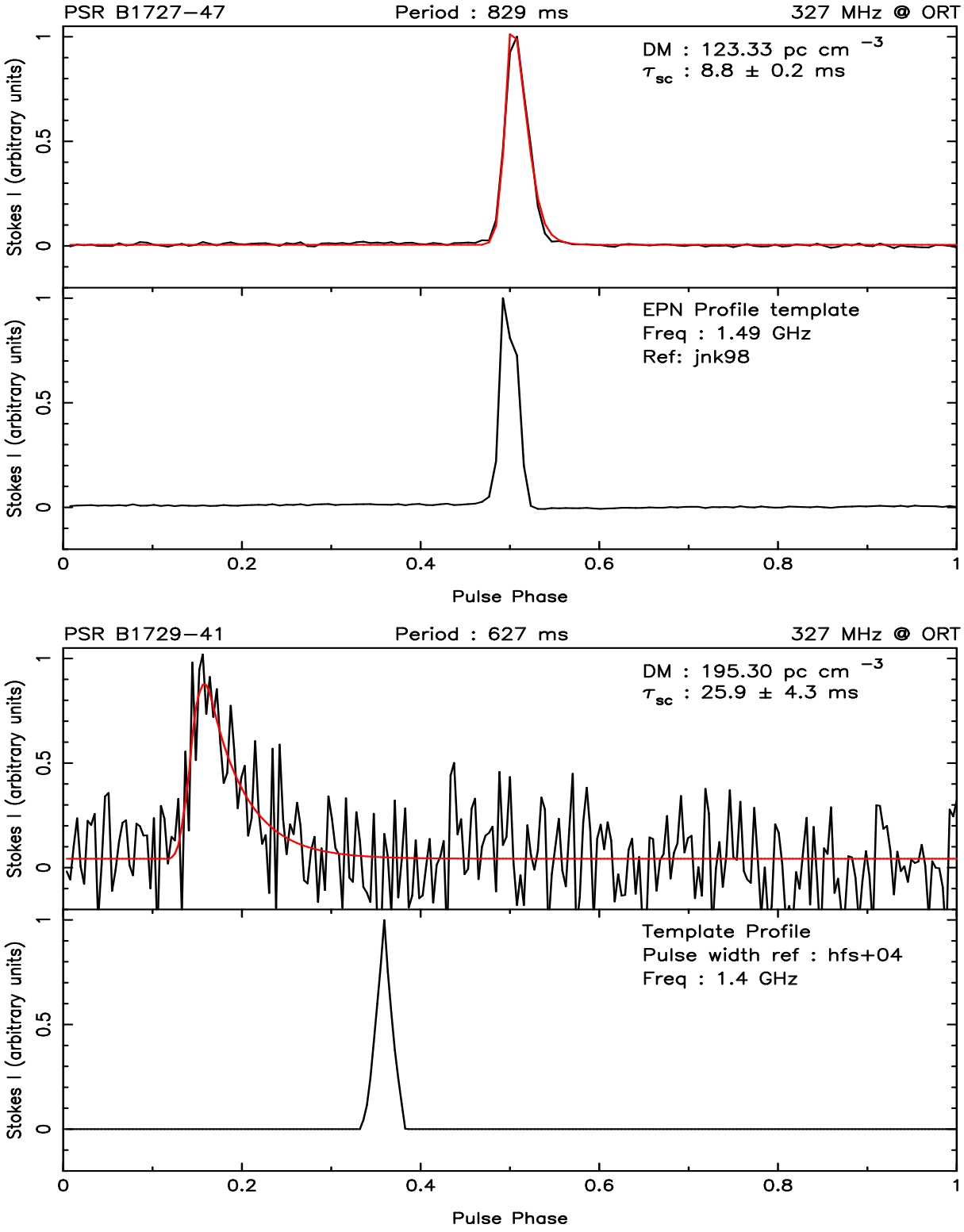

Fig. 26.— Same as in Fig. 1

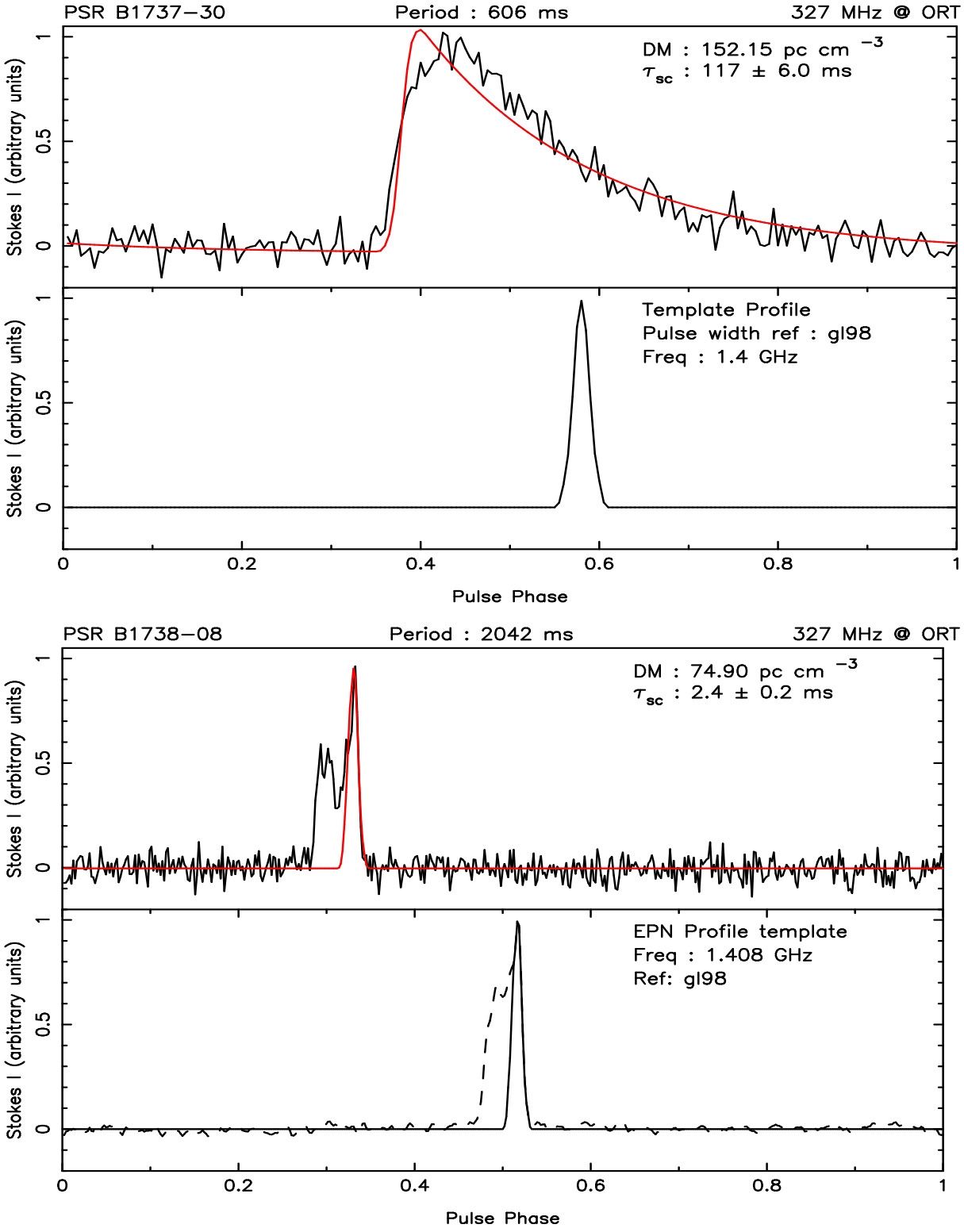

Fig. 27.— Same as in Fig. 1

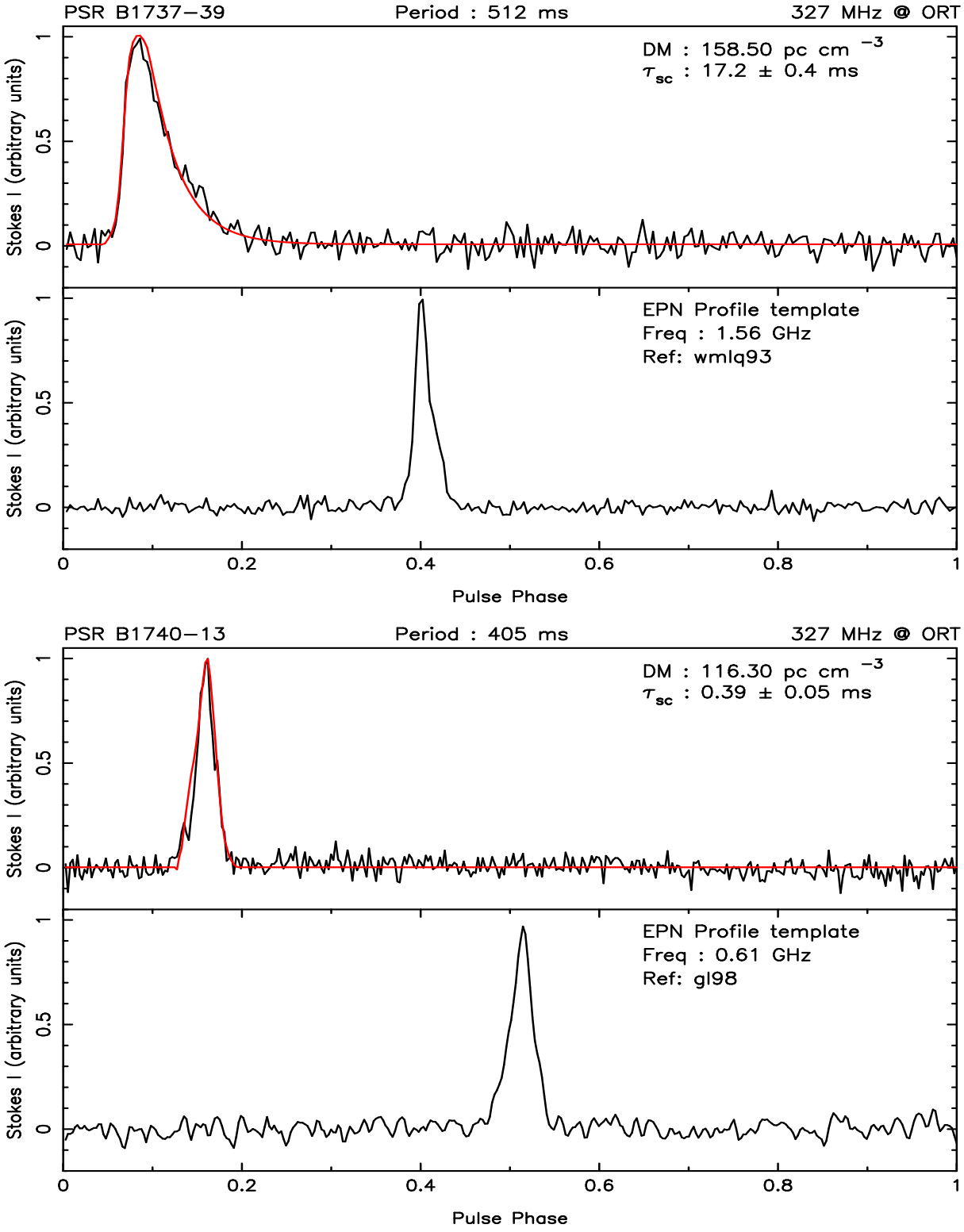

Fig. 28.— Same as in Fig. 1

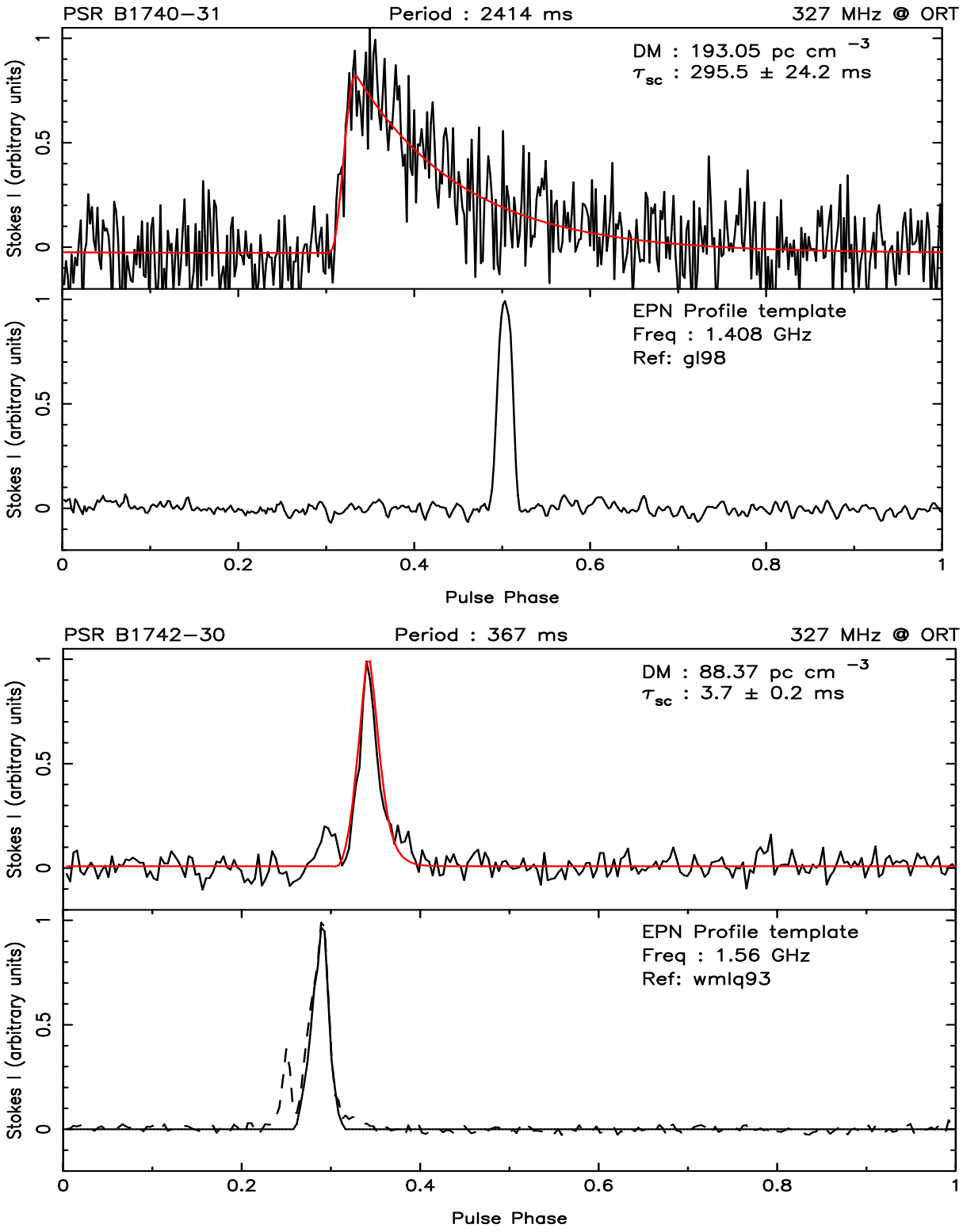

Fig. 29.— Same as in Fig. 1

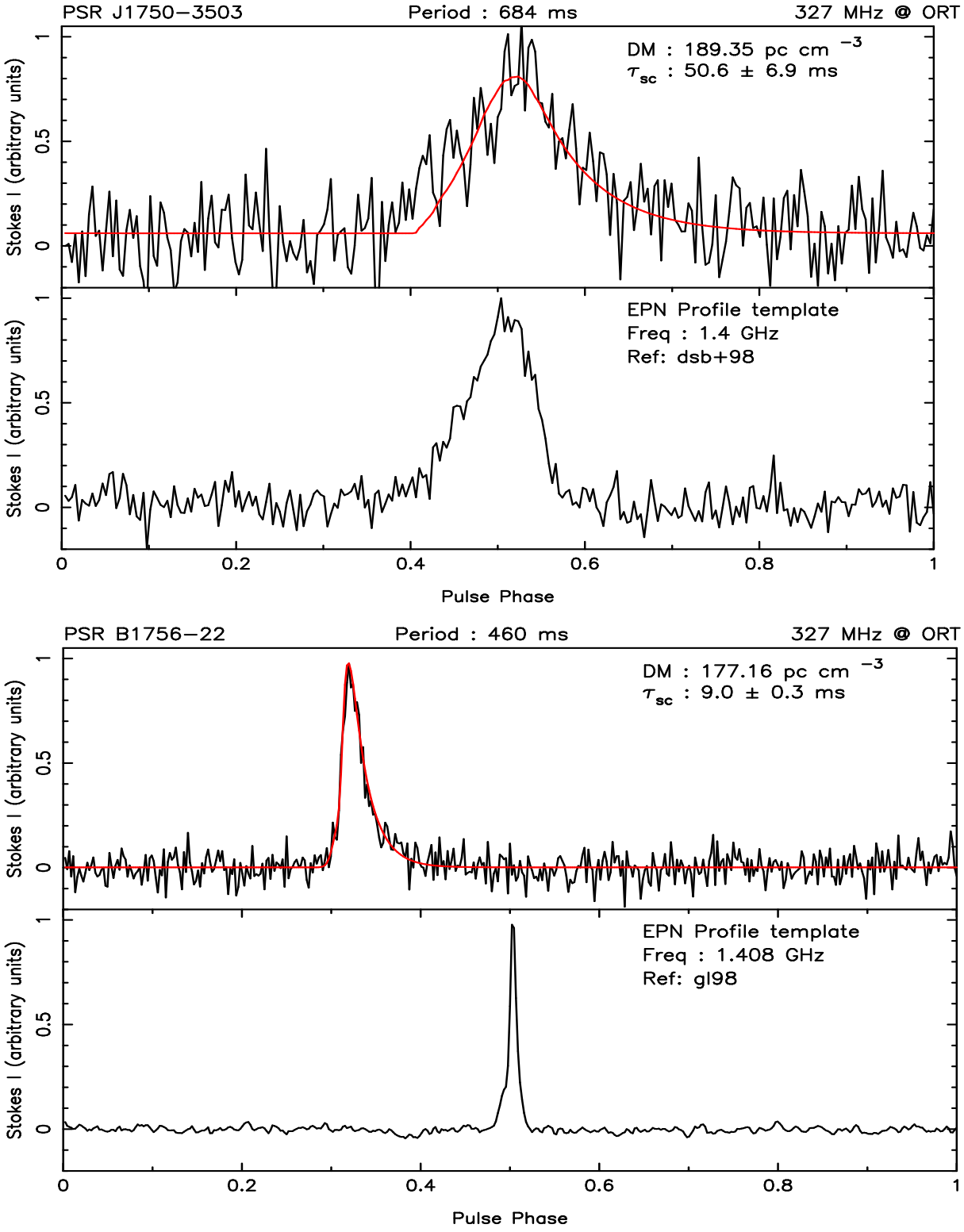

Fig. 30.— Same as in Fig. 1

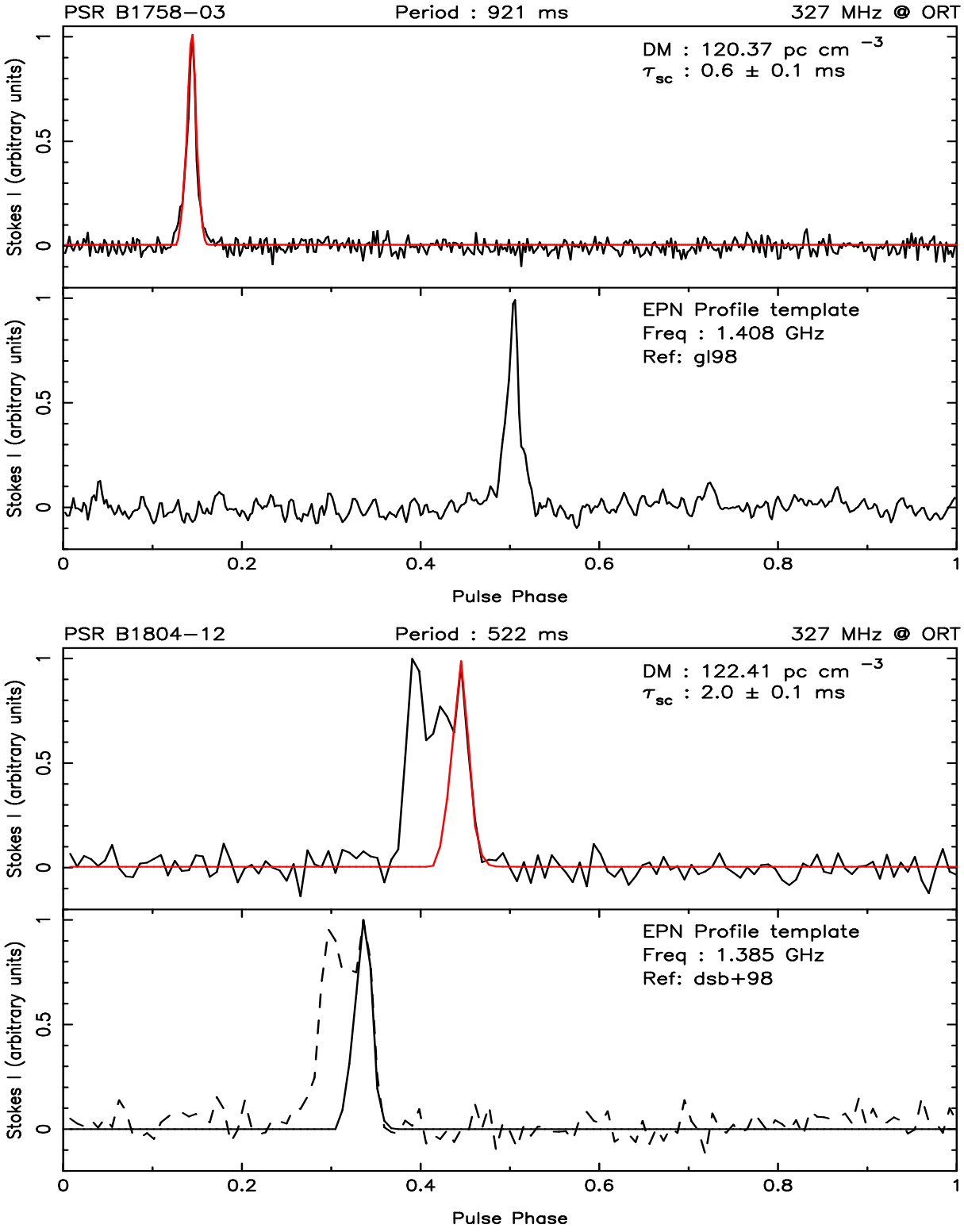

Fig. 31.— Same as in Fig. 1

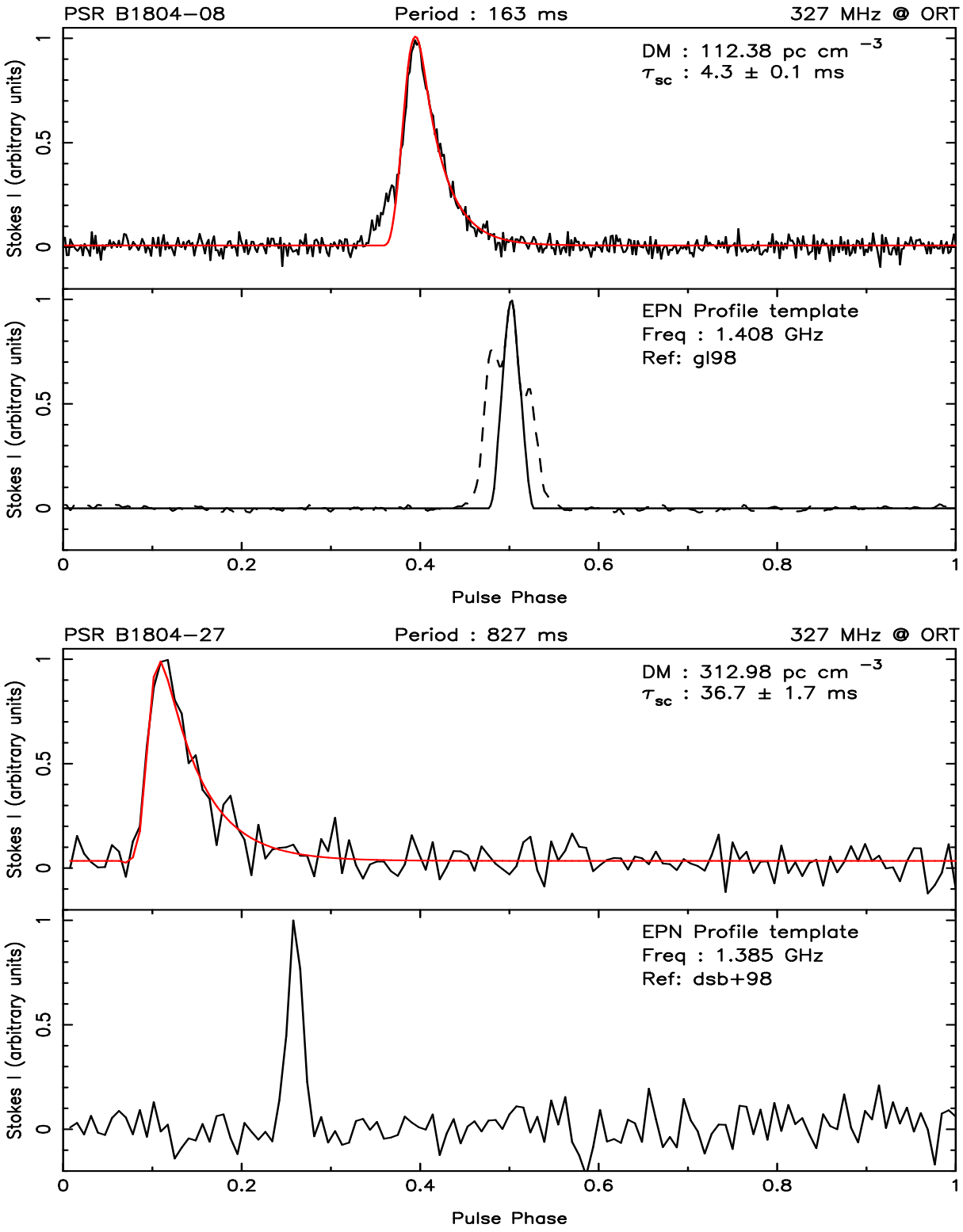

Fig. 32.— Same as in Fig. 1

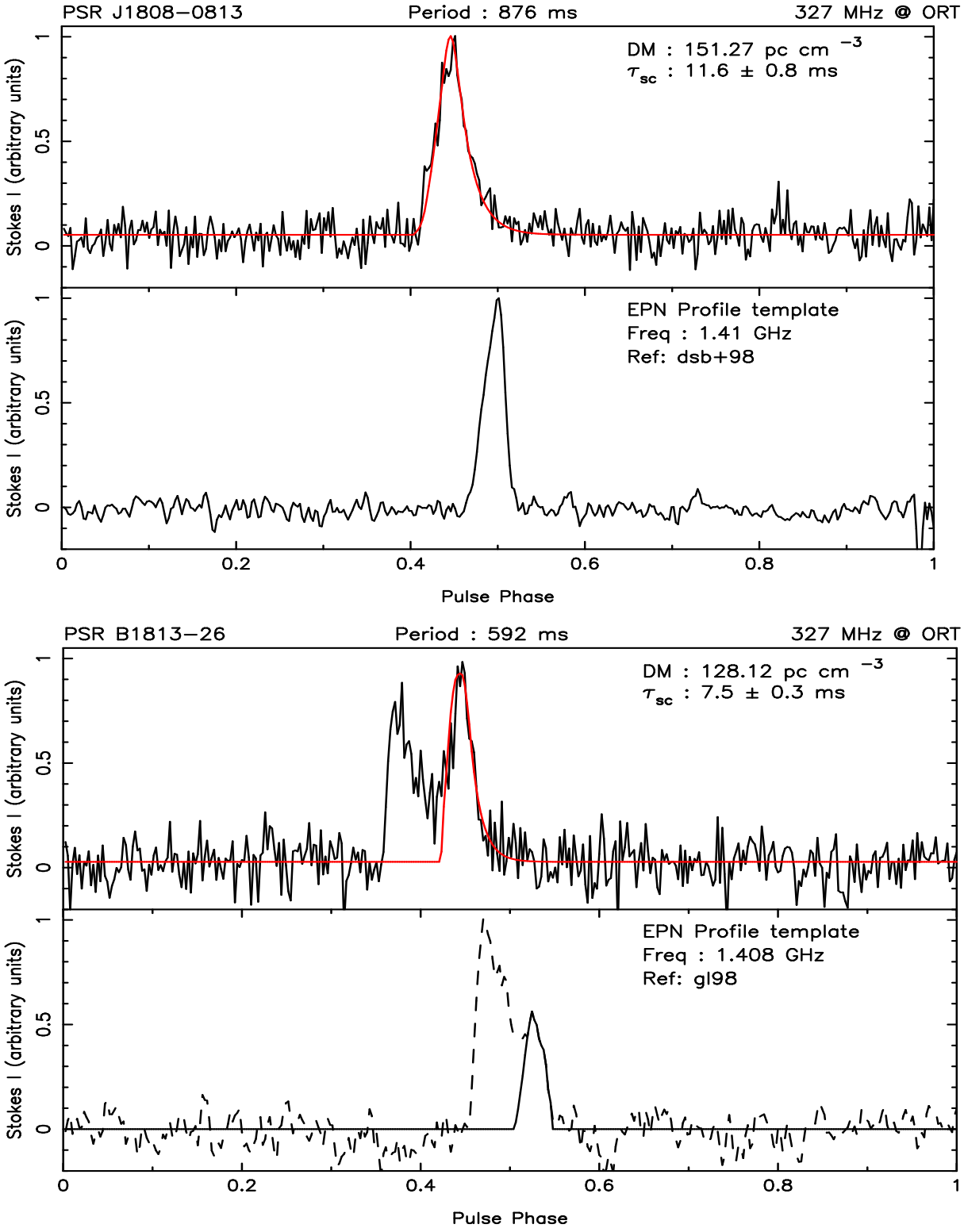

Fig. 33.— Same as in Fig. 1

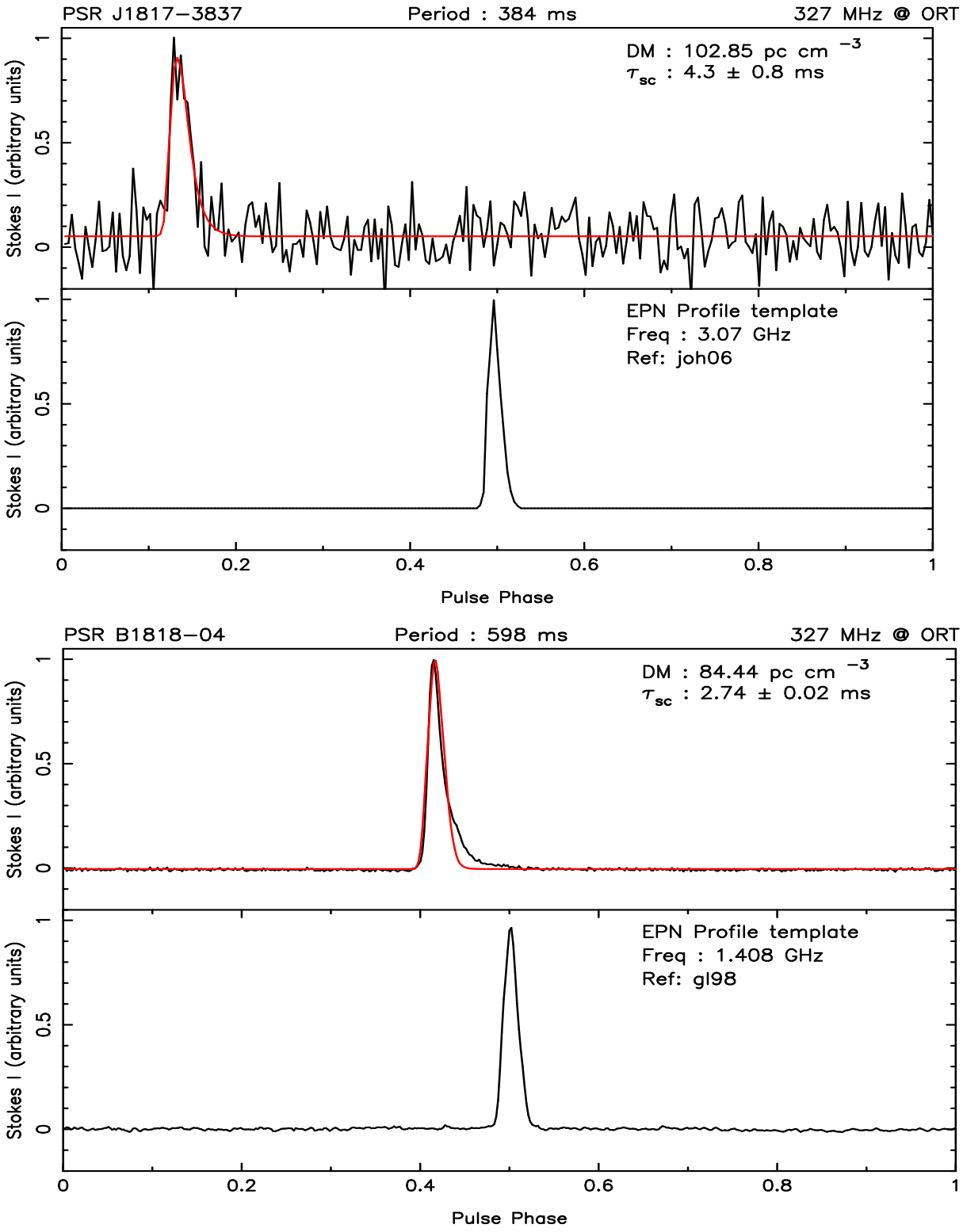

Fig. 34.— Same as in Fig. 1

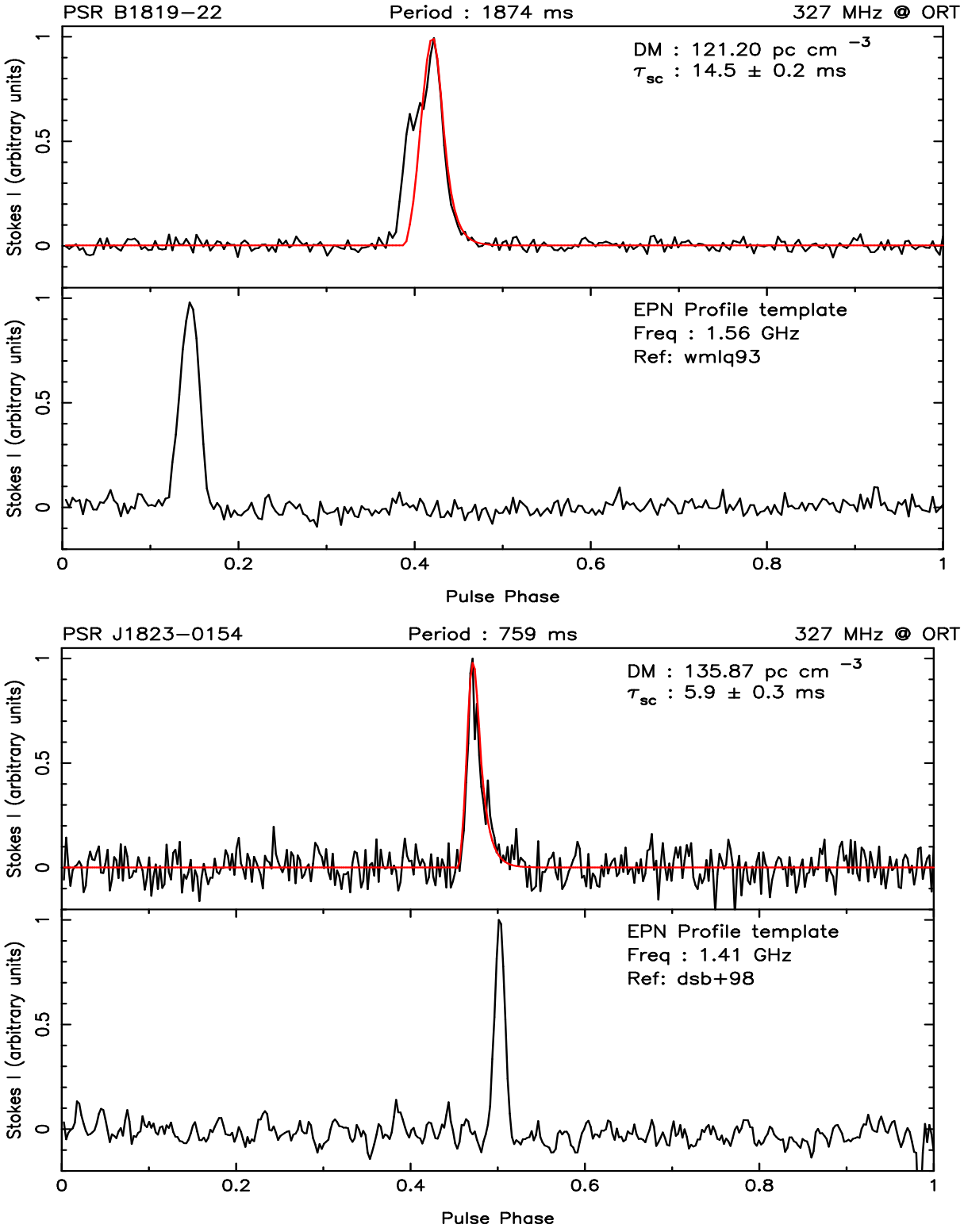

Fig. 35.— Same as in Fig. 1

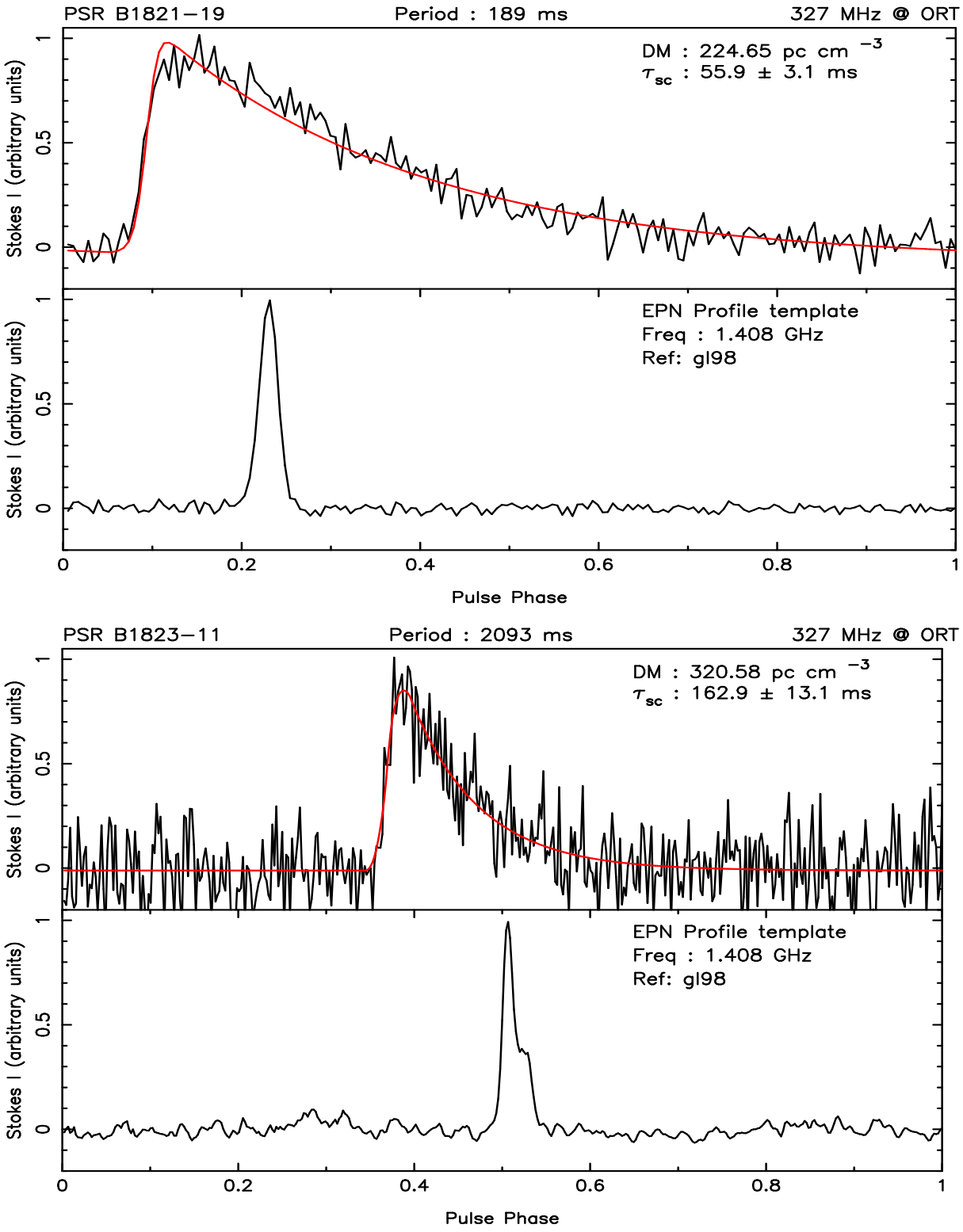

Fig. 36.— Same as in Fig. 1

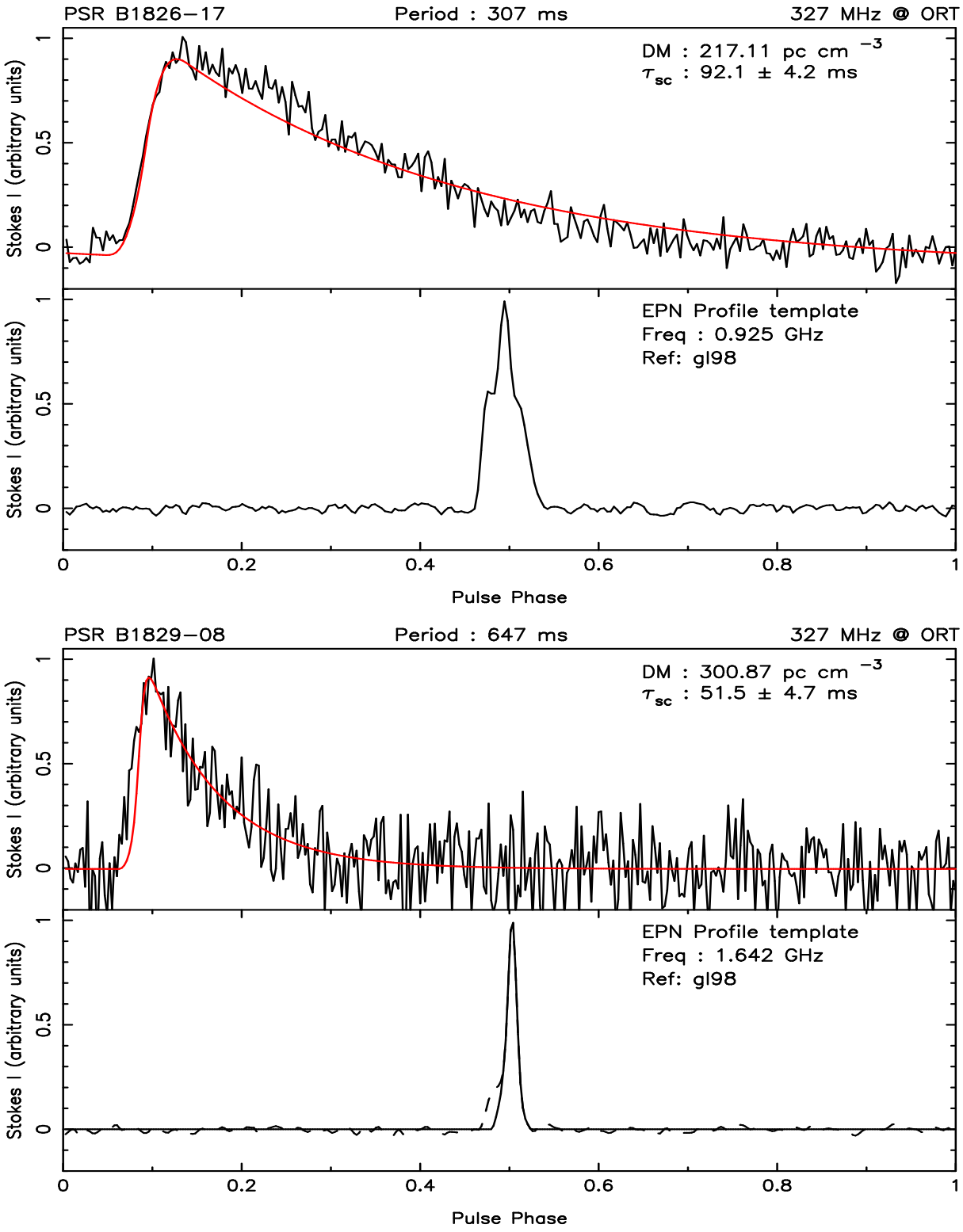

Fig. 37.— Same as in Fig. 1

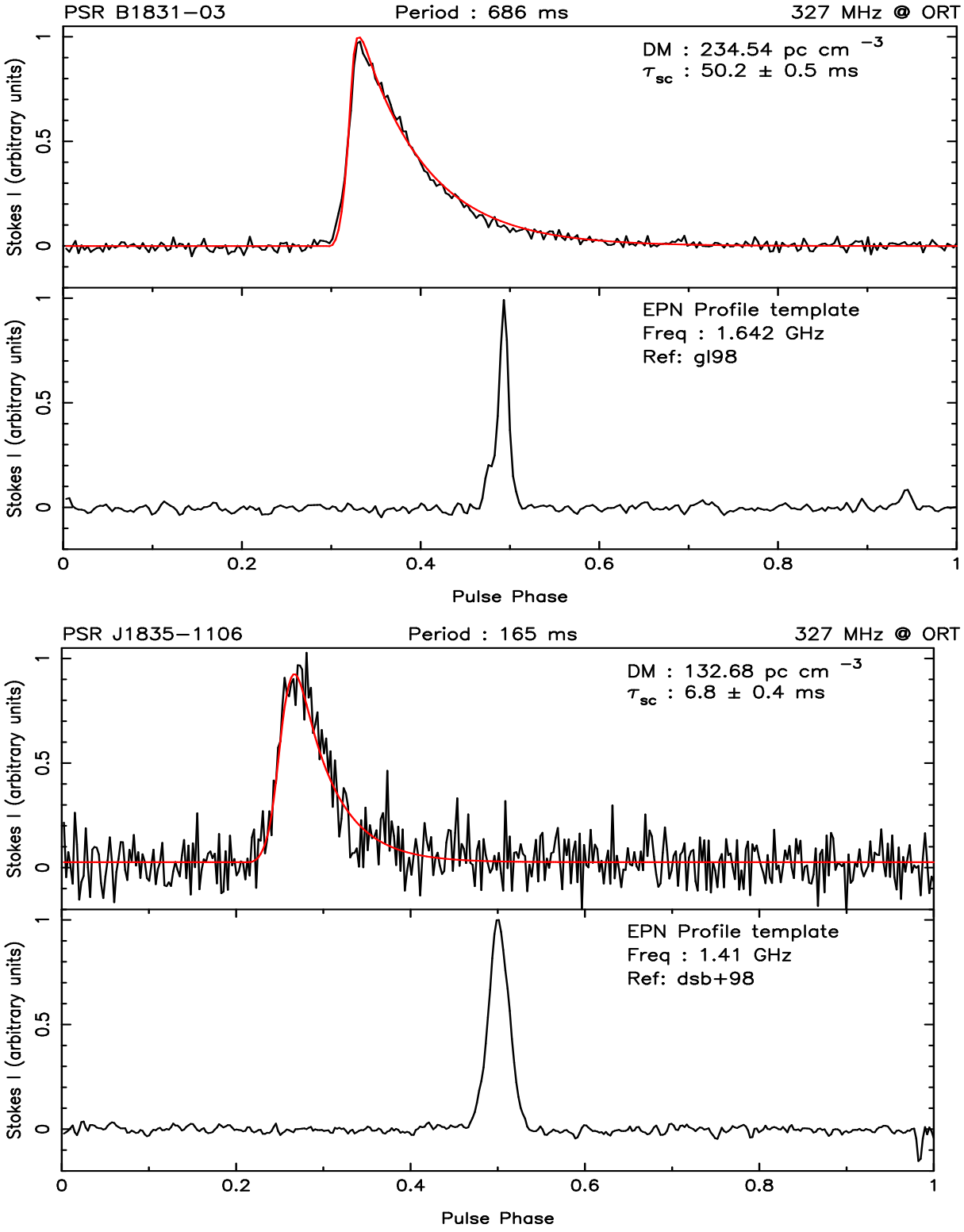

Fig. 38.— Same as in Fig. 1

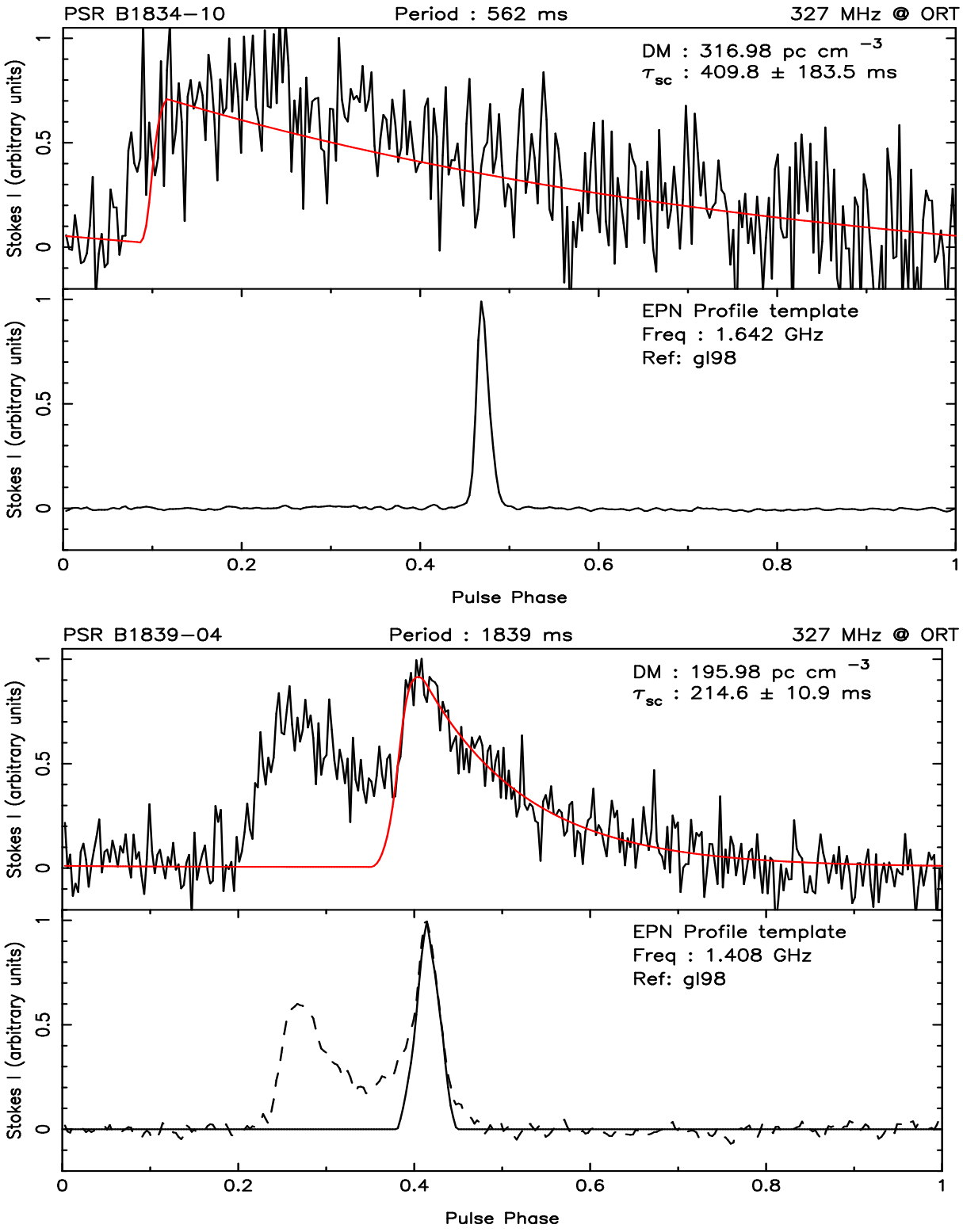

Fig. 39.— Same as in Fig. 1

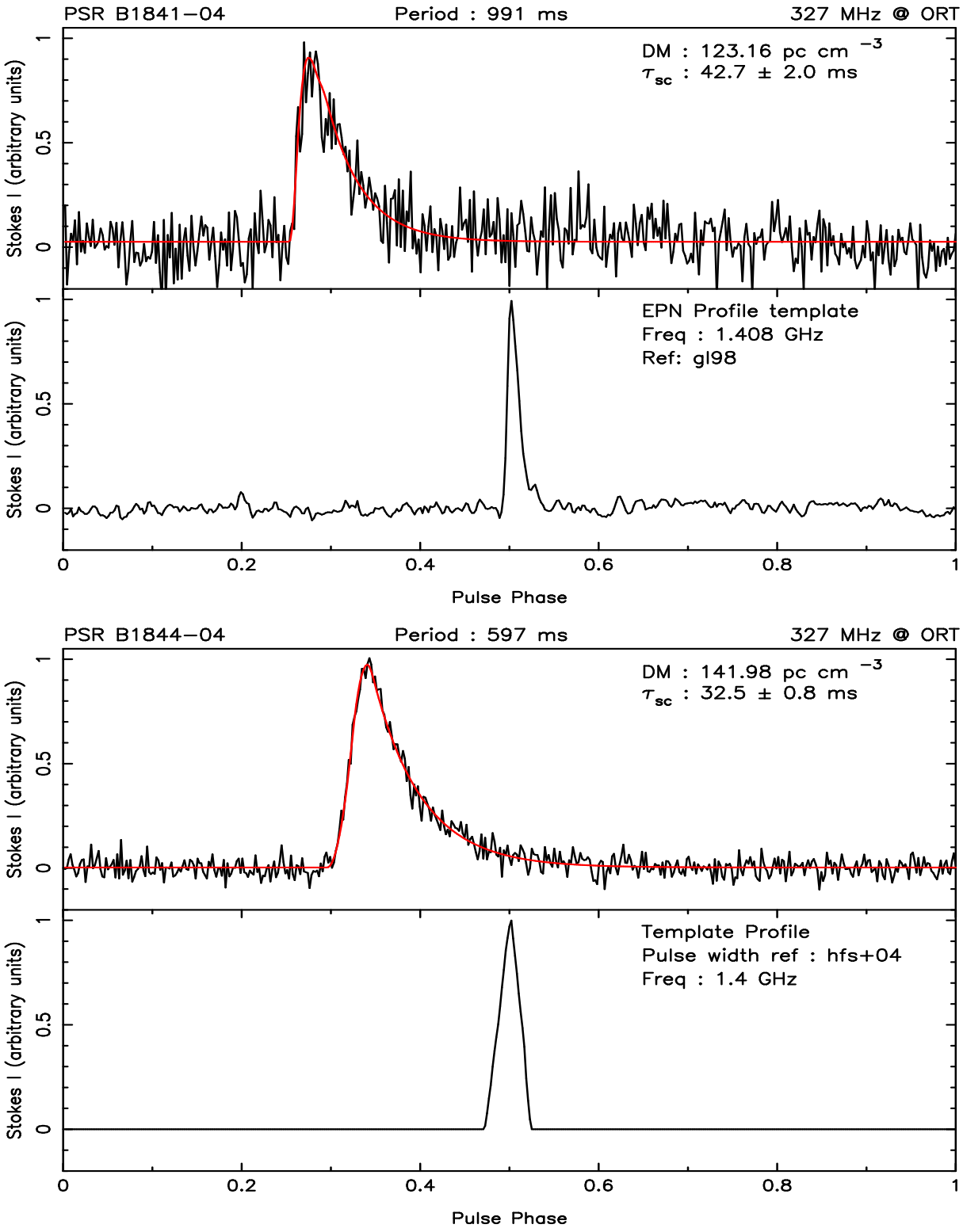

Fig. 40.— Same as in Fig. 1

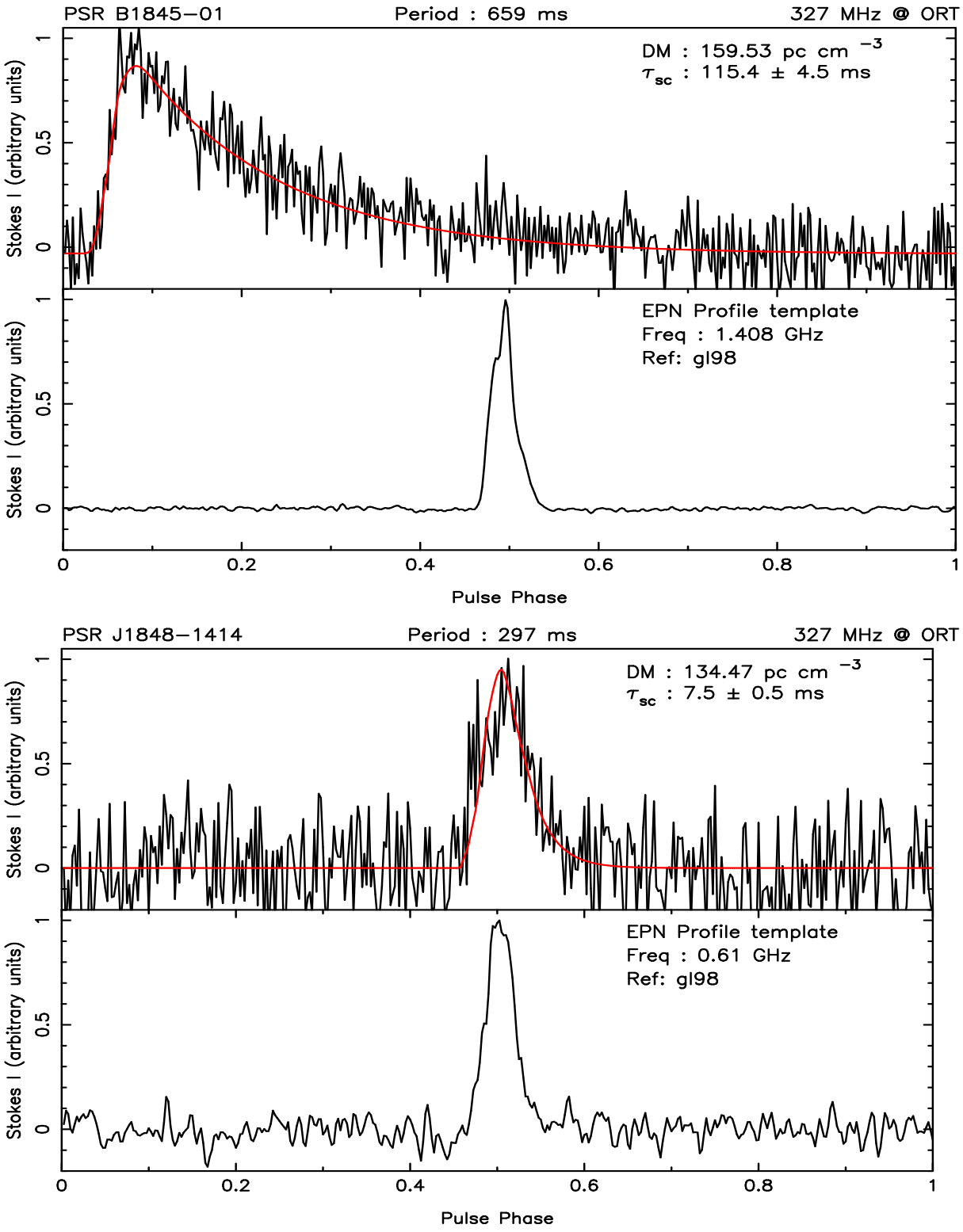

Fig. 41.— Same as in Fig. 1

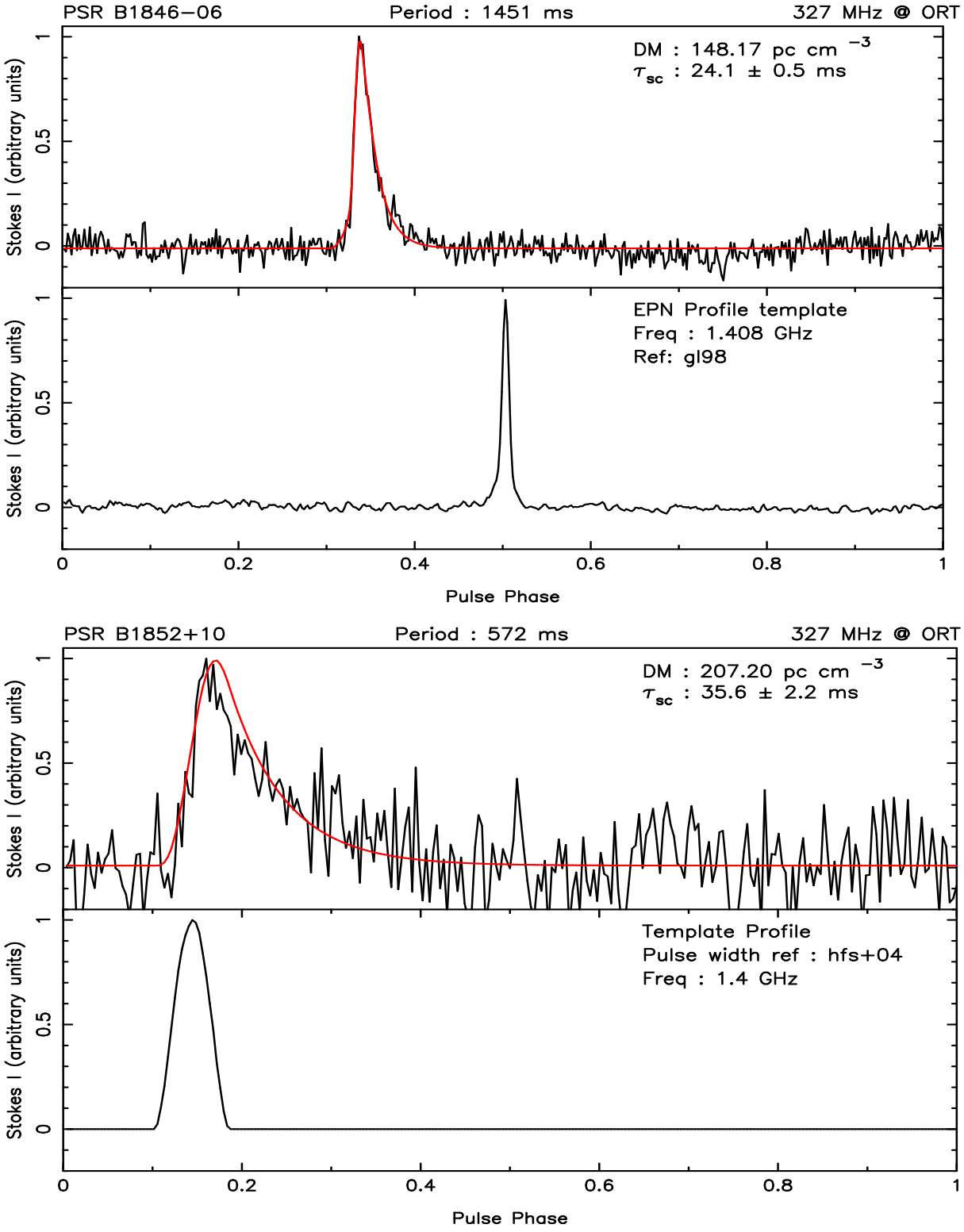

Fig. 42.— Same as in Fig. 1

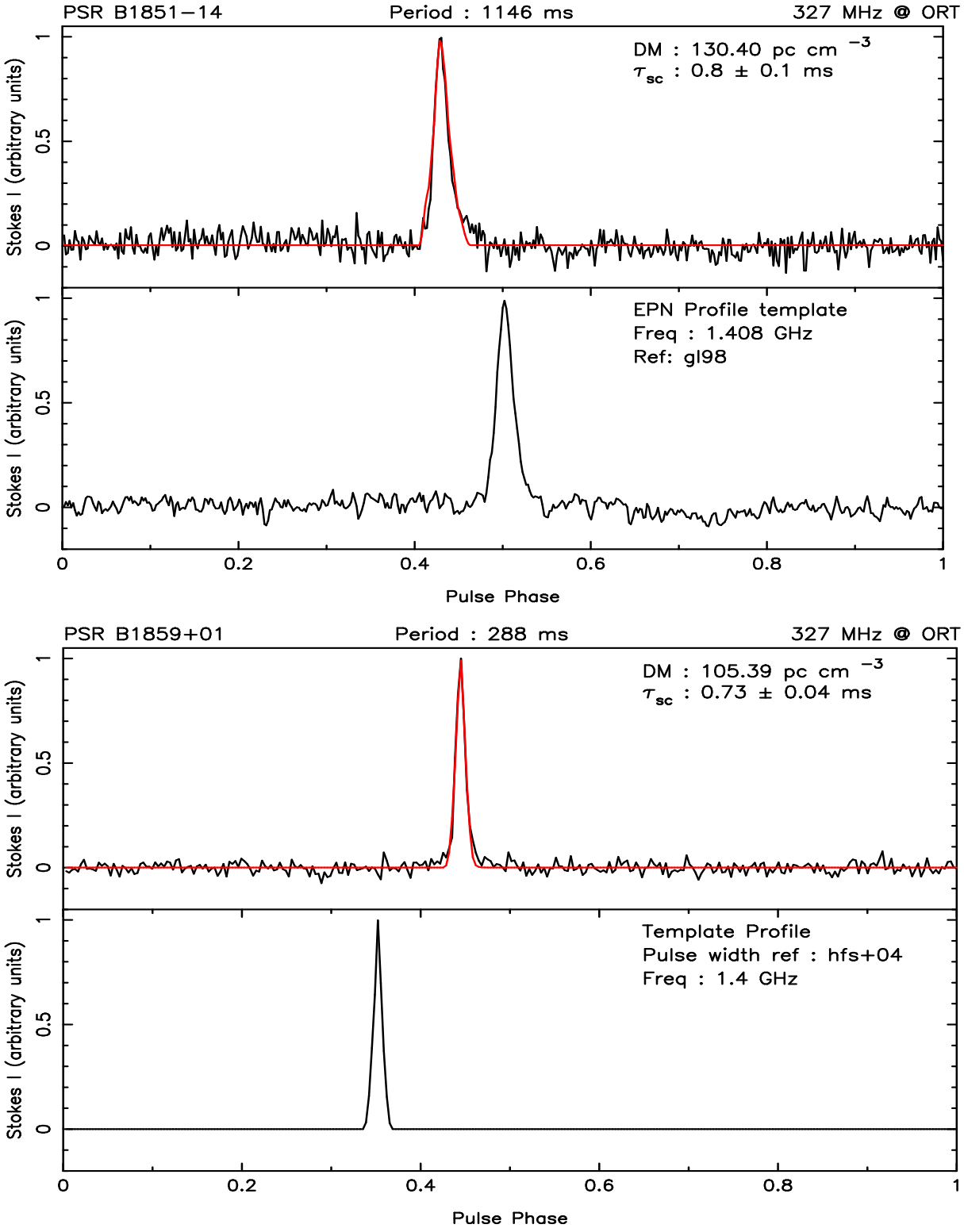

Fig. 43.— Same as in Fig. 1

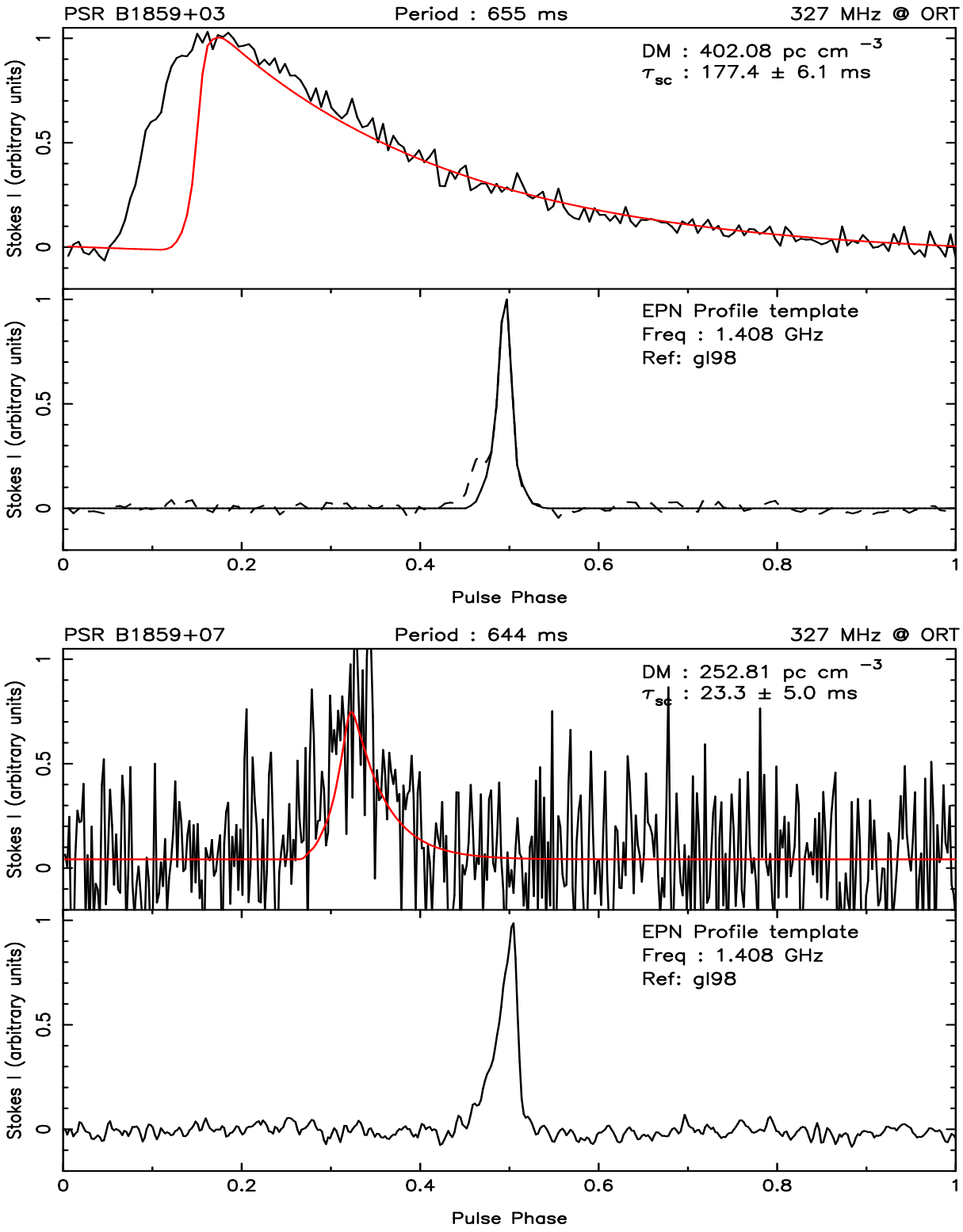

Fig. 44.— Same as in Fig. 1

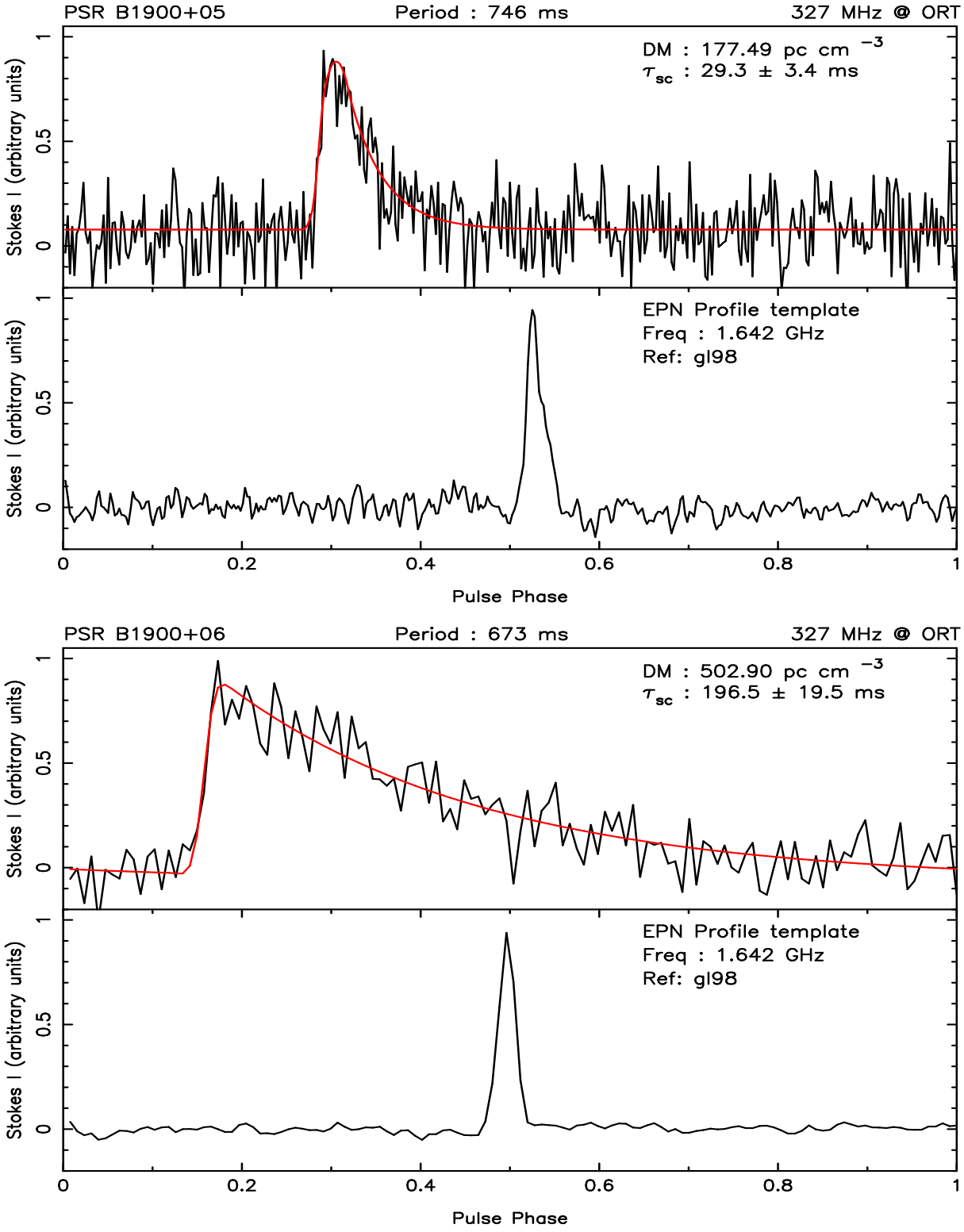

Fig. 45.— Same as in Fig. 1

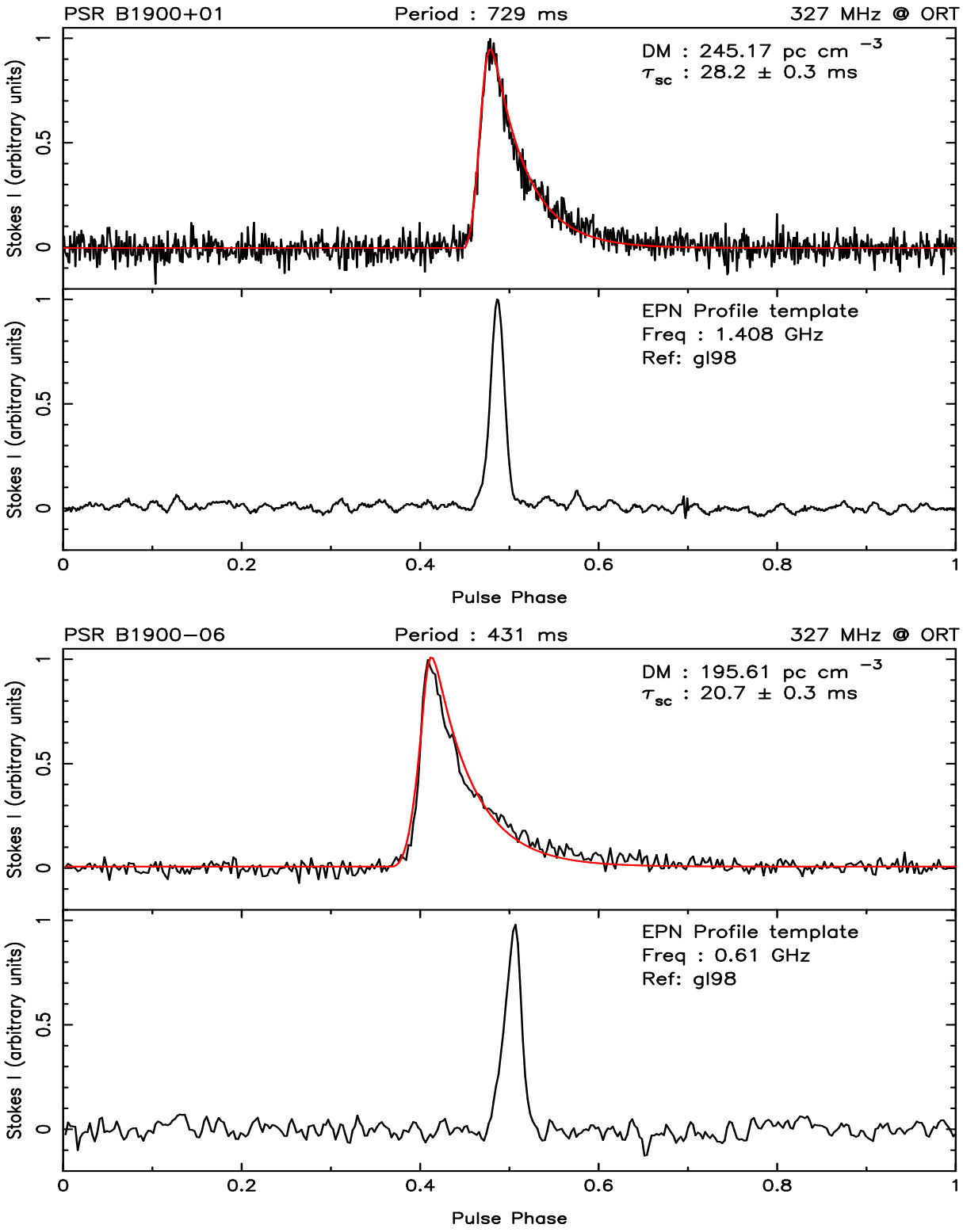

Fig. 46.— Same as in Fig. 1

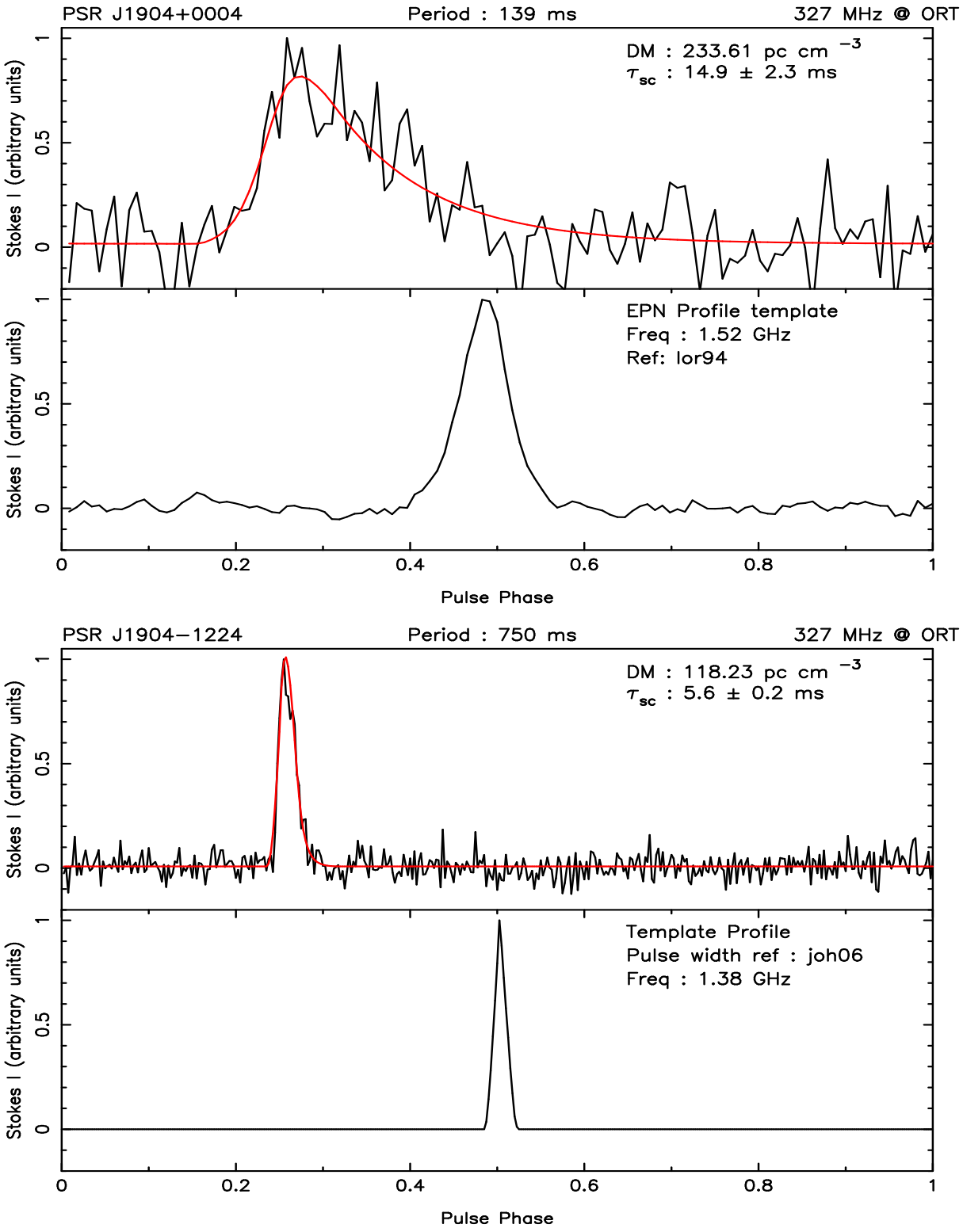

Fig. 47.— Same as in Fig. 1

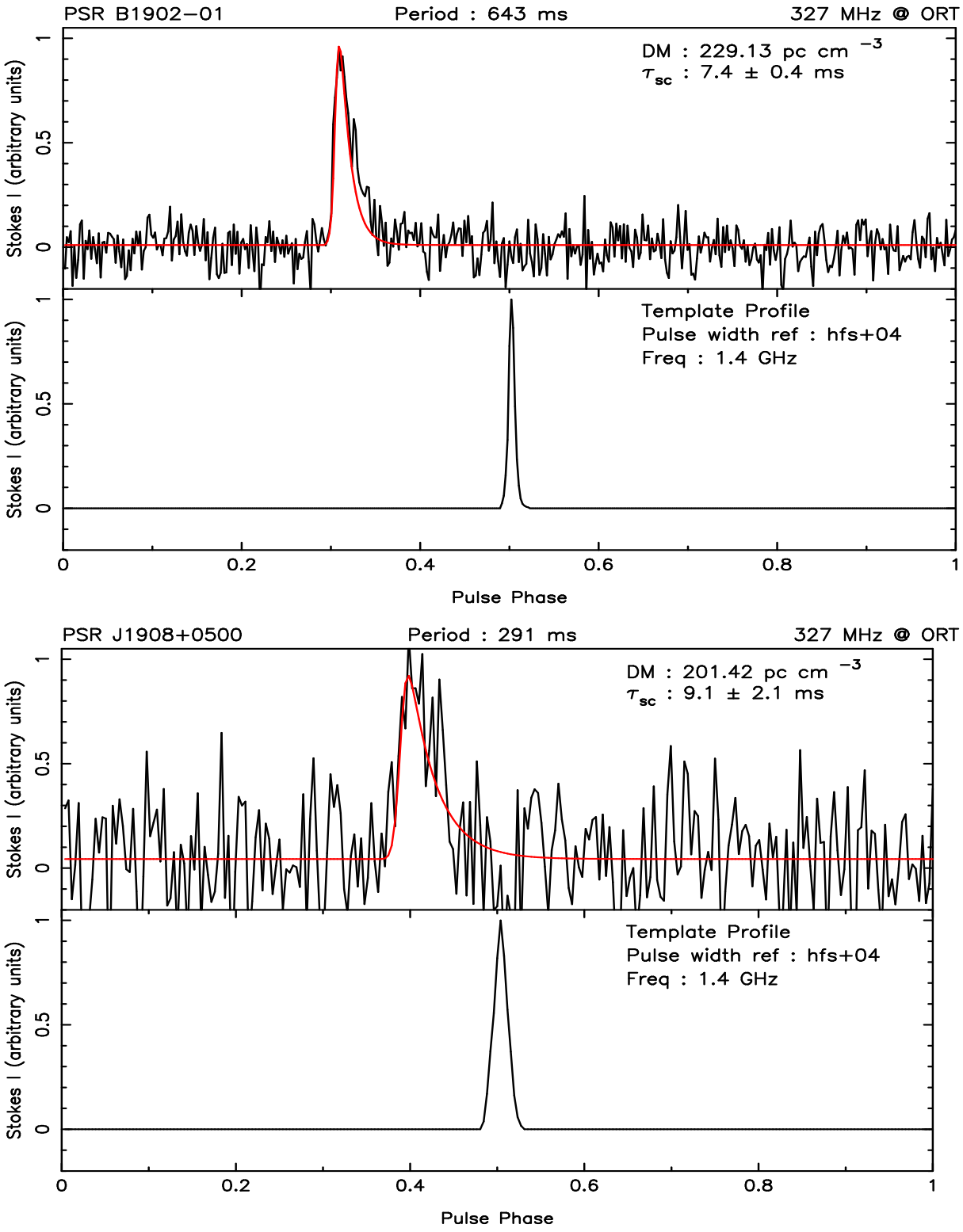

Fig. 48.— Same as in Fig. 1

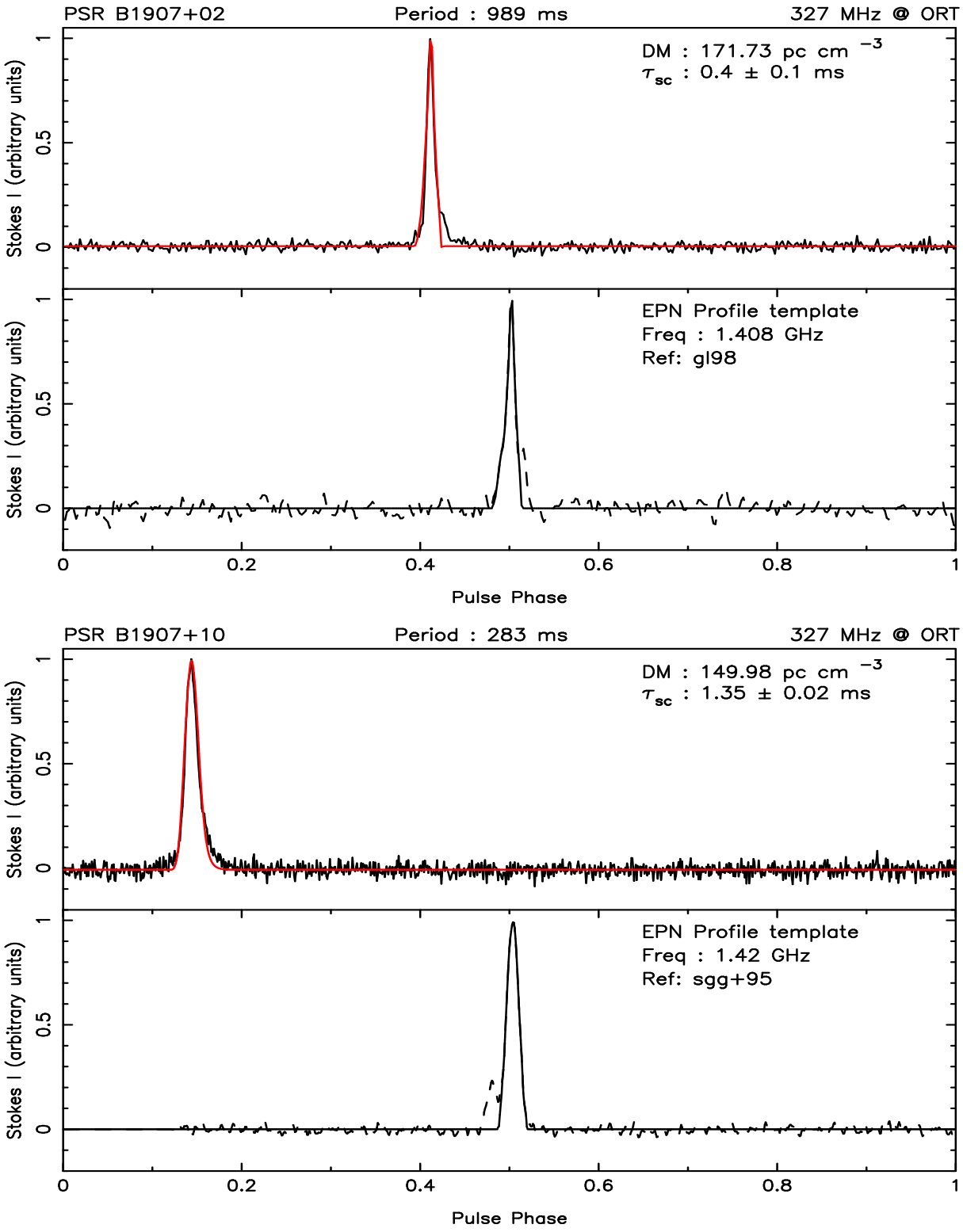

Fig. 49.— Same as in Fig. 1

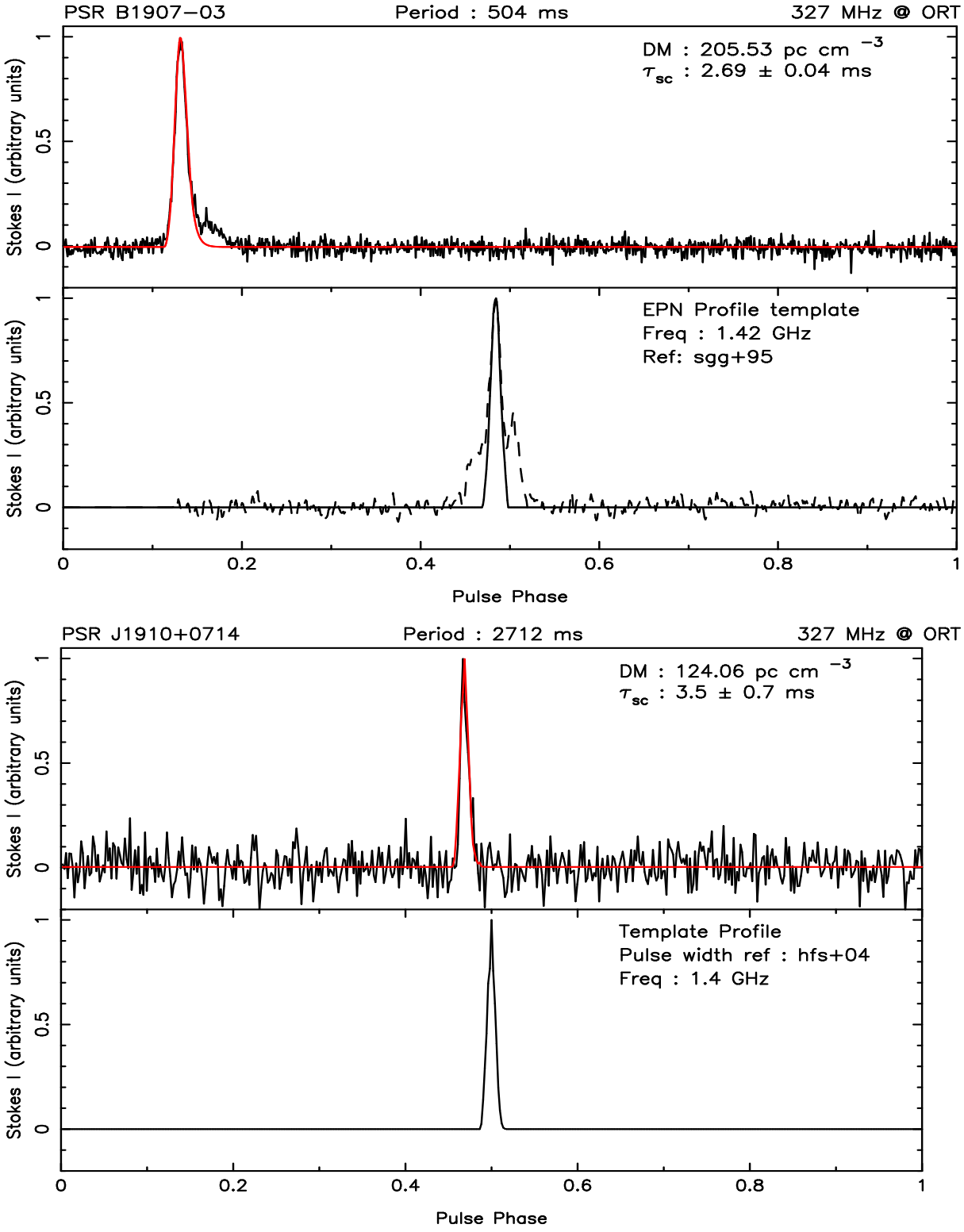

Fig. 50.— Same as in Fig. 1

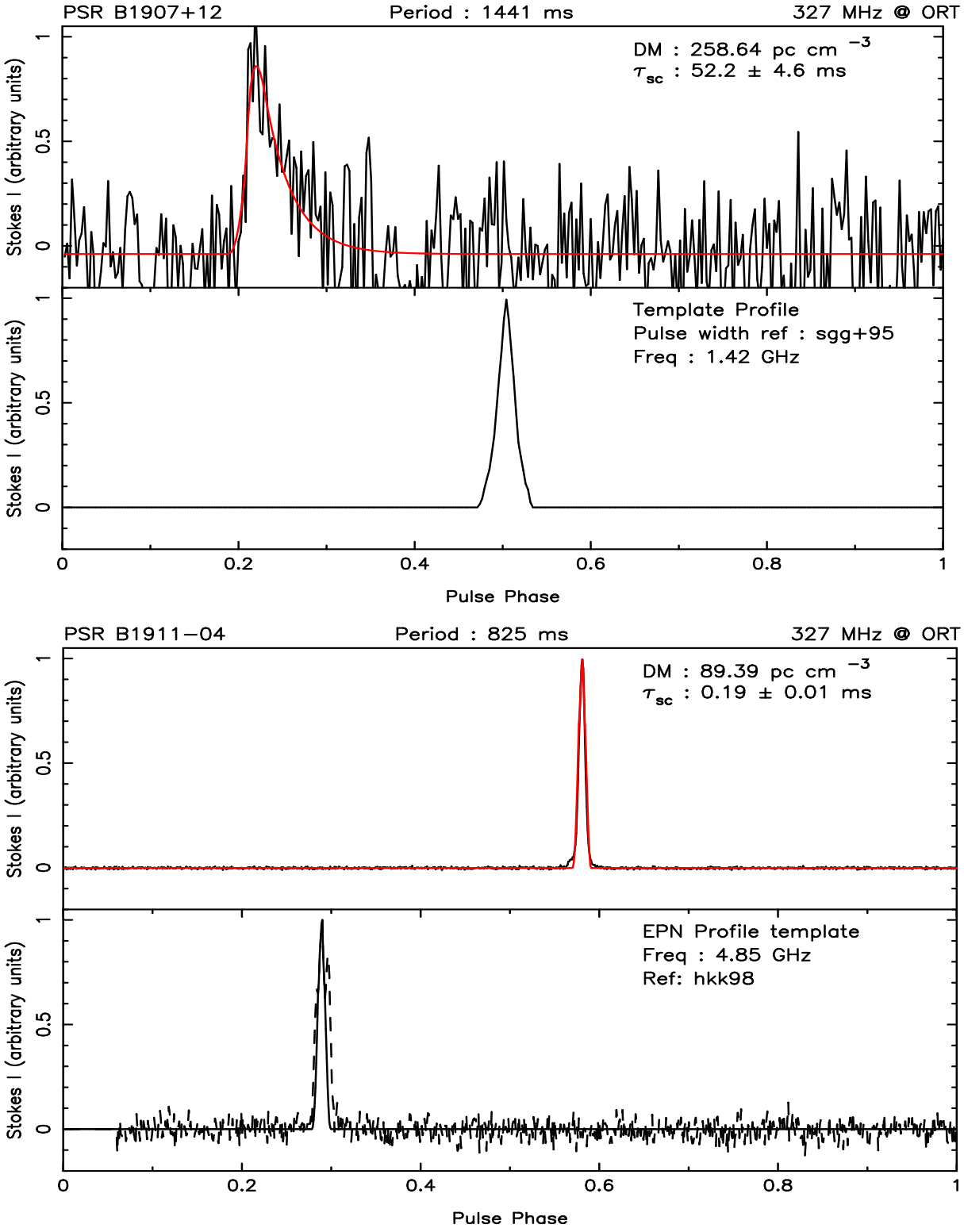

Fig. 51.— Same as in Fig. 1

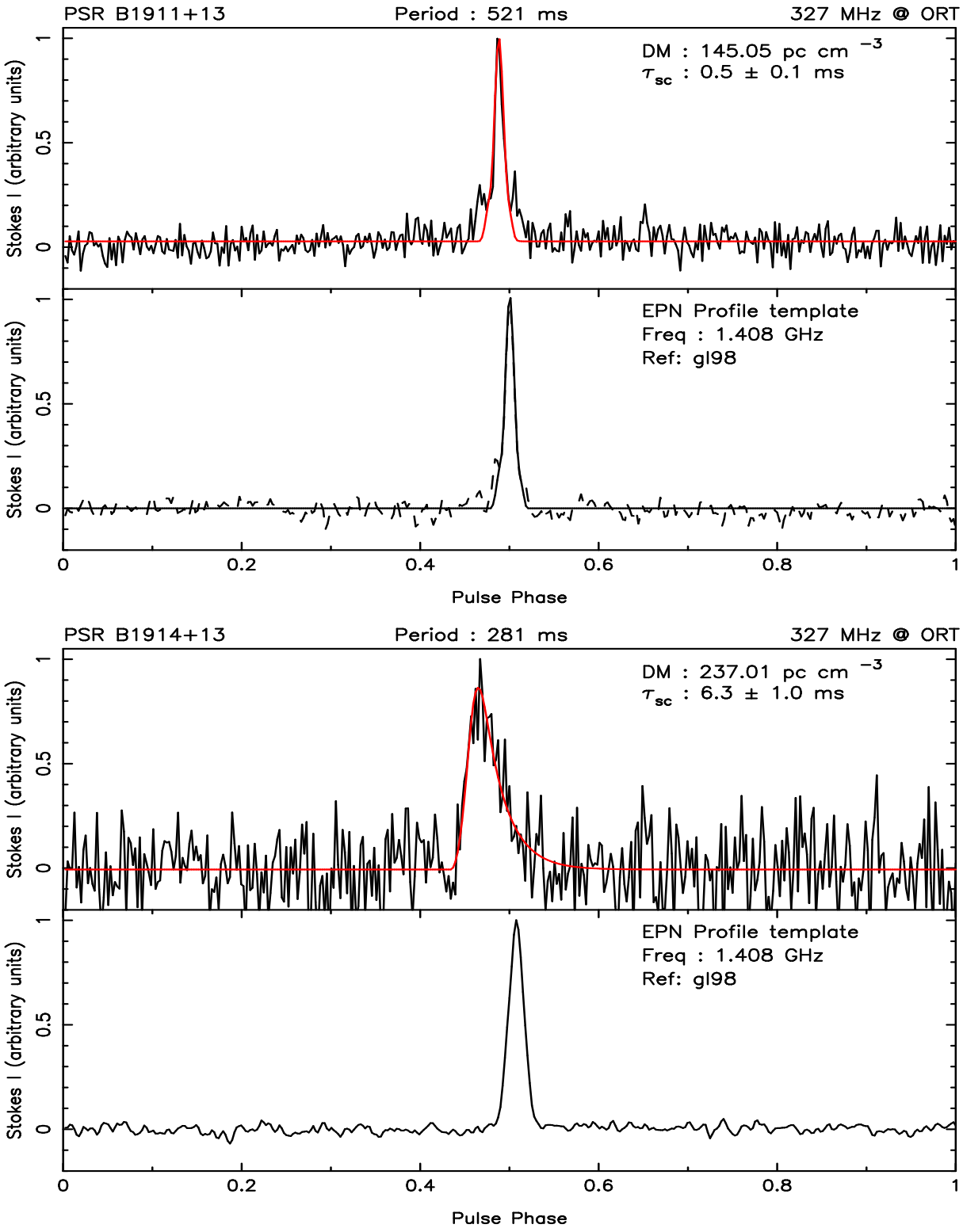

Fig. 52.— Same as in Fig. 1

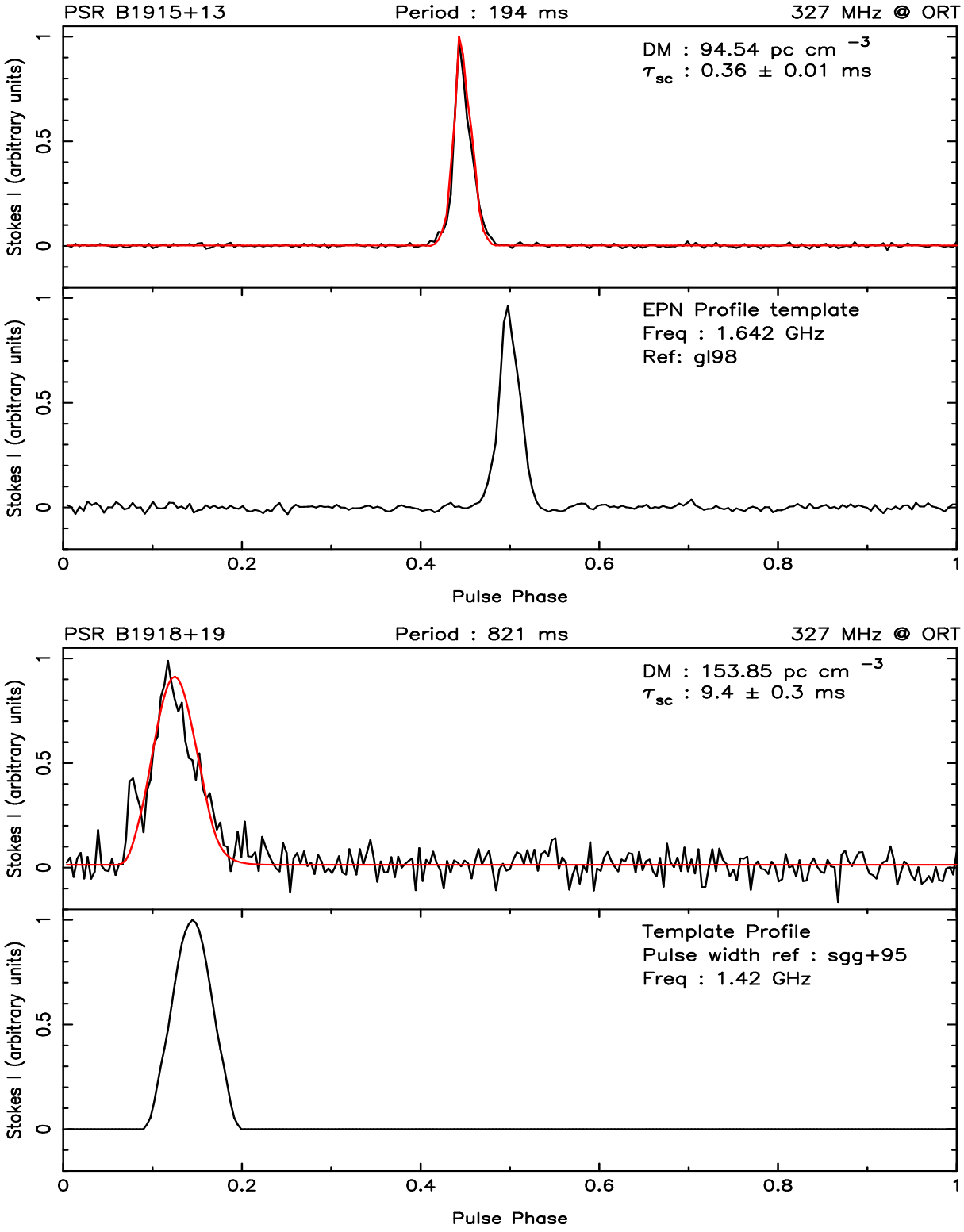

Fig. 53.— Same as in Fig. 1

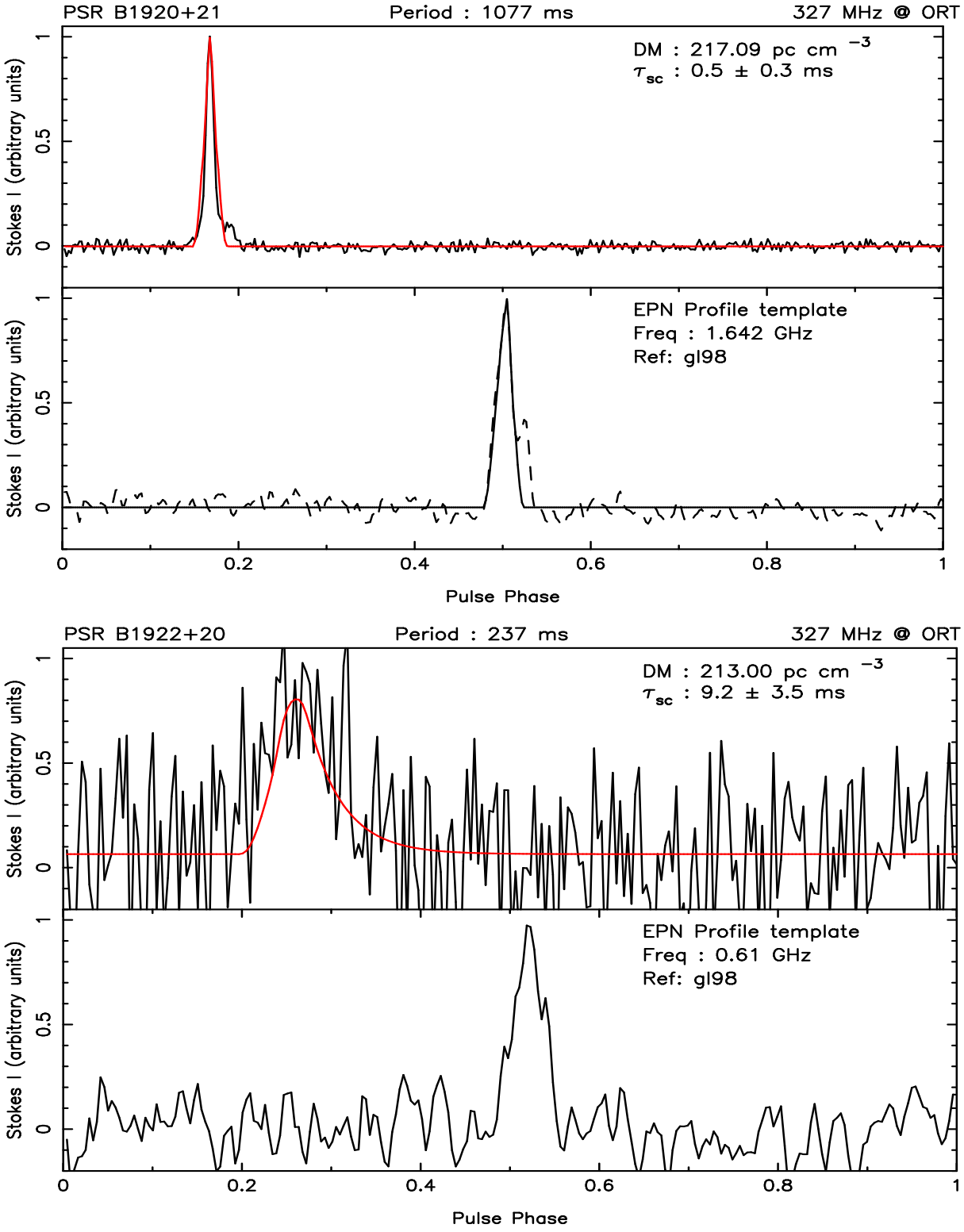

Fig. 54.— Same as in Fig. 1

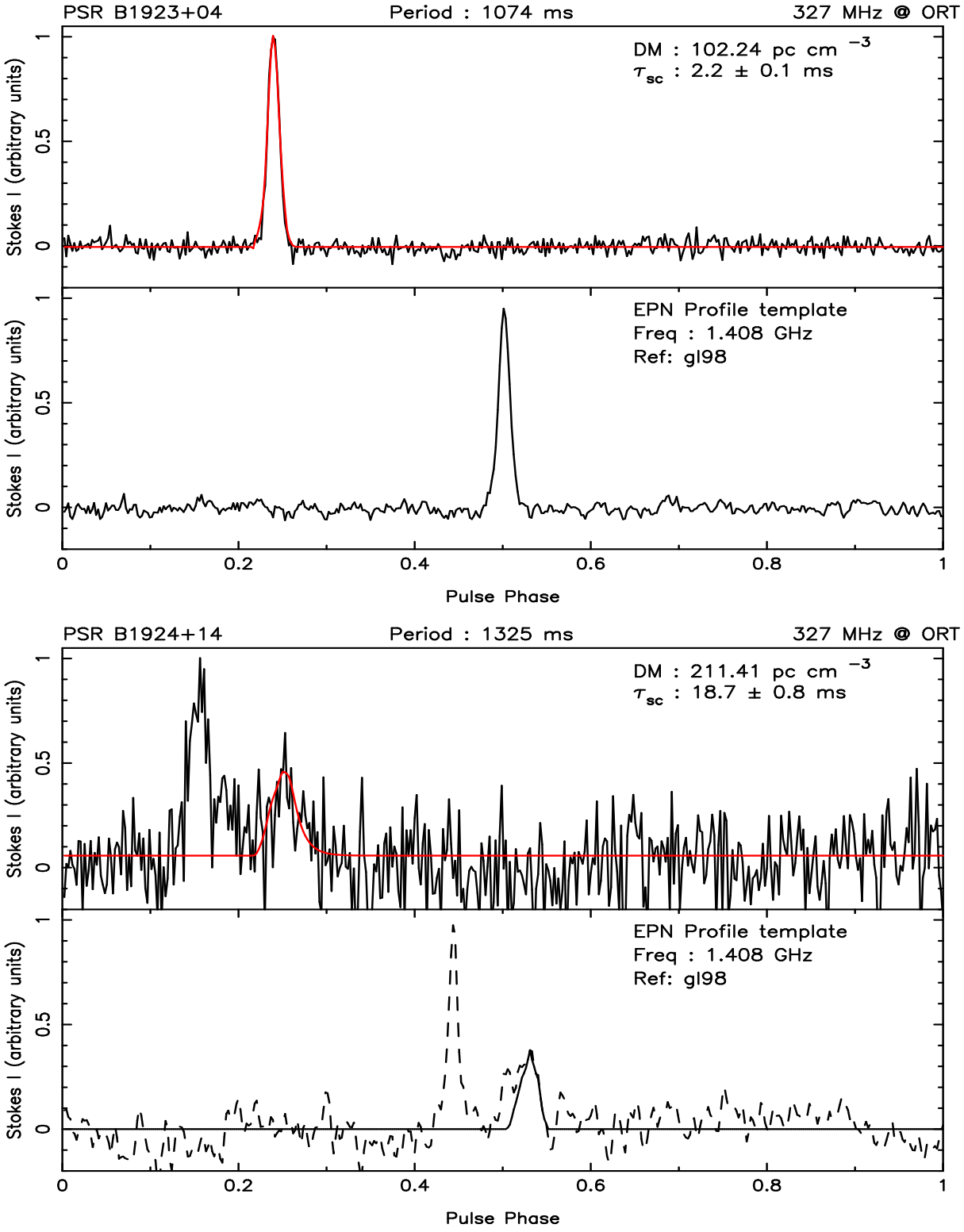

Fig. 55.— Same as in Fig. 1

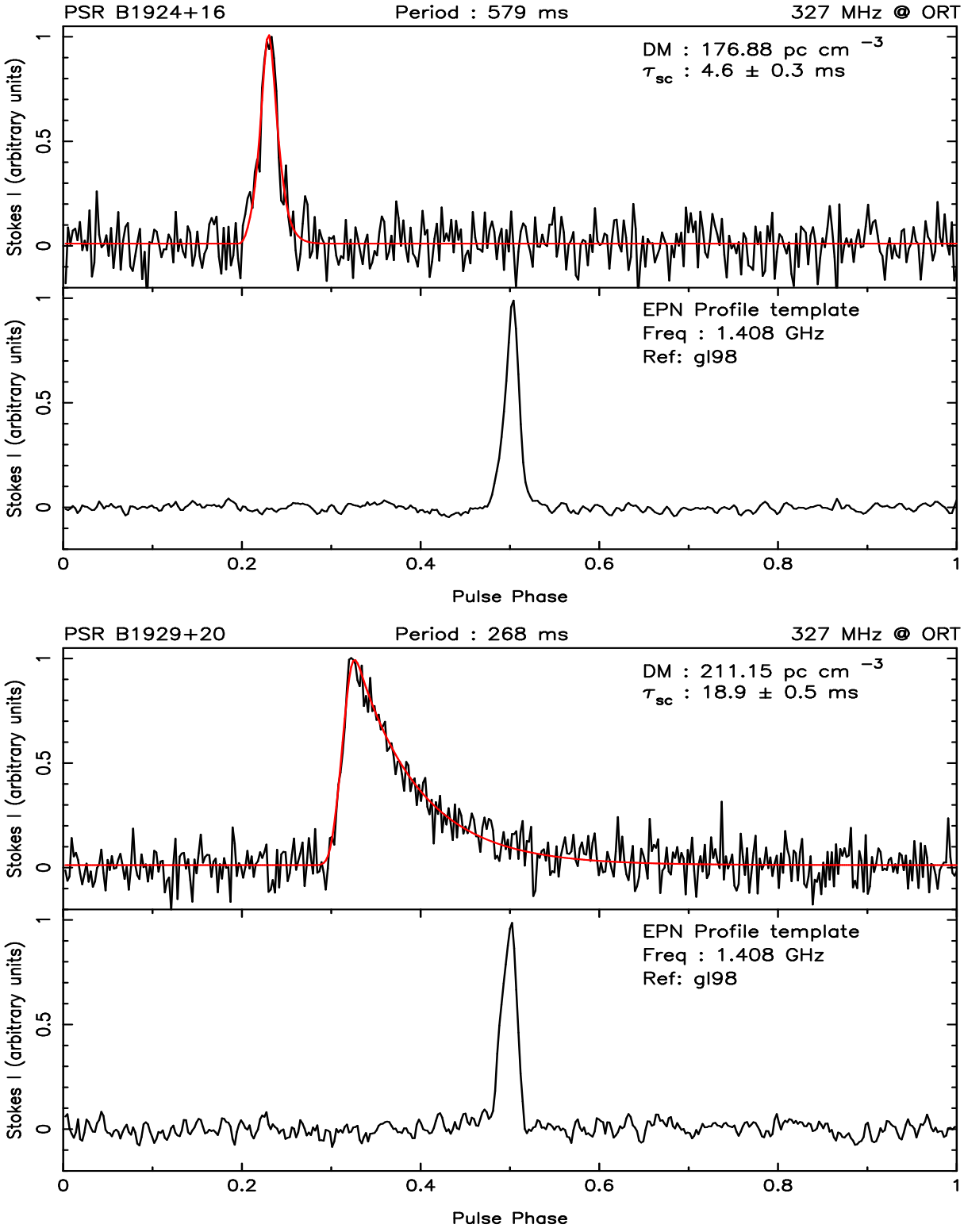

Fig. 56.— Same as in Fig. 1

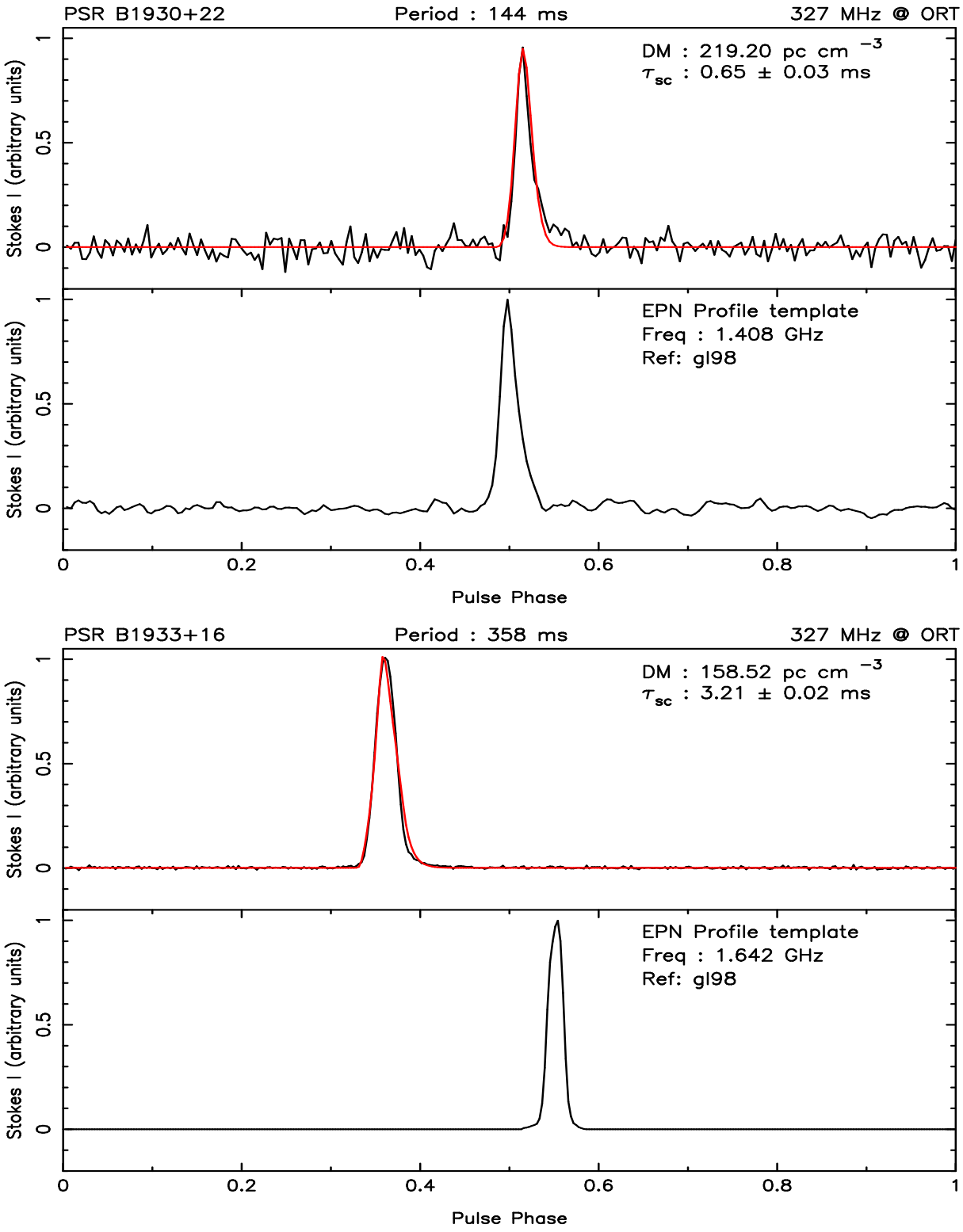

Fig. 57.— Same as in Fig. 1

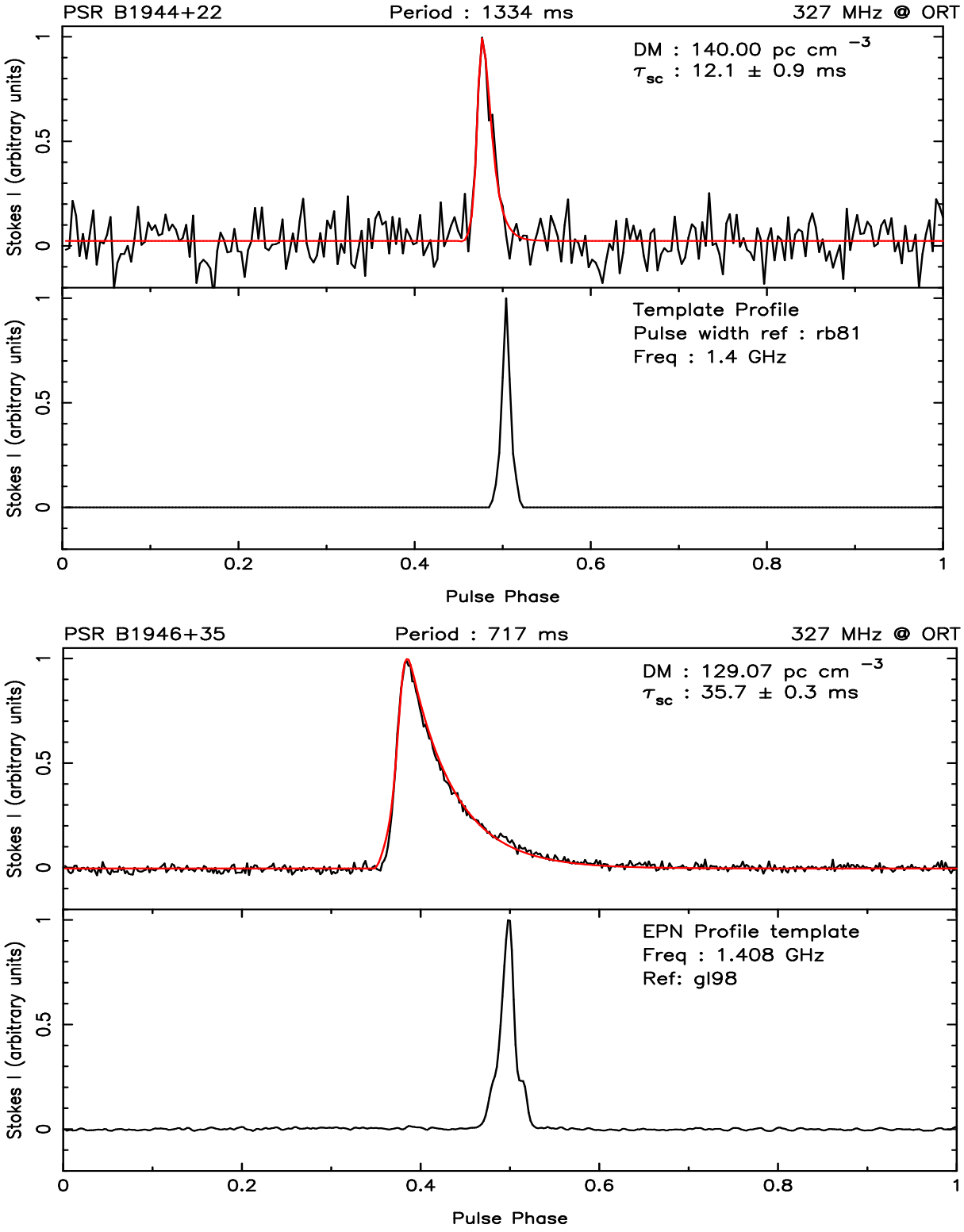

Fig. 58.— Same as in Fig. 1

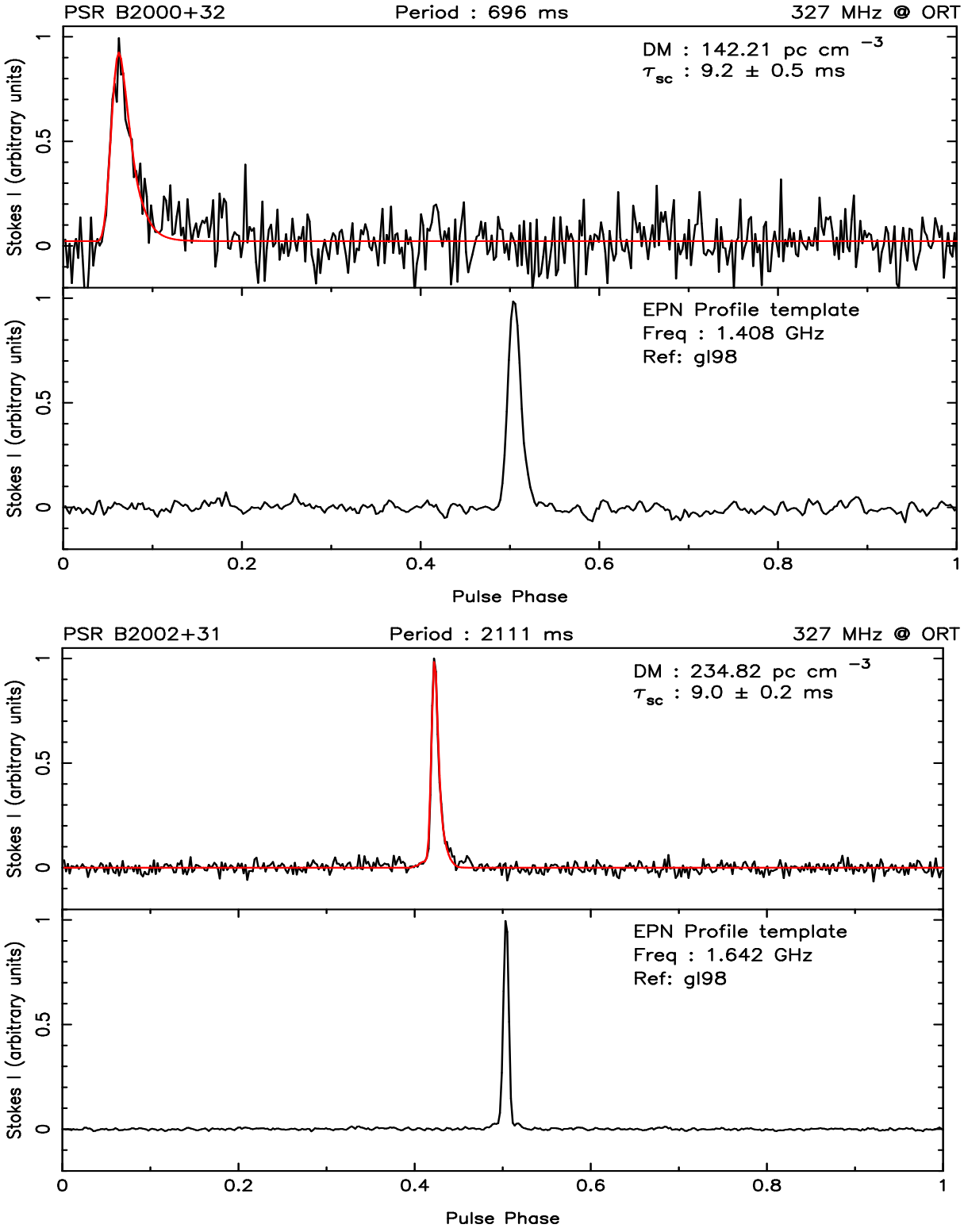

Fig. 59.— Same as in Fig. 1

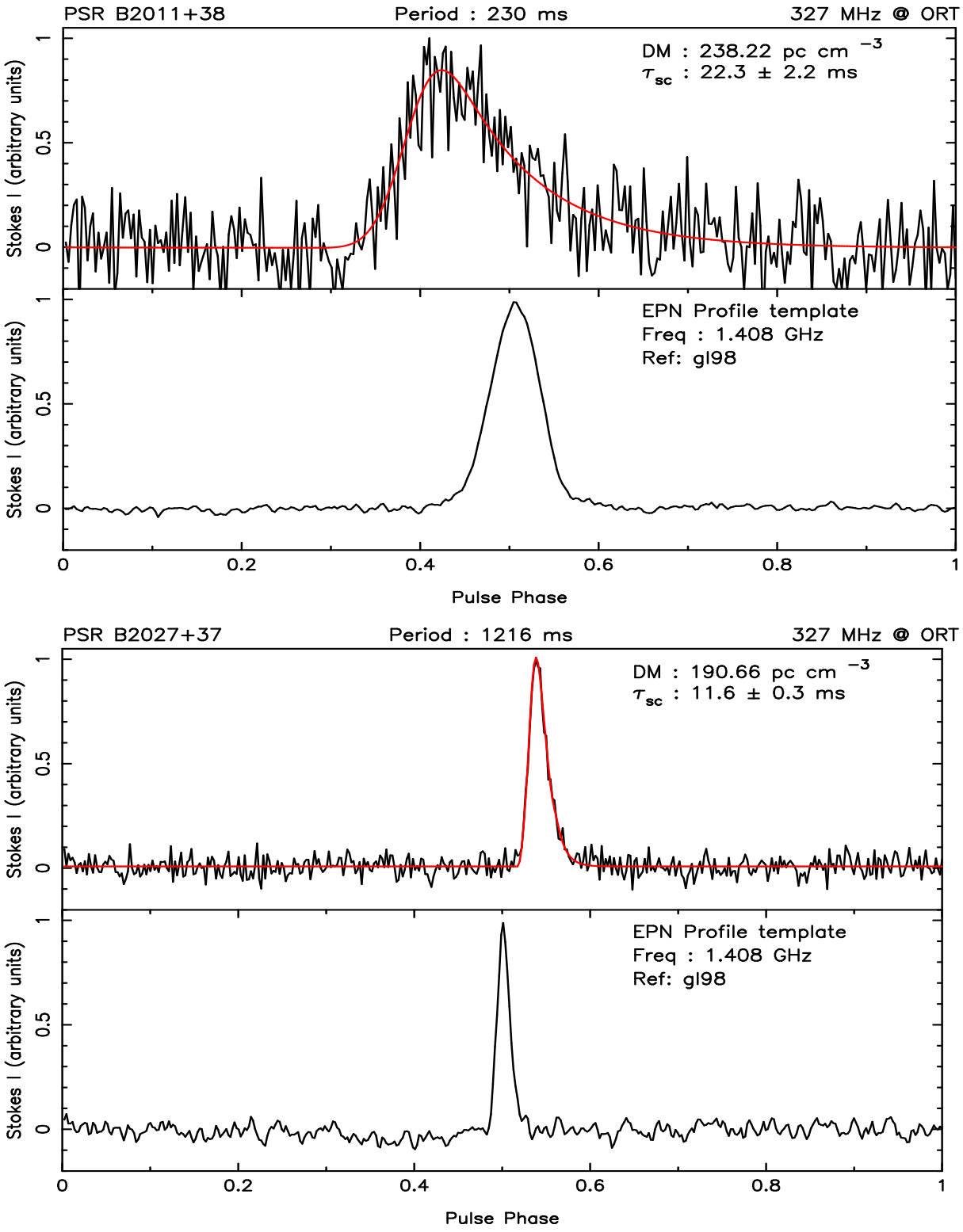

Fig. 60.— Same as in Fig. 1

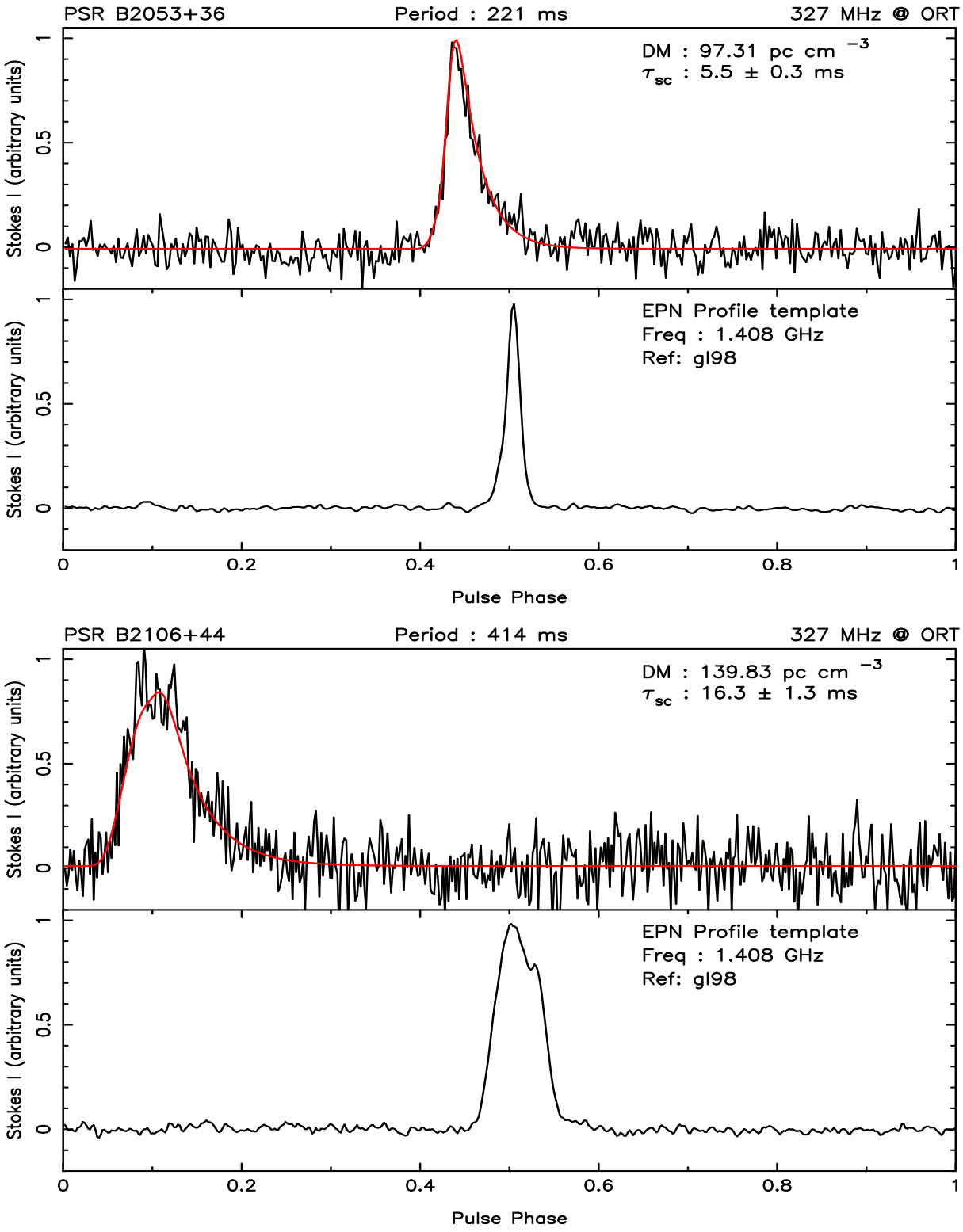

Fig. 61.— Same as in Fig. 1

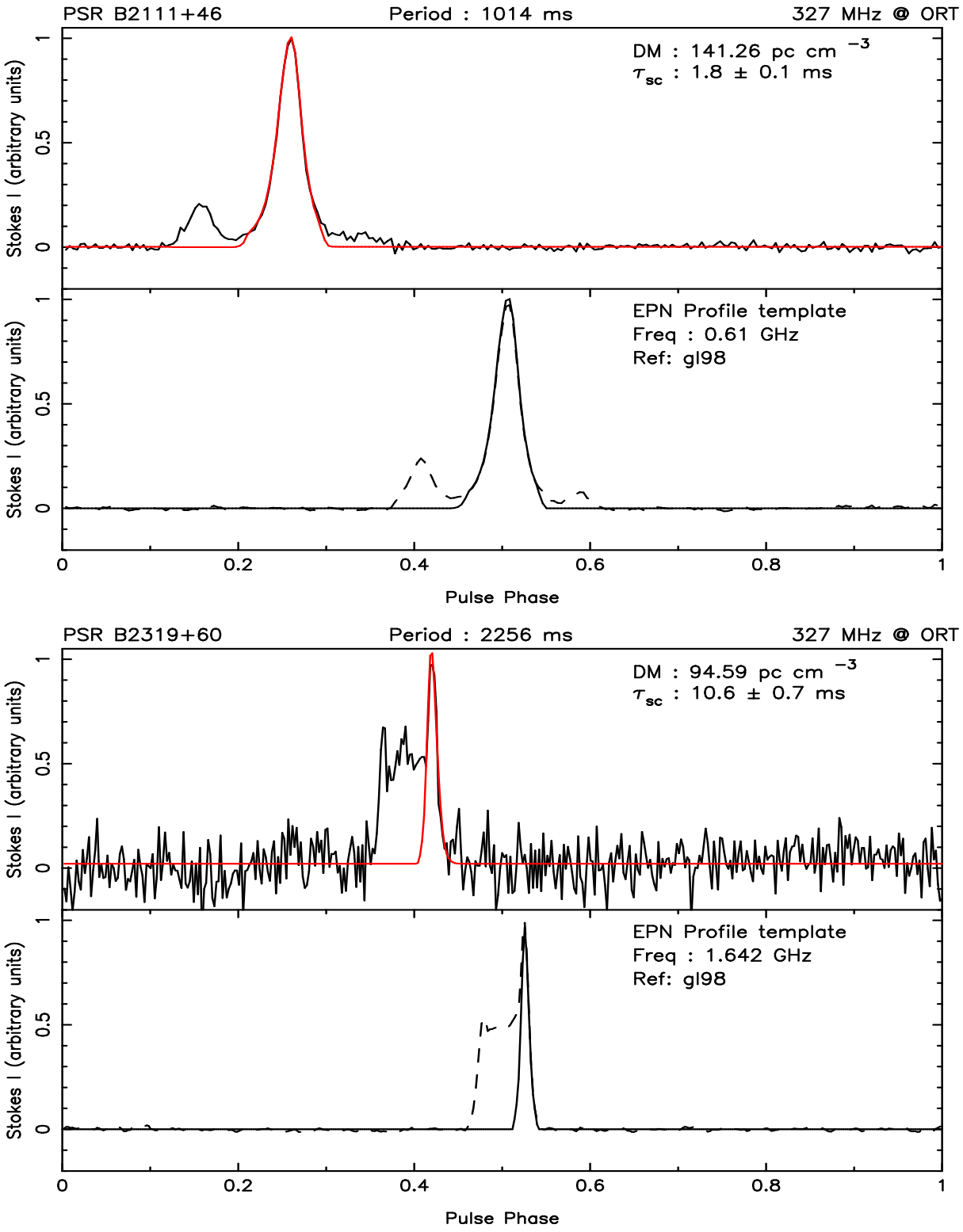

Fig. 62.— Same as in Fig. 1

2. Fit Results using pulse broadening function PBF2

As noted in section 2.2 of the main paper, there are 3 pulsars for which the transfer function $s(t) = \left(\pi^5 \tau_{sc}^3 / 8t^5\right)^{1/2} exp(-\pi^2 \tau_{sc}/4t)$ (also refered to as PBF2 function) is used to fit the data, since the exponential form proved to be inadequate. The results of the fits are given in Table. 2 and the plots are presented in Fig. 63

Table 2. Estimate of τ_{sc} using the PBF2 function. The table lists the pulsar's period in ms, dispersion measure in pc/cc, measured τ_{sc} with error, normalised χ^2 and number of degrees of freedom.

Sr. No.	PSR	Period (ms)	DM (cm^{-3} pc)	τ_{sc} ms	χ^2	N_{dof}
1	B1737-30	0.606924	152.15	62.2±2.5	0.5	196
2	B1834-10	0.562769	316.98	202.5±2.3	1.3	297
3	B1859+03	0.655511	402.08	102.5±0.7	1.4	170

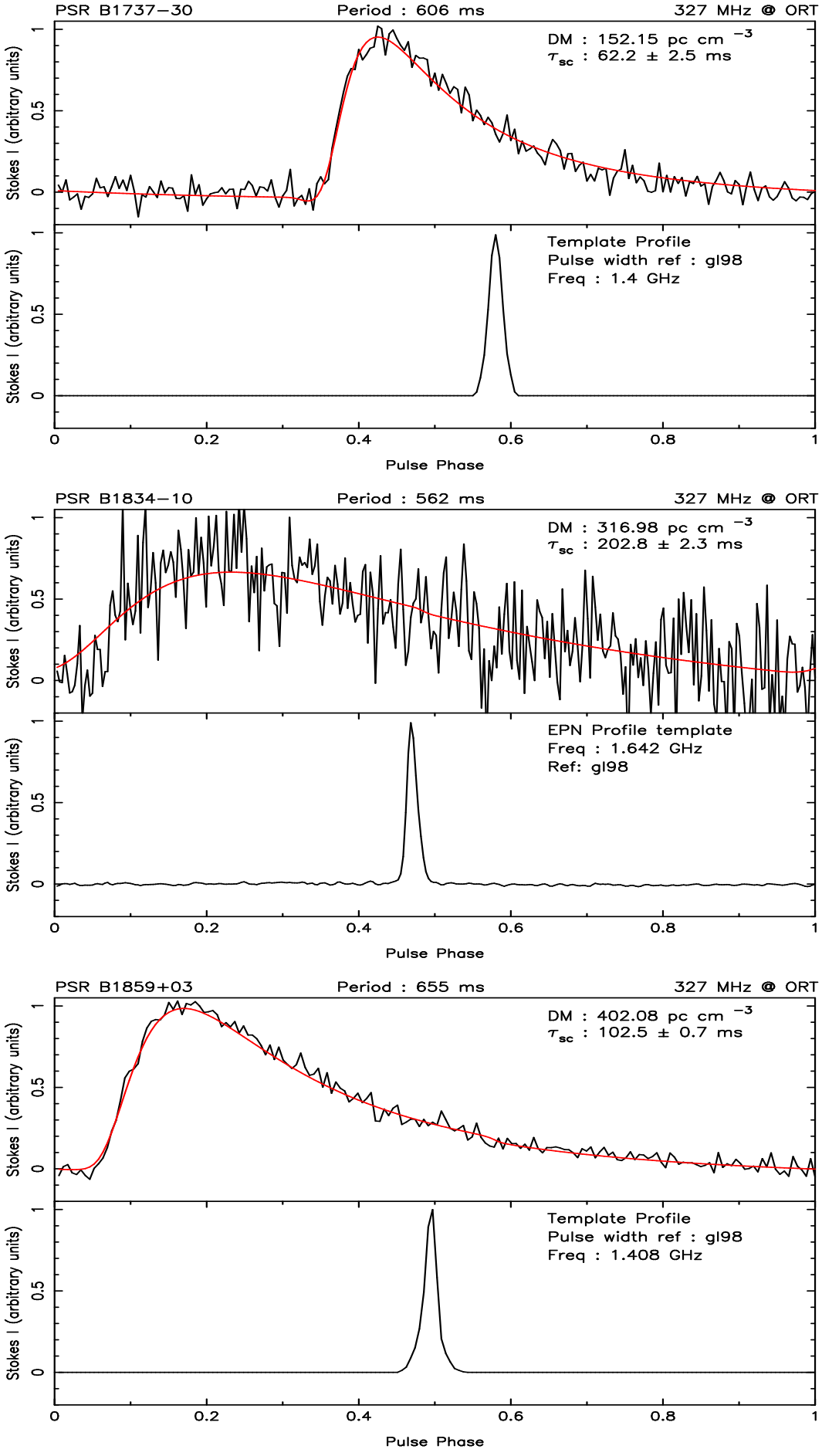

Fig. 63.— Same as in Fig. 1

3. Simulation for extracting τ_{sc} using multicomponent profiles

We present the results of simulations using the 2 component pulsar model as a template. In Figs. 65–70, the bottom panel is the template profile created using two Gaussian components defined as $A_1 exp(-(x-x_1)^2/\sigma_w^2) + A_2 exp(-(x-x_2)^2/\sigma_w^2)$ where, A_1 and A_2 are the amplitude of the Gaussians, x_1 and x_2 are the peak location of the Gaussians and σ_w is the width which is assumed to be same for both the Gaussians. The period of the pulsar is assumed to be 1024 ms. The resulting profile is convolved with an exponential transfer function of the form exp(-t/τ_{sc}) with the value of τ_{sc} as 30 ms. Multiple profiles were obtained by varying the amplitudes and the separation of the Gaussians. The trailing edge component of the profile thus obtained is processed to extract the value of τ_{sc} with the method as explained in the section 2.2 of the paper. The plots of all our simulations are given below. Each plot gives the separation of the components used and the amplitudes (given as a ratio of the two components) of the components along with the τ_{sc} obtained. Figure 64 shows the relation between τ_{sc} and the separation between the components. As one can see, the measured τ_{sc} is very close to the actual value of 30 ms when the separation between the components are larger. Also, when the separation between the components and/or the ratio of the amplitudes are too small, we tend to overestimate τ_{sc} by about 10%.

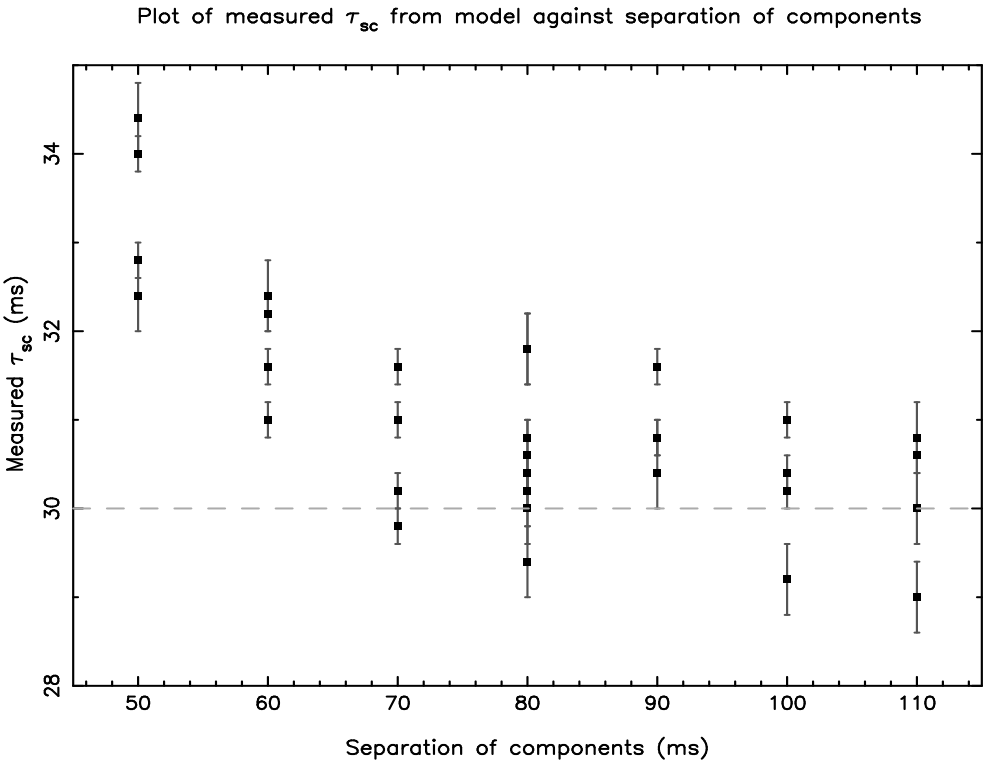

Fig. 64.— See text for details.

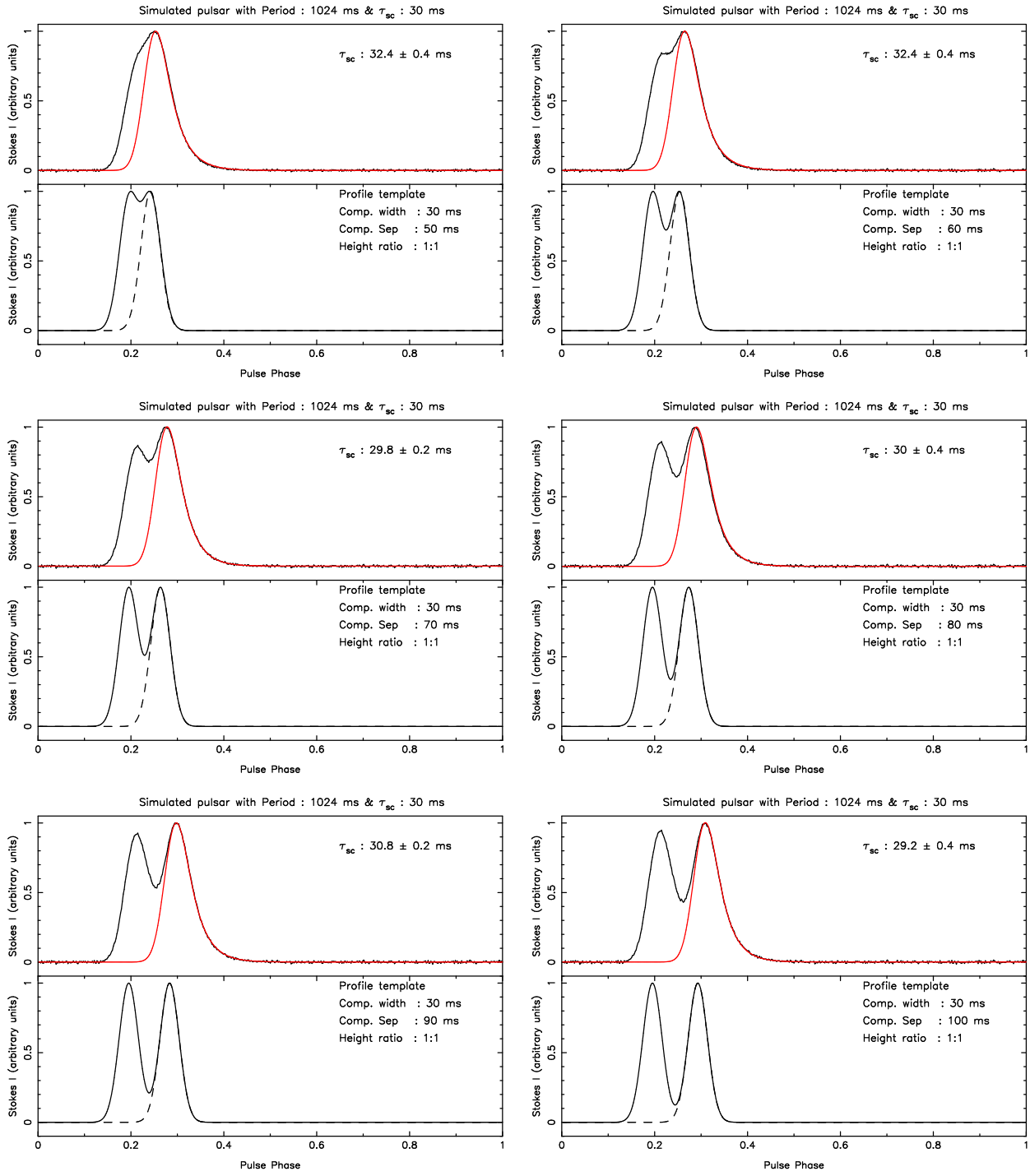

Fig. 65.— Same as in Fig. 1

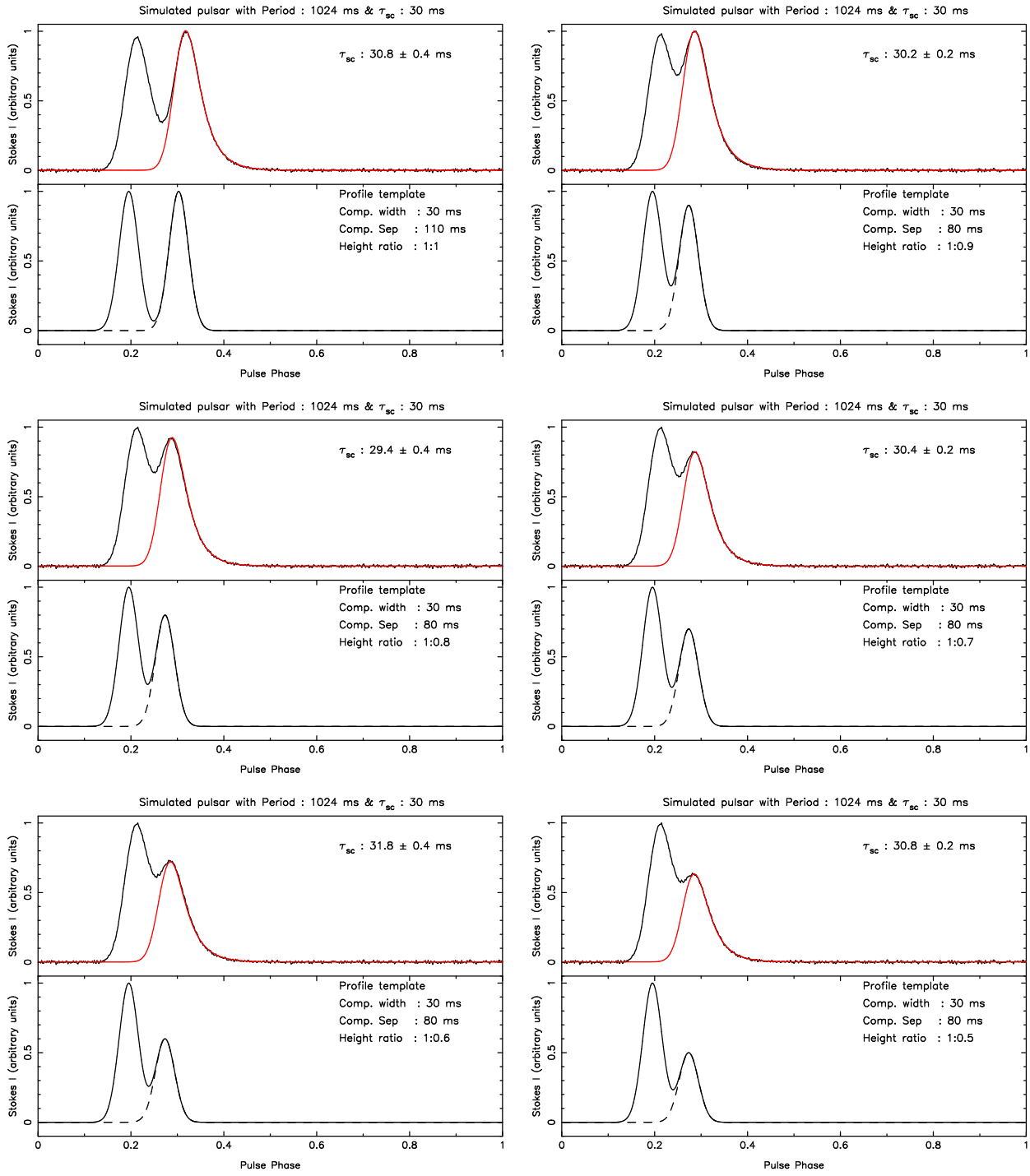

Fig. 66.— Same as in Fig. 1

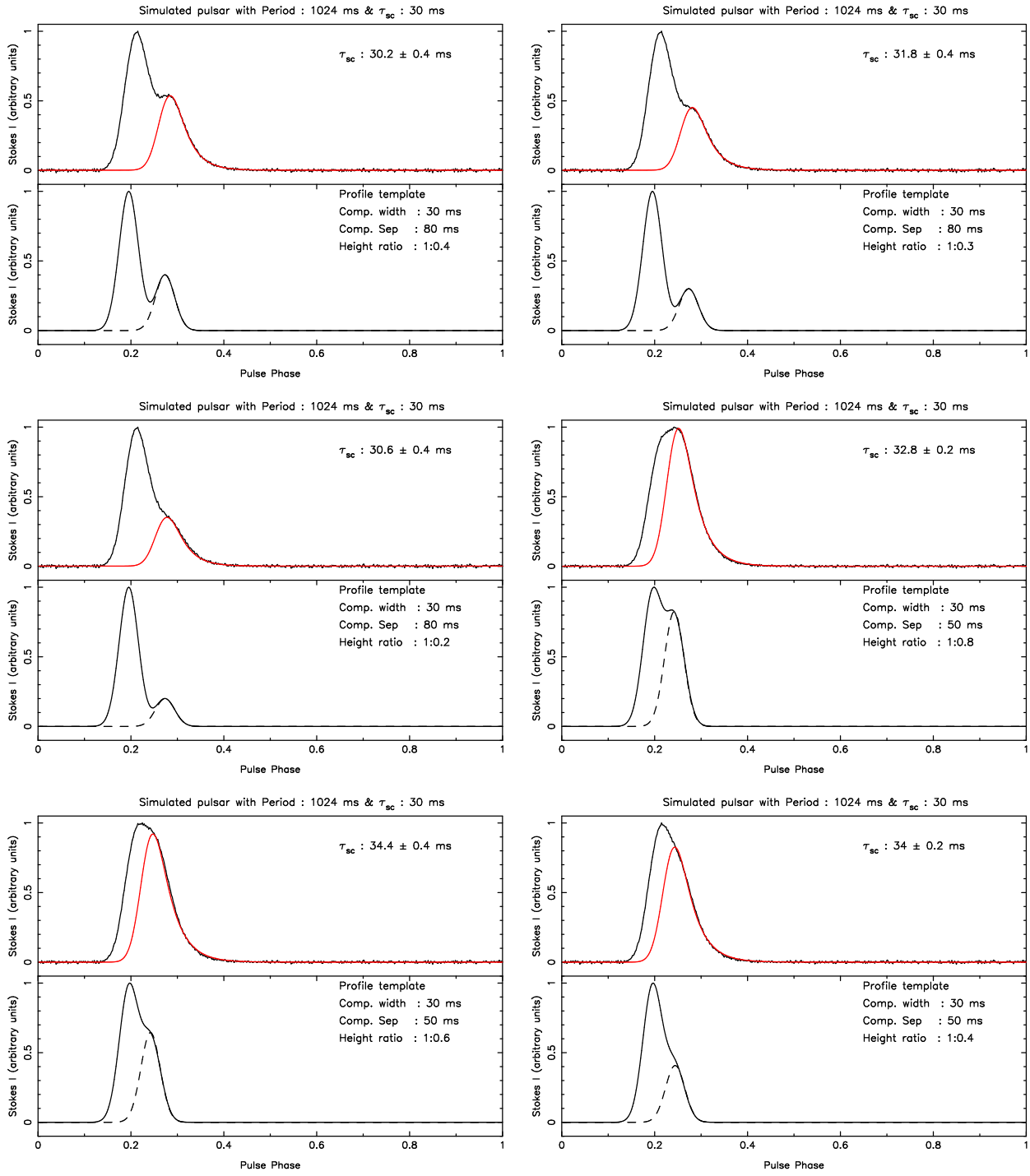

Fig. 67.— Same as in Fig. 1

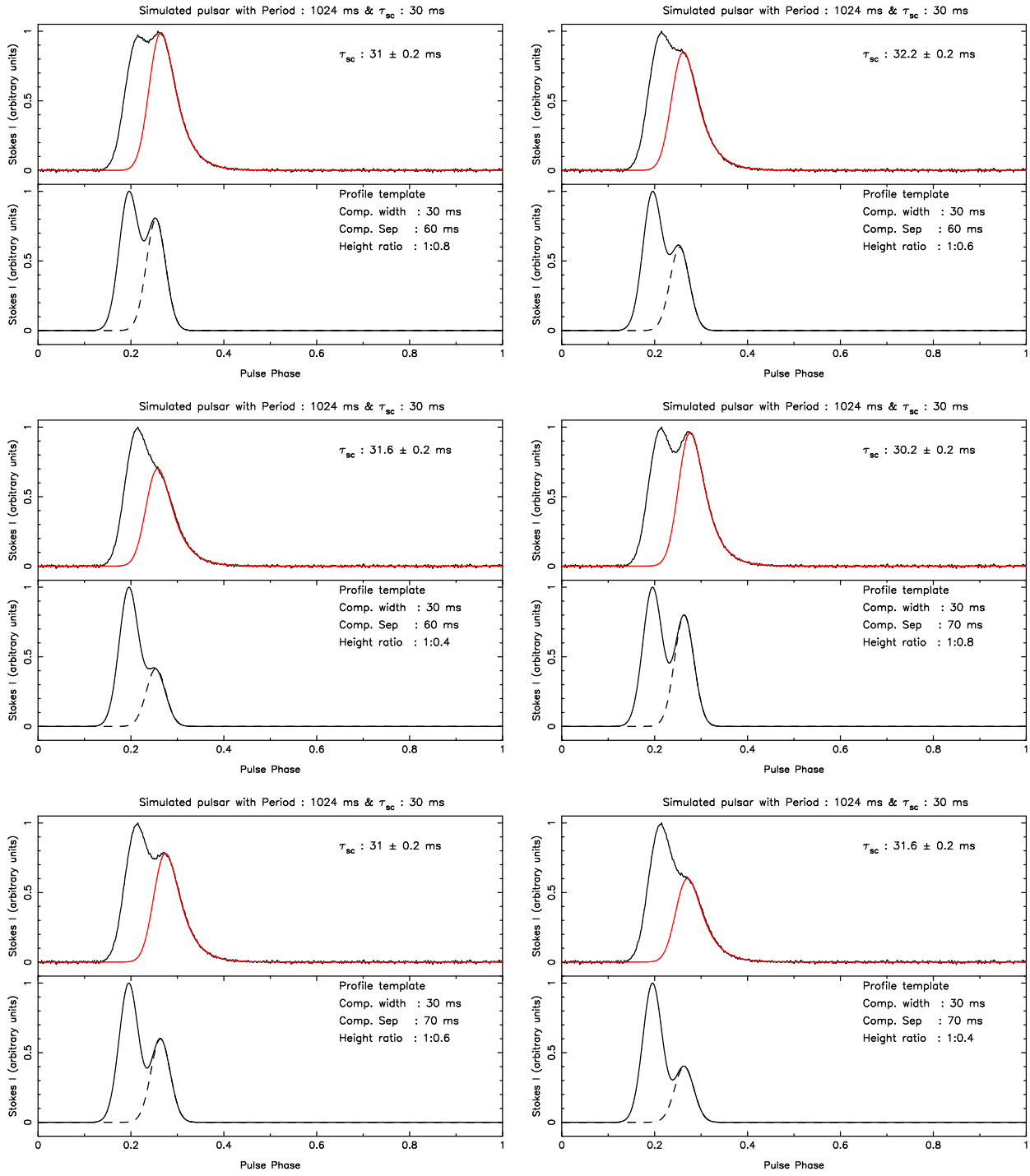

Fig. 68.— Same as in Fig. 1

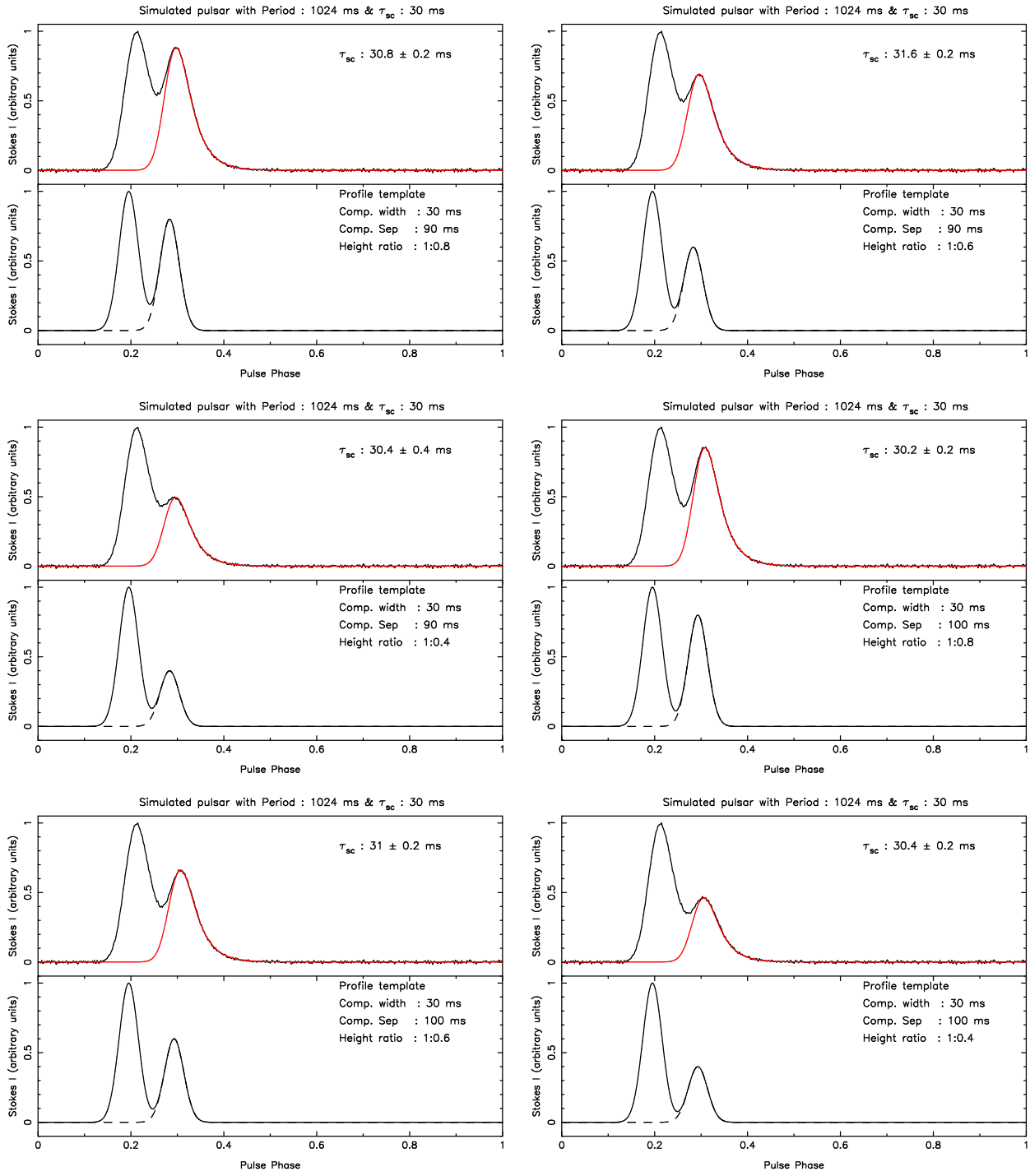

Fig. 69.— Same as in Fig. 1

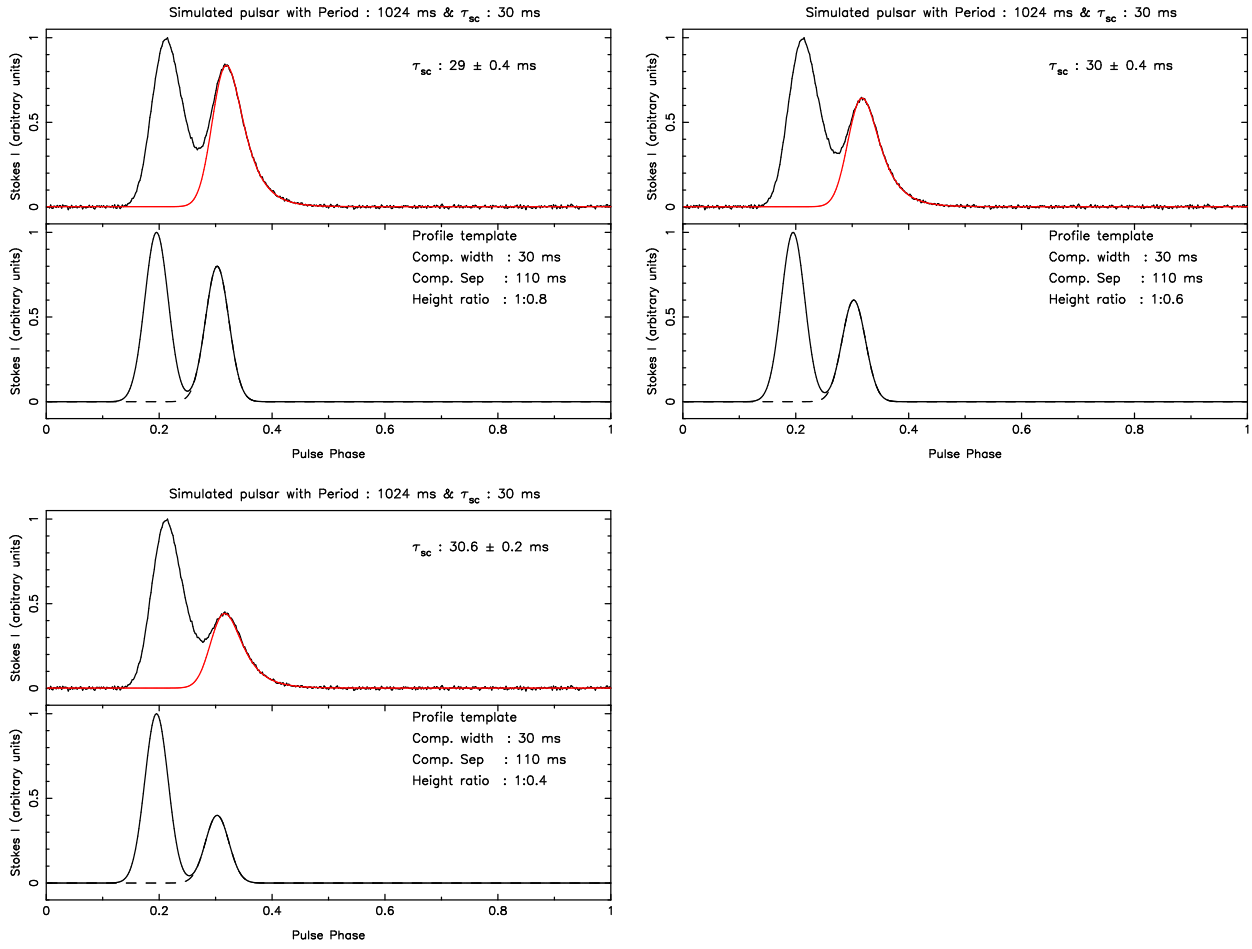

Fig. 70.— Same as in Fig. 1

REFERENCES

[antt94] Arzoumanian, Z., Nice, D. J., Taylor, J. H. & Thorsett, S.E., *Timing Behavior of 96 Radio Pulsars.* ApJ, 1994, 422, 671-680.

[bjb+12] Burke-Spolaor, S., Johnston, S., Bailes, M., Bates, S. D., Bhat, N. D. R., Burgay, M., Champion, D. J., D'Amico, N., Keith, M. J., Kramer, M., Levin, L., Milia, S., Possenti, A., Stappers, B. & van Straten, W., *The High Time Resolution Universe Pulsar Survey - V. Single-pulse energetics and modulation properties of 315 pulsars*, MNRAS, 2012, 423, 1351B.

[dsb+98] D'Amico, N., Stappers, B. W., Bailes, M., Martin, C. E., Bell, J.F., Lyne, A.G. & Manchester, R.N., *The Parkes southern pulsar survey - III. Timing of long-period pulsars*, MNRAS, 1998, 297, 28-40.

[gl98] Gould, D. M. & Lyne, A.G., *Multifrequency polarimetry of 300 radio pulsars*, MNRAS, 1998, 301, 235-260.

[hfs+04] Hobbs, G., Faulkner, A., Stairs, I. H., Camilo, F., Manchester, R. N., Lyne, A. G., Kramer, M., D'Amico, N., Kaspi, V. M., Possenti, A., McLaughlin, M. A., Lorimer, D. R., Burgay, M., Joshi, B. C. & Crawford, F., *The Parkes multibeam pulsar survey - IV. Discovery of 180 pulsars and parameters for 281 previously known pulsars.* MNRAS, 2004a, 352, 1439-1472.

[hkk98] von Hoensbroech, A., Kijak, J. & Krawczyk, A., *On the high frequency polarization of pulsar radio emission.* A&A, 1998, 334, 571-584.

[jnk98] Johnston, S., Nicastro, L. & Koribalski, B., *Scintillation parameters for 49 pulsars*, MNRAS, 1998, 297, 108-116.

[joh06] http://www.atnf.csiro.au/people/joh414/ppdata/index.html

[lor94] Lorimer, D. R., *PhD thesis*, 1994, The University of Manchester.

[qmlg95] Qiao, G. J., Manchester, R.N., Lyne, A. G. & Gould, D.M., *Polarization and Faraday rotation measurements of southern pulsars*, MNRAS, 1995, 274, 572-588.

[rb81] Rankin, J. M. & Benson, J. M., *Pulsar Polarization: Weak Sources and Emission Features at 430 MHz*, AJ, 1981, 86, 418-432.

[sgg+98] Seiradakis, J. H., Gil, J.A., Graham, D. A., Jessner, A., Kramer, M., Malofeev, V.M., Sieber, W. & Wielebinski, R., *Pulsar profiles at high frequencies. I. The data*, A&AS, 1995, 111, 205.

[tml93] Taylor, J. H., Manchester, R. N. & Lyne, A. G., *Catalog of 558 pulsars* ApJS, 1993, 88, 529-568.

[wmlq93] Wu, X., Manchester, R. N., Lyne, A.G. & Qiao, G., *Mean pulse polarization of southern pulsars at 1560 MHz.* MNRAS, 1993, 261, 630-646.